MTBITC-induced apoptosis and cell cycle arrest of human hepatoma (HepG2) cells:

A link between p53 and human telomerase ?

Inaugural - Dissertation

zur Erlangung des Grades einer Doktors der Humanbiologie (Dr. biol. hom.)

des Fachbereichs Humanmedizin

der Justus-Liebig-Universität Gießen

vorgelegt von: Evelyn Lamy

aus: Saarbrücken

Giessen im Jahr 2007

Aus dem Institut für Innenraum- und Umwelttoxikologie

des Fachbereichs Humanmedizin der Justus-Liebig-Universität Gießen

Direktor: Prof. Dr. V. Mersch-Sundermann

1. Gutachter: Univ. Prof. Dr. med. V. Mersch-Sundermann

2. Gutachter: Univ. Prof. Dr. med. A. Reiter

Tag der Disputation: 26.5.2008

Meinen Eltern & Alexander

Es ist nicht genug zu wissen, man muss es auch anwenden; es ist nicht genug zu wollen, man muss es auch tun.
Johann Wolfgang von Goethe

ACKNOWLEDGEMENTS

This thesis grew out of a series of dialogues with my supervisor Professor Dr. Volker Mersch-Sundermann, who gave me every opportunity to broaden my educational horizon and to develop my personality. He piqued my curiosity and provoked me in his very special manner to keep on track. I honestly could not have imagined having had a better mentor; his common-sense, his occasional cracking-of-the-whip, but also his patience with me is greatly appreciated. Especially his axioms will inspire me - or rather haunt me - for the rest of my life.

I thank all my research colleagues for providing a stimulating and fun environment in which to learn and grow. In particular, I wish to thank Dr. Richard Gminski, Ariane Ollman, Yvonne Völkel, Julia Schröder and Peter Brenk. Furthermore, I am indebted to Tao Tang, who made my life easier during the sometimes hard days in the lab. I will truly miss his all-inclusive catering. I especially would like to thank Dr. Thorsten Stahl (LHL, Wiesbaden) for wonderful conversations and the weekly dose of vitamin C.

Dr. Xinjiang Wu (University of Philadelphia, Faculty of Cancer Biology, USA) gave me a helping hand with the immunoblot technique and flow cytometry and Dr. Simone Helmig and Juliane Döhrel (Institute of Occupational Health Medicine, JLU Giessen) helped me with some molecular biology issues. They all gave me important thought-provoking impulses. Thanks to Prof. Dr. Peter Schreiner and Dr. Mike Kotke (Institute of Organic Chemistry, JLU Giessen) for the synthesis of MTBITC and to Prof. Dr. Firouz Darroudi (LUMC, the Netherlands) for providing the HepG2 cells. I also want to thank Ms. Deborah Lawrie-Blum (IUK, Freiburg) for proofreading this thesis.

Finally, I am forever indebted to my parents Horst and Monika Lamy and Alexander for their understanding, endless patience and constant encouragement and love I have relied upon throughout this time. I am also grateful to Mathilde, who is sitting right here beside me again, wondering curiously with her beautiful red eyes at what I might be doing.

On a different note, I would like to thank the black tea producers of India for keeping me awake, and the fair trade organization for making me feel okay about drinking so much tea. Last but not least, I am really thankful to my bicycle for keeping me fit and my heating for keeping me warm at the desk during the cold winter days in the office, although my male colleagues will probably shake their heads in complete bewilderment when reading this.

LIST OF ABBREVIATIONS

ANT	adenine nucleotide translocase
ATP	adenosine triphosphate
B(a)P	benzo(a)pyrene
Bp	base pair
BSA	bovine serum albumine
CDK	cyclin-dependent kinase
CPT	camptothecin
DEPC	diethylpyrocarbonate
DHR123	dihydrorhodamine123
DMEM	Dulbecco´s minimal essential medium
DMSO	dimethyl sulfoxide
DTNB	5.5´-dithiobis-2-nitrobenzoic acid
DTT	dithiothreitol
ELISA	enzyme linked immunosorbent assay
FACS	fluorescence activated cell sorting
FCS	fetal calf serum
FISH	fluorescent in situ hybridization
FITC	fluorescence
FL	fluorescence channel
GC-MS/MS	gas chromatograph, coupled to a mass spectrometer
GLS	glucosinolate
GSH	glutathione
H2O2	hydrogen peroxide
HCC	hepatocellular carcinoma
HRP	horseradish peroxidase
HSP	heat shock protein
hTERT	human telomerase reverse transcriptase
hTR	human telomerase RNA template molecule
IARC	international agency for research on cancer
IFN-a	interferon a
ITC	isothiocyanate
JC-1	5,5',6,6'-tetrachloro-1,1',3,3'-tetraethylbenzimidazolcarbocyanine iodide
LMP	low melting point

MDM2	murine double minute oncogene
MDR	multidrug resistance
MES	2-(N-morpholino)ethanesulfonic acid
MESF	molecules of equivalent soluble fluorochrome
MFI	mean fluorescent intensity
MMP	mitochondrial membrane potential
MPA	meta-phosphoric acid
mRNA	messenger ribonucleic acid
MRP	multidrug resistance proteins
MTBITC	4-methylthiobutylisothiocyanate
MW	molecular weight
NMP	normal melting point
O*	superoxide
OATP	organic anion transporting polypeptide
OH	hydroxyl-
OTM	Olive tail moment
p53	tumor suppressor gene product p53
PAH	polycyclic aromatic hydrocarbon
PBS	phosphate buffered saline
PCR	polymerase chain reaction
PEITC	phenylethyl isothiocyanate
P-gp	P- glycoprotein
RH123	rhodamine123
ROS	radical oxygen species
RT	room temperature
RTL	relative telomere length
SCGE	single cell gel electrophoresis assay
SDS-PAGE	sodium dodecyl sulfate polyacrylamide gel electrophoresis
SFN	sulforaphane
SIM	single ion mode
SOD	superoxide dismutase
ssDNA	single stranded DNA
T	temperature
TEAM	triethanolamine

TMB	3,3`,5,5`-tetramethylbenzidine
TNB	5-thio-2-nitrobenzoic acid
TRAP	telomeric repeat amplification protocol
TUNEL	terminal uridine deoxynucleotidyl transferase dUTP nick end labelling
UV	ultra violet
Wt	wildtype

I. ABSTRACT

Experimental data provide strong evidence for the effective inhibition of tumorigenesis by isothiocyanates (ITCs), enzymatic cleavage products of glucosinolates in *Brassica* vegetables like e.g. cabbage, broccoli or brussel sprouts. A number of ITCs have been identified as strong inhibitors of cell proliferation and apoptosis inducing agents which presents the chance for therapeutic impact of ITC-treatment on malignant transformed cells. Although much is known about ITC-induced apoptosis, many questions remain to be answered. The present study aimed to investigate the chemopreventive properties of 4-methlythiobutylisothiocyanate (MTBITC), which are still largely unknown despite its substantial quantitative presence in food plants. Thereby, this study focused on the hypothesis that p53-dependent induction of apoptosis leads to suppression of telomerase. Human telomerase is stably expressed in the majority of cancer cells but absent in normal tissues which outlines the importance of this enzyme and its compounds in the process of carcinogenesis and provides a promising target for a selective therapeutic approach of malignancies. Proof of a connection between telomerase regulation and the induction of apoptosis by ITCs would present an important detail for a better understanding of the chemotherapeutic properties of these compounds.

As a result, this study showed for the first time the suppression of the telomerase catalytic subunit hTERT and the holenzyme activity in malignant transformed cells mediated by an ITC. This was accompanied by a G2/M phase arrest of the cell cycle and apoptosis induction observed by internucleosomal DNA fragmentation, flow cytometry analysis and the detection of single stranded apoptotic DNA. A collapse of the mitochondrial membrane potential, as analysed by flow cytometry with the probe JC-1 and the suppression of the anti-apoptotic multi-domain Bcl-2 protein Bcl_{xL}, were preceeded by glutathione depletion. Thereby, DNA strand breakage, induced by MTBITC-treatment probably presented the initial step in the growth suppression machinery. This DNA damage was followed by an increase in the protein level of the tumor suppressor p53 and subsequent by the initialization of $p21^{WAF1}$ protein expression. But also, the activation of p63 expression by MTBITC-treatment could be shown for the first time. As a conclusion, the present findings support the idea of an existing extra-telomeric, cell cycle regulation function of telomerase in HepG2 cells. The results of this study also showed that irrespective of the intense

degradation kinetics of MTBITC, the strong cytostatic effect of the ITC was not markedly affected by it and suggests that although ITCs are only present at maximum concentrations in a living system for a rather short time, this might be sufficient to exert their therapeutic effects.

I. ZUSAMMENFASSUNG

Die Inhibition der Tumorigenese durch Isothiocyanate (ITC), enzymatische Abbauprodukte von Glucosinolaten in *Brassica*-Gemüsen wie z. B. Kohl, Brokkoli oder Rosenkohl, ist durch experimentelle Daten belegt. Eine Reihe an ITC wurde als Wachstumsinhibitoren und Apoptose-induzierende Stoffe identifiziert, was die Möglichkeit eines Therapieansatzes bei maligne-transformierten Zellen durch ITC birgt. Obwohl bereits einiges über ITC-vermittelte Apoptose bekannt ist, bleiben noch viele Fragen offen. Die vorliegende Studie zielte darauf ab, die chemopräventiven Eigenschaften von 4-Methylthiobutyl isothiocyanat (MTBITC) zu untersuchen, welche noch größtenteils unbekannt sind, trotz der beachtlichen Quantität von MTBITC in Lebensmittelpflanzen. Dabei fokussierte diese Studie auf die Hypothese, dass p53-vermittelte Apoptoseinduktion eine Inhibition der Telomerase zur Folge hat. Humane Telomerase wird in den meisten Krebszellen stabil exprimiert, ist aber in normalen Geweben nicht detektierbar, was die Bedeutung dieses Enzyms und seiner Komponenten in der Karzinogenese hervorhebt und ein vielversprechendes Ziel für einen selektiven therapeutischen Ansatz bei malignen Tumoren darstellt. Der Beweis einer Verbindung zwischen Telomeraseregulation und der Apoptoseinduktion durch ITC würde ein wichtiges Detail für ein besseres Verständnis der chemotherapeutischen Eigenschaften dieser Stoffe darstellen.

Als Ergebnis der hier vorliegen Studie konnte zum ersten Mal die Unterdrückung der katalytischen Untereinheit der Telomerase hTERT und der enzymatischen Aktivität durch ITC-Behandlung in malignen Zellen gezeigt werden. Dieser Effekt wurde begleitet von einem Zellzyklusarrest in der G2/M-Phase und Apoptoseinduktion, nachgewiesen durch internukleosomale DNA-Fragmentierung, durchflusszytometrische Analyse und der Detektion von apoptotischer Einzelstrang-DNA. Dem Zusammenbruch des

mitochondrialen Membranpotenzials, durchflusszytometrisch analysiert mittels JC-1, und der Unterdrückung des anti-apoptotischen multi-Domänen Bcl-2-Proteins Bcl_{XL} ging eine Absenkung des Glutathionspiegels voran. Dabei stellen die durch MTBITC verursachten DNA-Strangbrüche vermutlich den initialen Schritt in der Proliferationsinhibition dar. Diese DNA-Schäden waren von einem Anstieg des Tumorsuppressor p53-Proteins begleitet und im Folgenden von der Initialisierung der $p21^{WAF1}$-Expression. Zum ersten Mal konnte hier auch die Aktivierung der Expression des p63-Proteins durch MTBITC-Behandlung gezeigt werden. Schlussfolgernd unterstützen die vorliegenden Ergebnisse das Konzept einer existierenden extra-telomeren, Zellzyklus-regulierenden Funktion der Telomerase in HepG2-Zellen. Die Ergebnisse dieser Untersuchung zeigen auch, dass ungeachtet der rapiden Degradation von MTBITC im untersuchen *in vitro*-Modell, die starken zytostatischen Effekte des ITCs auf die Zellkultur nicht merklich betroffen waren. Dies deutet darauf hin, dass obwohl nachgewiesener Weise ITC nur für relativ kurze Zeit Maximalkonzentrationen *in vivo* erreichen, dies dennoch ausreichend sein kann, um einen therapeutischen Effekt auszuüben.

II. INTRODUCTION

2.1 ITCs in Disease and Cancer Prevention

A number of studies support the assumption that isothiocyanates (ITCs) affect the risk of developing chronic diseases such as cancer (Bianchini and Vainio, 2004; Conaway et al., 2002; Hecht, 1999). These sulphur-containing metabolites have been identified as the agents responsible for lowering cancer risk in people eating diets rich in cruciferous vegetables and have therefore recently attracted intense research interest. The association between cancer risk and brassica vegetable consumption derived from cohort, as well as case-control studies, have been summarized in large part by van Poppel and co-workers (van Poppel et al., 1999).

Approximately 120 individual glucosinolates (GLSs) - the glucopuranose-containing precursor products of ITCs - have been isolated chiefly from species of the family *Brassicaceae* and allied families (Fahey et al., 2001). The ITCs are formed by myrosinase-derived hydrolysis of GLSs, following cell damage by chewing, cutting, or processing the vegetable (Holst and Williamson, 2004). Despite the great variety of structure homologues so far, experimental research on the cancer preventive properties of ITCs limit to only a fractional number thereof.

2.2 4-Methylthiobutylisothiocyanate (MTBITC)

The ITC 4-methylthiobutylisothiocyanate (MTBITC, erucin) was fist characterized in steam volatile oils of brassica vegetables by Buttery and co-workers in 1976 (Buttery et al., 1976). It has been detected in a large number of brassica vegetables, and is present in considerable amounts in these plants as shown by Zeuner (Zeuner, 2005). However, it is only recently that its chemopreventive properties have been addressed, dealing with the cytostatic features of this ITC in human leukaemia cells (Fimognari et al., 2004a; Fimognari et al., 2004b). MTBITC is particularly of interest, not only because of its quantitative presence in plants, but because it has been shown that sulforaphane (SFN), which has been extensively studied and is one of the most potent chemopreventive ITC known to date, is oxidized *in vivo* to its structure analogue MTBITC (Kassahun et al., 1997). In their study, 12 % of the NAT-conjugate of MTBITC was recovered in rats treated with SFN and 67 % of a SFN-metabolite was detected in animals administered MTBITC. These findings provoke a closer look at the bioactivity of MTBITC.

2.3 Chemopreventive properties of ITCs

The cancer chemopreventive (i.e. prophylactic *and* therapeutic) activities of ITCs have been reviewed previously by Thornally (Thornalley, 2002). These include the tandem and cooperating inhibitory effects on phase I cytochrome P450 metabolizing enzymes (probably by a combination of enzyme suppression and direct inhibition of their catalytic activities, which thereby lowers the levels of ultimate carcinogens formed) and the enhanced expression of phase II enzymes. ITCs also contribute to the induction of multidrug resistance (MDR) transporters, which in consequence actively facilitate the secretion of xenobiotic compounds (Harris and Jeffery, 2007). But more than that, recently, a number of ITCs have been identified as strong inhibitors of cell proliferation and apoptosis inducing agents (Wu et al., 2005),which presents the chance for *therapeutic* impact of ITC-treatment on malignant transformed cells.

2.4 Apoptosis induction and cell cycle regulation by ITCs

Because of the structure analogy of ITCs, their mechanisms of apoptotic action are similar although the cell death pathway (intrinsic, extrinsic or both) at the least seems to be strongly dependent on the cell type (Keum et al., 2004). A majority of the studies have focused on the mitochondria-mediated intrinsic path of apoptosis induction by ITCs, which is initialized by an alteration in the mitochondrial membrane permeability and cytochrome c release into the cytoplasm. This release is mediated by mitochondrial membrane proteins of the Bcl-2 family, either acting pro-apoptotic (e.g. Bax, Bak, Bad) or anti-apoptotic (e.g. Bcl-2, Bcl_{xL}). The subsequent recruitment and activation of caspase 9 leads to the cleavage of caspase 3 and internucleosomal DNA fragmentation. This process occurs under the premise of sufficient ATP to maintain the integrity of the cell and to provide the necessary energy for enzymatic degradation. An updated, more detailed description of the topic is provided by Zhang and his group (Zhang et al., 2006). Additionally to apoptosis-induction, ITCs have also been shown to arrest cell cycle progression at the G1, S or G2/M phase (Rose et al., 2003; Tang and Zhang, 2004; Zhang et al., 2003). Which outcome prevails is quite likely to depend on balancing signals from various sources. In a number of these systems, however, cell death induction could be observed in dependence to the p53 status *in vitro* and *in vivo* (Huang et al., 1998; Kuang and Chen, 2004).

2.5 The p53 family

The p53 gene family is one of the most important tumor suppressor families known to date, inducing growth suppression or apoptosis, once activated. All three members (p53, p63 and p73) share similar transcriptional functions, although their execution function has varying efficiency (Shimada et al., 1999). Regulation of the p53 protein occurs on both mRNA and protein level, whereas the murine double minute (MDM2) oncogene plays the most central role by conjugation of p53 with ubiquitin, which leads to its proteosomal degradation (Iwakuma and Lozano, 2003). A review on p53-dependent apoptosis pathways is provided by Shen et al. (Shen and White, 2001). p63 shares substantial structural and functional homology with p53, suggesting a comparable function as a tumor suppressor in human cancer. Unlike p53, p63 gives rise to multiple protein isoforms due to differential mRNA splicing and alternative promoter utilization. When overexpressed, p63 has been shown to bind p53 DNA target sites, transactivate p53-responsive genes and induce cell cycle arrest and apoptosis in mammalian cells in a p53-like manner (Calabro et al., 2002).

2.6 The relationship between telomeres, telomerase and p53

p53 plays a crucial role not only in the limitation of cellular proliferation by apoptosis induction or cell cycle arrest, but it has also been shown by several authors that p53 transcriptionally suppresses the activation of human telomerase reverse transcriptase (hTERT) (Saito et al., 2004; Shats et al., 2004; Stampfer et al., 2003) suspecting a p53-dependent regulatory path for hTERT control in human cells.

hTERT presents the catalytic subunit of telomerase (Bryan et al., 1998), a ribonucleoprotein complex, consisting - besides hTERT - of an RNA template molecule (hTR) (Feng et al., 1995) and a number of telomerase associated proteins (Chang et al., 2002; Smogorzewska and de Lange, 2004). Although hTR is constitutively expressed in all tissues, hTERT expression seems to be restricted to telomerase-positive tissue, indicating that hTERT is the limiting factor for the enzyme activity (Bodnar et al., 1998). A positive correlation has been found by several authors between the amount of hTERT mRNA and the enzymatic activity of telomerase, suggesting that the enzyme activity is regulated directly at the gene transcriptional level of hTERT (Cong et al., 1999; Ducrest et al., 2002; Yi et al., 1999). The hTERT gene possesses two p53 binding motifs upstream of the 5`core promotor region at –1877 and –1240 relative to the start of transcription. The binding of stabilized p53 with the assistance of the transcription factor SP1 at these two motifs of

hTERT represses the hTERT promotor (Kanaya et al., 2000). Besides this, regulation of telomerase occurs on the level of posttranslational protein-protein interaction and protein-phosphorylation. Recently, the heat shock protein 90 (HSP90) chaperon complex has been demonstrated to bind to hTERT and contribute in a large part to the holenzyme activity (Akalin et al., 2001). A proposed model suggests that both HSP90 and p23 bind to hTERT and influence proper assembly with hTR to form the active enzyme (Forsythe et al., 2001). In consideration of the fact that hTERT is primarily nuclear and HSP90 is prevalent in the cytoplasm, it has been proposed that telomerase assembly occurs in the nucleus or that –in contrast to other chaperone targets- HSP90 remains associated with the functional enzyme.
Telomerase is continuously repressed in most normal somatic tissues, except for stem and germ cells. In contrast to this, 80 to 90 % of cancer cells stably express this enzyme (Shay and Bacchetti, 1997), which is reactivated during malignant transformation. This (re)activation provides unlimited proliferation capacity for the tumor cells by *de novo* synthesis of telomeric $(TTAGGG)_n$ sequences, circumventing the "end-replication problem" of DNA synthesis (Kim et al., 1994; Smogorzewska and de Lange, 2004). Telomerase activity has been shown to be strongly correlated with the state of malignancy in transformed cells and is discussed as a useful molecular marker in the prognosis of cancer (Triginelli et al., 2006; Zhang et al., 1999). Moreover, its reactivation in most human cancers outlines the importance of this enzyme and its subunits in the process of carcinogenesis and provides a promising target for a *selective* therapeutic approach to malignancies.
Only recently, it has been found that telomerase exerts extra-telomeric effects (Perrault et al., 2005). Besides the catalytic function of hTERT, it directly takes part in protecting the chromosome ends from signalling into cell cycle arrest and/or apoptosis (Blackburn, 2000). Telomeres form a higher order t-loop structure, with their 5´overhangs invading and being buried in-between double stranded telomeres and hTERT is critical for maintaining the capping of telomeres (Griffith et al., 1999). The loss of this capping function would generate one or more free telomere ends. This could lead to end-to-end fusions and degradation of chromosomes, which in consequence could be recognized by specific DNA-damage sensors, including p53. A chemical-induced rapid degradation of the telomeric repeats triggering apoptotic death has been described in several systems (Ramirez et al., 2003). Recent studies by Cao and co-workers (Cao et al., 2002) discovered that hTERT owns a similar subcellular distribution pattern as p53 throughout mitosis suggesting the possibility, that hTERT and p53 cooperate to maintain normal mitotic spindle function

during chromosome segregation. Thereby, hTERT starts to dissociate from chromosomes in the mitotic prophase and binds successively to microtubule spindles at metaphase. In anaphase, hTERT finally localizes around the daughter chromatids. The precise mechanism of this extra-telomeric function however is under current research and needs to be refined and further detailed.

2.7 Objectives and hypothesis

As described above, the impairment of cell growth by specific hTERT targeting can be sustained by two pathways. First, successive telomere shortening as a result of prolonged inhibition of the telomerase enzyme activity. This process requires a period of several months, depending on the proliferation rate of a cell, finally leading into cellular senescence. The second pathway comprises the loss of the hTERT-mediated capping function of telomerase which results in the initialization of apoptotic signalling.

The present study aimed to test the hypothesis that p53-dependent induction of apoptosis, mediated by ITCs, leads to suppression of telomerase in a human malignant transformed cell line. This was investigated in the human hepatoma HepG2 cell line, a wildtype p53 cell line with strong telomerase activity and short telomeres. Since ITCs are metabolized *in vivo* mainly by phase I and II enzymes to their mercapturic acid-derivatives in the liver, this cell line qualified for the question at issue. 4-methylthiobutyl-ITC was exemplarily tested for this hypothesis. MTBITC was especially interesting due to its substantial quantitative presence in food plants and the fact that its chemopreventive properties are largely unknown. Although much is known about ITC-induced apoptosis, many questions remain to be answered. Proof of a connection between telomerase and the induction of apoptosis by ITCs would present an important detail for better understanding of the chemotherapeutic properties of these compounds in human-derived cells.

In detail, the following aims were addressed:

- to investigate the effects of MTBITC on the proliferation of HepG2 cells and to characterize the apoptotic origin
- to determine the role of p53 family members in programmed cell death
- to analyse the influence of MTBITC on telomerase and telomere length
- to determine cofounders of the observed findings
- to investigate the stability and degradation kinetics of MTBITC in the applied system

III. MATERIAL

3.1 The human cell culture model HepG2

A large part of the studies dealing with the p53-dependent regulation of telomerase have been carried out with non-physiological overexpression of p53 or have lacked isogenic controls (Lin and Elledge, 2003). In contrast to this, in the present work, the experiments were carried out with the human derived hepatoma cell line HepG2, a hepatocellular carcinoma (HCC) cell line expressing physiological levels of p53. HepG2 are a telomerase positive cell line with rather short telomeres of around 5.6 kb in length (Furuta et al., 2003). They were originally derived in 1979 from an 11-year old Argentine boy (Aden et al., 1979), with the intention of replacing fresh human hepatocytes in early toxicology screening. This cell line has been successfully cultured for more than 100 passages (Silvers et al., 1994).

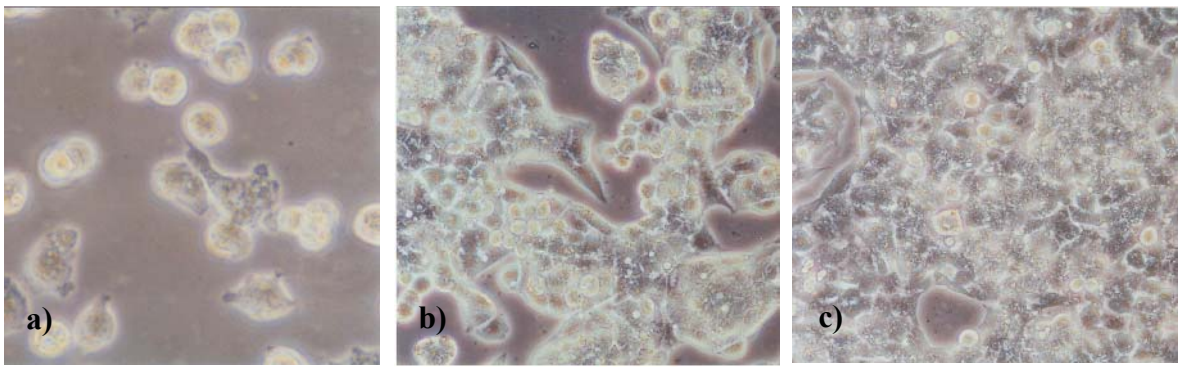

Figure 1: HepG2 cells in different growth states: a) 24 hours, b) 3 days and c) 6 days after seeding

3.1.1 Biochemical characterization

HepG2 cells are considered to be suitable *in vitro* models of the HCC since they have been shown to possess similar characteristics typical for primary hepatocytes. Under cell culture conditions, they secrete most of the plasma proteins, like e.g. fibrinogen and albumin as well as apolipoproteins (Knowles et al., 1980). HepG2 cells also exhibit carrier-mediated bile acid uptake, functionally resembling the multispecific organic anion transporting polypeptide (OATP) of the human liver (Kullak-Ublick et al., 1996). But more interesting is the fact that they express considerate levels of Phase III transporters, including the

multidrug resistance proteins MRP1, MRP2 and the P- glycoprotein P-gp (Harris and Jeffery, 2007).

The successful application of HepG2 cells in genetic toxicology is mainly based on the capability of the cells to synthesize enzymes of the xenobiotica metabolism, reflecting the metabolism of normal human hepatocytes (Hewitt and Hewitt, 2004; Wilkening and Bader, 2003; Wilkening et al., 2003). This is in advantage to cells which have to be externally supplemented with these enzymes (e. g. by the addition of arochlor induced S9-mix from rats) for activation of promutagens or –carcinogens (Doostdar et al., 1993; Knasmuller et al., 1998).

3.1.2 Tumor suppressor gene product p53 status

The tumor suppressor gene p53 is located on the short arm of chromosome 17 and is known to be frequently deleted and abnormally expressed in several HCC derived cell lines (Hosono et al., 1991). For the HepG2 cell line, however, several groups have shown a normal wildtype (wt) expression of p53 (Puisieux et al., 1993). The mRNA level and protein level of p53 have been reported as normal with a half-life of the p53 protein in this cell line to be less than 30 min. (Bressac et al., 1990; Puisieux et al., 1993).

3.2 General material

For cell culture technique, immunoblotting, sterile filtration of chemicals and GC-MS/MS analysis, the following materials shown in table 1 were used:

Table 1: Materials used for cell culture, sterile filtration, immunoblotting and GC-MS/MS analysis

Material	Cat. No.	Distributor
96-well plate, non-sterile, transparent	32409522	Greiner bio-one
96-well plate, sterile	655180	Greiner bio-one
cell culture flask 025 cm^2 with 0.22 µM filter cap	831810002	Sarstaedt
cell culture flask 075 cm^2 with 0.22 µM filter cap	658.175	Sarstaedt
cell culture flask 175 cm^2 with 0.22 µM filter cap	831.812.002	Sarstaedt
cell scraper	541070	Greiner bio-one
centrifuge conical tubes, PA 16 x 51 mm, 5.5 ml vol	358122	Beckman Instruments
Hyperfilm ECL, 18 x 24 cm	RPN3103K	Amersham Bioscience
Hyperfilmcassette, 18 x 24 cm	RPN13642	Amersham Bioscience
Millex FG (PTFE) Syringe driven filter unit, 0.2 µm	SLFG025LS	Millipore

Millex GP Syringe driven filter unit, 0.22 µm	SLGP033RS	Millipore
Nescofilm nitrocellulose membrane, hybond ECL	2569.1 RPN 3103K	Roth Amersham Bioscience
Sterile filter (bottle top) syringe, singel use, sterile 0.8 x 40 mm	SCGPT02RE REF304432	Millipore Becton Dickenson
whatmanpaper, 17CVR, 46 x 57 cm	3017915	Whatman Internat. Inc.
11 mm crmp cp alum PTFE	392611627	Varian
Crimp Top wide opening vial 2 ml 12 x 32 mm glass Microliter syringe 10 µl	392611635 Syrc L10-26 S-AS	Varian Hamilton

3.3 Chemicals

Standard chemicals were obtained from the Sigma-Aldrich Group (Taufkrichen), Serva (Heidelberg), Lifetechnologies (Karlsruhe) and Merck (Darmstadt). In addition, the following alphabetically arranged chemicals shown in table 2 were used:

Table 2: Chemicals used for the experiments and their specifications

Chemicals	Purity	Cat. No.	Distributor
2-Mercapto-Ethanol	> 98 %	805740	Merck
2-Propanol Aceton	99.5 % > 99.9 %	8067 1.000.14.2500	J. T. Baker Merck
Acrylamide solution, 30 % (37,5:1) Agarose	 for electrophoresis	A3626,0250 11404	Applichem Serva
Developer Rapid Fixer		G138i A+B+C G334i A+B	Agfa Agfa
Ammoniumpersulfat Boric acid	 p. a.	A9164 1.001.651.000	Sigma-Aldrich Merck
Cyclohexane DEPC	for synthesis	8.222.68.2500 K028.3	Merck Roth
Digitonin Dimethylsulfoxide (DMSO)	 cell culture grade	D141 A3672,0100	Sigma-Aldrich Applichem
Dithriothreitol (DTT) D-Mannitol	99%	D-9779 M9546	Sigma-Aldrich Sigma-Aldrich
Dodecylsulfat-Na-Salt (SDS) EDTA disodium salt dihydrate	 p.a.	20760 8043.2	Serva Roth
Ethanol Ethylacetate	p. a. for synthesis	32205 8.222.772.500	Riedel-de-Haen Merck
Glycerol Glycin	p.a.	3783.1 10.670.500	Roth Applichem

Glyzin		A1377.5000	Applichem
Hydrochloric acid fuming	37%	1.003.171.000	Merck
Maleic acid		63190	Sigma-Aldrich
Metaphosphoric acid		M6288	Sigma-Aldrich
Methanol	p.a.	65543	Fluka
Sodium chloride		3957.2	Roth
Sodium hydroxide		6771.1	Roth
Sucrose	99 + %	S-0389	Sigma-Aldrich
TEMED	> 99 %	2367.3	Roth
Triethanolamine		T5,830-0	Sigma-Aldrich
Tris	99.9 %	4855.2	Roth
Triton X-100		1.086.431.000	Merck
Tween 20	for electrophoresis	P5927	Sigma-Aldrich

3.4 Cell culture reagents

For culture of the HepG2 and CCRF-CEM cell line the reagents in table 3 were utilized. All cell culture reagents were sterile filtered (0.2 µm). The medium for HepG2 cells consisted of DMEM, supplemented with 15 % FCS and 50 µg/ml gentamycin; for culture of CCRF-CEM cells, RPMI medium containing 10 % FCS was used. The prepared media were stored at 4 °C and pre-warmed to 37°C before use.

Table 3: Reagents for the culture of the HepG2 and CCRF-CEM cell line

Cell Culture Reagents	Cat. No.	Distributor
DMEM low Glucose (1 g/l) with L-Glutamin	E15-806	PAA
DMEM w/o phenol red	11880	Invitrogen
Dulbeccos PBS w/o Ca^{2+}/Mg^{2+}	H15-002	PAA
Fetal calf serum (FCS), Gold	A15-649	PAA
Gentamycin solution (50 mg/ml)	47991.01	Serva
L-Glutamine 200 mM	M11-004	PAA
RPMI w/o L-glutamine	E15-039	PAA
Trypsin, 2.5 % (10 x) in PBS	L 11-001	PAA

3.5 Antibodies

The antibodies for immunoblotting experiments are listed in table 4,. Primary antibodies were derived from immunized mice or rabbits, the secondary HRP-labelled IgG antibodies

were derived from goat or horse. The antibodies were purchased as ready made solutions and applied at the given dilution factor in the immunoblotting experiments.

Table 4: Primary and secondary antibodies

Antibody	Source	Specificity	Dilution factor	Cat. No.	Distributor
b-Actin (AC-74)	mouse	monoclonal Ab	1:3000	A 5316	sigma
Bcl-xL	rabbit	monoclonal Ab	1:500	2762	cell signalling
HSP70	rabbit	polyclonal Ab	1:1000	4872	cell signalling
HSP90	rabbit	polyclonal Ab	1:1000	4874	cell signalling
hTERT (C-term)	rabbit	monoclonal Ab	1:500	1531-1	epitomics
MDM2 (D-12)	mouse	monoclonal Ab	1:100	sc-5304	santa cruz
p21 Waf1/cip1 (DCS60)	mouse	monoclonal Ab	1:500	2946	cell signalling
p53 (BP53-12)	mouse	monoclonal Ab	1:2000	P 5813	sigma
p63 (87C53)	mouse	monoclonal Ab	1:100	ab11995	abcam
Mouse IgG, HRP-linked	goat		1:4000	7076	cell signalling
Rabbit IgG, HRP-linked	horse		1 :4000	7074	cell signalling

3. 6 Electrophoresis reference bands

To monitor the progress of protein separation and transfer efficiency and for the identification of proteins in the polyacrylamide gels, the molecular weight marker listed in table 5 was used. Additionally, table 5 contains the DNA markers, applied to verify the size of the amplified telomerase fragments.

Table 5: Molecular weight markers for protein and DNA analysis

Chemicals	Cat. No.	Distributor
Precision Plus Protein Dual Color Standard	161-0374	Biorad
DNA Ladder 100 bp (0,1µg/µl)	12228692	Invitrogen
DNA Ladder, 50 bp (1 µg/µl)	10416-014	Invitrogen

3.7 Assay kits

For the assessment of cell proliferation, formation of single stranded apoptotic DNA, glutathione content of HepG2 cells, telomerase activity and telomere length determination, the kits in table 6 were used.

Table 6: Kits implemented in the investigations with HepG2 cells

Assy kits	Cat. No.	Distributor
Apoptosis Elisa Kit, ssDNA	APT225	Chemicon
Cell Proliferation Reagent, WST 1	11644807001	Roche
Glutathione Assay Kit	ALX850038-K101	Alexis
TeloTAGGG Kit	2013789	Roche
Telomere PNA Kit/FITC for flow cytometry	K5327	Dako

3.8 Staining solutions

The staining solutions applied in the experiments are listed in table 7.

Table 7: Staining solutions

Chemical	Cat. No.	Distributor
Bradford Reagent	B6916	Sigma-Aldrich
Dihydrorodamine (DHR123)	D1054	Sigma-Aldrich
Erythrosin B	20096-4	Sigma-Aldrich
Ethidium bromide (10 mg/ml)	E1510	Sigma-Aldrich
JC-1	T3168	Invitrogen
Propidium Iodide	81845	Fluka
SYBR Gold (10.000 x)	S11494	Molecular Probes

3.9 Equipment and software

Besides the standard laboratory equipment, the following apparatus were used for the experiments:

- Infinite M 200 microplate reader, Tecan Group Ltd., Germany
- Geldocumentation Imager 2000, Intas, Germany
- High Performance Centrifuge Avanti J-30 I, Beckman Coulter, Germany
- FACSCalibur with sorter, BD, Germany

  FSC Diode 488 nm

  SSC PMT 488 nm

  FL1 PMT 515-545 nm

  FL2 PMT 564-606 nm

  FL3 PMT >650 nm
- Gas chromatograph CP-3800, coupled to a 1200 Quadrupole MS/MS, Varian, Germany

with a CombiPAL auto sampler and a factorFour fused silica capillary column (VF-35ms, 30 m x 0.25 mm (i.d.), 0.25 µm film thickness, Varian, Germany

For data acquisition and analysis the following computer software was used:

- Gel-Pro Express 4.0, Intas, Germany (Densitomentric protein analysis)
- Magellan 5.0, Tecan, Germany (Multiplate fluorescence and absorbance measurement and analysis)
- FACStation Software 3.5, BD, Germany (Flow cytometric data acquisition)
- Cellquest pro, BD, Germany (Flow cytometric data analysis)
- Modifit LT, Verity Software House Inc., UK (Flow cytometric data analysis)
- QuickCal 2.3, Bangs Laboratories, Inc., USA (Flow cytometric data analysis)
- Comet 5.5, Optilas, Germany (Assessment of DNA damage and data analysis)
- Analysis Macro 2000, Kinetic Imaging Ltd, UK (Assessment of DNA damage and data analysis)

3.10 Media, Buffers, Solutions

The buffers required for DNA laddering experiments are listed in table 8.

Table 8: Buffers and their chemical composition for the DNA laddering assay

Buffer/Solution	Chemical/Solution	Weighted sample/ Volume	Final concentration
TBE-buffer (10x)	Tris	108 g	89 mM
	Borsäure	55 g	89 mM
	EDTA	9.3 g	0.05 M
	Aqua dest.	1000 ml	
	Storage: RT 1-2 months		
TE-buffer pH 8.0	Tris (1M)	10 ml	10 mM
	EDTA	0.17 g	1 mM
	Aqua dest.	990 ml	
	adjust pH with HCl		
	Storage: RT		
TTE-buffer	Triton X-100	100 µl	0.2 %
	TE-buffer	50 ml	
	Storage: + 4°C		

DNA loading buffer (10x)	bromophenol blue 1.25 % 0.5 M EDTA, pH 8,0 Glycerol Aqua dest. Storage: RT	1 ml 0.5 ml 2.5 ml 1 ml	50 mM

Table 9 contains the compositions of the buffers and solutions needed for the conduction of the comet assay.

Table 9: Buffers and their chemical composition for the comet assay

Buffer/Solution	Chemical/Solution	Weighted sample/ Volume	Final concentration
LYSIS SOLUTION (PH 10)	NaCl EDTA NaOH Triton X-100 Aqua dest. Storage: + 4°C for 24 h	146.1 g 37.2 g 8 g 10 ml 1000 ml	2.5 M 0.2 M 0.2 M 1%
DNA UNWINDING	NaOH Aqua dest.	12 g 1000 ml	0.3 M
ELECTROPHORESIS BUFFER (PH 13)	NaOH EDTA Aqua dest.	12 g 0.37 g 1000 ml	0.3 M 2 mM
NEUTRALISATION BUFFER (PH 7.5)	Tris Ajust pH with HCl	48.44 g	0.4 M
AGAROSE	normal melting point NMP NMP LMP PBS w/o Ca^{2+}, Mg^{2+}	100 mg 70 mg 50 mg 10 ml, each	1% 0.7 % 0.5 %

The solutions and buffers prepared for the immunoblotting of proteins are listed in table 10.

Table 10: Buffers and their chemical composition for immunoblotting of proteins

Buffer/Solution	Chemical/Solution	Weighted sample/ Volume
SDS stock solution	SDS 10 % (w/v)	100 g
	aqua dest.	1000 ml
	Storage: RT	
1.5 M Tris-HCl (pH 8.8)	Tris	181.71 g
	aqua dest.	1000 ml
	adjust pH with HCl	
	Storage: RT	
0.5 M Tris-HCl (pH 6.8)	Tris	60.57 g
	aqua dest.	1000 ml
	adjust pH with HCl	
	Storage: RT	
1 M Tris stock solution	Tris	121.14 g
	aqua dest.	1000 ml
	Storage: RT	
1.92 M Glycin stock solution	Glyzin	144.13 g
	aqua dest.	1000 ml
	Storage: RT	
electrophoresis buffer (10 x)	Tris	30.3 g
pH 8.3	Glyzin	144 g
	SDS (10%)	100 ml
	aqua dest.	900 ml
	Storage: + 4°C	
APS solution (10 %)	Ammoniumpersulphat (APS)	100 mg
	aqua dest.	1 ml
	Storage: + 4°C, for 24 h	
Transfer buffer	1.92 M Glyzin	100 ml

	10 % SDS Methanol aqua dest. Storage: 4 hours	2.5 ml 200 ml 672.5 ml
Tris based saline (TBS) (10 x)	NaCl aqua dest. Storage: RT	80 g 1000 ml
Tris based saline (TBS) (1 x)	Tween 20 Storage: + 4°C, for 2 weeks	1 ml
0.1 M Tris pH 8.6	Tris-HCl Aqua dest. Adjust pH with HCl Storage: RT	 1000 ml
Solution A	0.1 M Tris-HCl pH 8.6 Luminol Storage: + 4°C, in the dark	200 ml 50 mg
Solution B	p-hydroxycumaric acid DMSO Storage: RT, in the dark	11 mg 10 ml

3.11 Test substance and controls

- 4-Methylthiobutylisothiocyanate (MTBITC, Erucin)
  MTBITC (purity > 99.9 %) was synthesized by Prof. Dr. Schreiner, Dept. of Organic Chemistry, University of Giessen, Germany. The purity and specificity of MTBITC was verified by NMR and GC-MS/MS analysis. MTBITC was dissolved in sterile DMSO and stored at –80°C.

The following chemicals listed in table 11 were used for experimental setup and positive controls in the experiments.

Table 11: Chemicals used for experimental setup and positive controls. The chemicals were either dissolved in DMSO or distilled water.

Chemical	Cat. No.	Distributor/Source
Benzp(a)pyrene (> 97%)	B-1760	Sigma-Aldrich
Camptothecin	1100	TOCRIS
hydrogen peroxide (30%)	A 0626,025	Applichem
TMPyP4 (> 95%)	613560	Calbiochem
Valinomycin (> 98%)	94675	Fluka

- Dimethyl sulfoxide (DMSO)

  As solvent control either dimethyl sulfoxide (DMSO) or distilled water were used. Both were sterile filtered before use. Since DMSO has been shown to be cytotoxic to complex mammalian cell systems, the effect of the solvent, especially on apoptosis induction and the mitochondrial membrane potential (MMP) of HepG2 cells was tested in preliminary experiments. No alteration of the test parameters could be detected at a concentration of 0.1 % DMSO, which was then used in all further experiments. Noticeably, in concentrations exceeding 0.3 %, alterations in ssDNA formation and an influence on the MMP occurred in the treated cultures.

- Benzo(a)pyrene (B(a)P)

  As positive control for the Comet Assay, the procarcinogen benzo(a)pyrene (B(a)P) was used at a final concentration of 100 µM. This five-ring PAH is classified by the IARC as a probable human carcinogen (2A) and is clearly positive mutagenic in short term assays with metabolic activation. B(a)P has been successfully applied as positive control in genotoxicity studies in the HepG2 model (Mersch-Sundermann et al., 2004).

- Camptothecin (CPT)

  Exposure of cells to 6 µM CPT for 24 h was used as positive control in the apoptosis assays. This plant alkaloid indirectly causes apoptosis by binding to the enzyme topoisomerase I rendering cells to apoptosis induction by the formation of DNA single strand breaks (Capranico et al., 2007).

- Hydrogen peroxide (H_2O_2)

  The measurement of oxidative stress in HepG2 cells was done using 10 µM H_2O_2, incubated for 1 h, as positive control. H_2O_2 has been successfully used earlier in studies investigating the usefulness of DHR123 as probe for ROS detection (Henderson and Chappell, 1993; Royall and Ischiropoulos, 1993). It does not react outside the cell with DHR123, but this reaction only takes place within peroxidase-positive cells (Henderson and Chappell, 1993).

- TMPyP4

  The cationic porphyrin TMPyP4 was used as positive control for telomerase measurement at a concentration of 300 µM. TMPyP4 is able to bind to and stabilize G-quadruplexes in human telomere sequences, resulting in the inhibition of telomerase activity (Grand et al., 2002).

- Valinomycin

  The ionophore valinomycin was used at a concentration of 10 µM in flow cytometric analysis of the mitochondrial membrane potential (MMP). This macrocyclic dodecadepsipeptide possesses high specificity for potassium ions (K^+) and facilitates the movement of K^+ through lipid membranes leading to the breakdown of the mitochondrial membrane potential (Safiulina et al., 2006).

IV. METHODS

4.1 General cell culture

HepG2 cells were supplemented with fresh culture medium every second to third day. The cells were passaged about once a week. All cell treatment steps described in this chapter were carried out with fluids pre-warmed to 37°C.

4.1.1 Cryoconservation & reanimation of the cell culture

HepG2 cells were stored at minus 200°C in liquid nitrogen until use. For cryoconservation, the cells were harvested by trypsination, resuspended in culture medium and pelleted at 700 g, 5 min., RT. The supernatant was decanted and 2 x 10^6 cells/ml resuspended in 1 ml of cryoconservation medium (DMEM containing 15 % FCS and 10 % DMSO). The cell suspension was transferred to a cryo cup and cooled at around 1 °C/min to minus 200°C.
For defrosting, the cells were put into a water bath at 37 °C and subsequently pelleted at 700 g, 5 min, RT. The cells were washed twice with culture medium, resuspended in 5 ml fresh culture medium and transferred to a T25 culture flask for cultivation. 24 h later, the medium was refreshed to remove dead cells.

4.1.2 Cell culture and passage

Subconfluent cell cultures were harvested by trypsination: adherent HepG2 cells were washed twice with PBS and incubated with a 0.1 % trypsin-EDTA-solution for 4 min at 37°C. The enzymatic reaction was stopped with culture medium and the cell number/vitality determined by erythrosine B staining and counting in a Neubauer chamber. An appropriate amount was then transferred to a new culture flask and incubated in a cell culture incubator at standard conditions (95 % humidity, 5 % CO_2, 37°C).

4.1.3 Procedure of chemical exposure

For chemical exposure, HepG2 cells were seeded in T25 culture flasks at a density of 1-2 x 10^6 cells or 96 -well plates at a density of 1 x 10^4 cells. Exponential growing cells were then treated with the chemicals for the indicated time points.

4.2 Assessment of cell proliferation and viability

Cytotoxicity can occur in the inner of a cell without disturbing the cellular membrane; therefore, a sensitive marker of enzymatic activity was used for the detection of cell growth. Cellular damage inevitably results in loss of the ability of the cell to maintain and provide energy for metabolic function and growth. This reduction in metabolic activity can be detected with the WST-1 assay. WST-1 is a tetrazolium salt which is cleaved to formazan by cellular enzymes. Recent studies support the assumption that WST-1 is reduced extra-cellular or at the plasma membrane by a mechanism involving superoxide (Berridge et al., 1996). An expansion in the number of viable cells results in an increase in the overall activity of mitochondrial dehydrogenases in the sample. This augmentation in enzyme activity leads to an increase in the amount of formazan dye formed, which directly correlates to the number of metabolically active cells in the culture. The formazan dye produced is then quantified by a scanning multiwell spectrophotometer (ELISA reader) by measuring the absorbance of the dye solution at 405 nm.

The assay was carried out with a kit from Roche, according to the manufacturers´ instructions. The appropriate cell concentration and incubation time of WST-1 was determined in preliminary experiments. This was particularly of importance since the mitochondrial activity varies considerably between cell types and cell number. A 1 h-incubation of cells with WST-1 resulted in the best signal intensity permitting the observation of a change in cell proliferation over 100 orders of magnitude. For further experiments, a number of 1 x 10^4 cells/100 µl were used. The assay was carried out three times in triplicate.

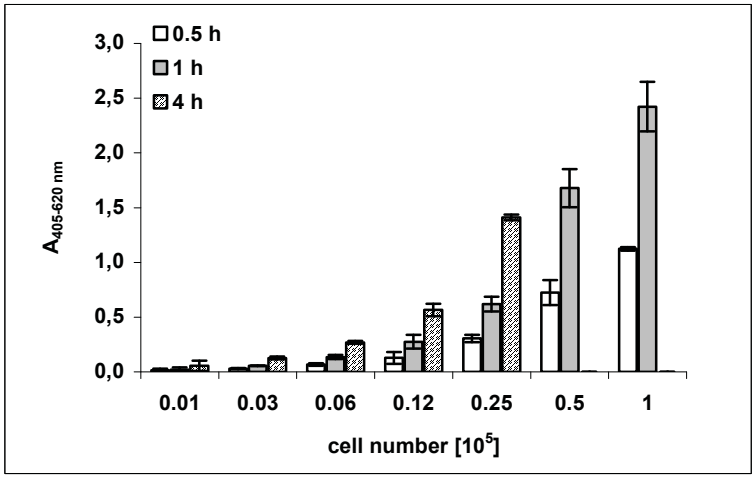

Figure 2: Kinetics of the metabolism of WST-1 in HepG2 cells. The cells were grown at the indicated cell number for 24 h and then incubated with 10 µl WST-1 for 0.5 to 4 h. Absorbance at 405 nm (reference 620 nm) was determined in an ELISA reader. The bars represent the mean of three independent experiments ± standard deviation.

4.3 Techniques for the assessment of apoptosis induction

A first estimation of apoptosis induction by MTBITC was obtained with the DNA laddering assay, and the measurement of the "subG1" DNA content. For quantification of apoptosis induction and as a more specific marker, the ELISA-based detection of single stranded apoptotic DNA was carried out. The assessment of apoptosis induction with different methodologies is important for the verification of the results since the degree of DNA degradation to oligo- or mononucleosomal-size fragments does not always take place during apoptosis or varies in a broad range, depending on the stage and pathway of apoptosis, cell type and often the nature of the apoptosis-inducing agent.

4.3.1 DNA degradation by internucleosomal fragmentation (DNA laddering)

During apoptosis, a series of morphological visible reorganisations occur in the cell: chromatin condensation, loss of cell volume and membrane blebbing. In parallel to that, DNA fragmentation occurs in the majority of cells, representing a biochemical hallmark of apoptosis. An endogenous Ca^{2+}, Mg^{2+}-dependent endonuclease is believed to be responsible for DNA cleavage, breaking double stranded DNA at internucleosomal sites (Golstein et al., 1991). Therefore, apoptotic DNA cleavage results in the formation of characteristic fragments of oligonucleosomal size (180-200 bp). This observation was first described by Wyllie (Wyllie, 1980). Qualitative determination of DNA fragmentation can be visualized by agarose gel electrophoresis analysis. Treated samples were harvested by scraping and washed twice with PBS before lysing with 600 µl of lysis buffer for 15 min on ice. Next, the cell debris was spun down by centrifugation at 15.000 g, 15 min, 4°C and the DNA- containing supernatant transferred to a 2 ml eppendorf cup. The solution was treated with 20 µl RNAse (Dnase free) for 1 h at 37°C and subsequently with 30 µl Proteinase K for another hour at 50°C. Then, the DNA was precipitated by addition of 600 µl of 100 % 2-propanol and 20 µl of 5 M NaCl. A DNA pellet was derived by another centrifugation step (15.000g for 30 min at 4°C), the supernatant decanted and the DNA washed with 70 % ethanol. After decanting, the purified DNA pellet was dried for 10 min at RT and finally the DNA was dissolved in 50 µl TE Buffer, supplemented with loading buffer at a final concentration of 1 x and loaded onto a 2 %-agarose gel. 20 µg of a 100 bp marker were taken as reference for the laddering. The voltage was set to 50 V for 30 min and then set to 100 V for another 3 h. The detection of the ladder was carried out by staining of the gel with an ethidium bromide solution (10 µg/ml) for 20 min and subsequent detection under UV light.

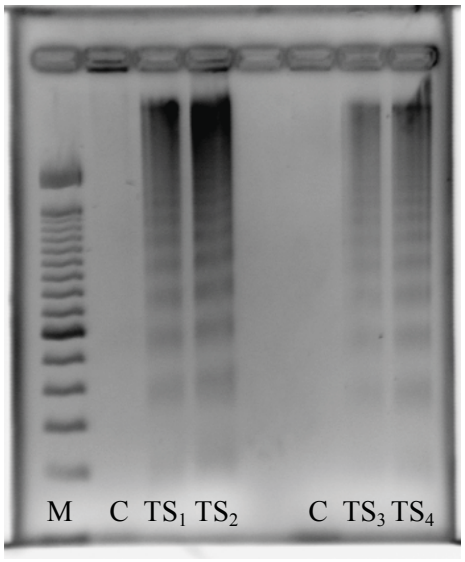

Figure 3: Experimental setup of the DNA laddering assay by CPT-treatment of HepG2 cells. Induction of internucleosomal DNA fragmentation was detected after treatment of HepG2 cells with 6 µM CPT for 24 h. The fragmented DNA was separated in a 2 % agarose gel and stained with 10 µg/ml ethidium bromide. (M= DNA 100 bp marker, C= a.d. treated cells; TS_1 & TS_3 = 2 x 10^6 cells, treated with CPT; TS_2 & TS_4 = 4 x 10^6 cells, treated with CPT. High salt alcoholic precipitation of DNA was conducted immediately (TS_1 & TS_2) or overnight (TS_3 & TS_4).

4.3.3 Measurement of the subG1 DNA content

In a first approach to quantify apoptosis induction by MTBITC, the cellular DNA content was measured after permeabilization of HepG2 cells by fixation with 70 % ethanol. Since the alcohol fixation does not fully preserve highly degraded DNA within the apoptotic cells, this fraction of DNA leaks out during subsequent cell rinsing with aequous solutions. As a consequence, apoptotic cells containing only fractional DNA can be identified on a DNA content frequency histogram as cells being less stainable than G1 cells, the generally called “sub-G1” or “hypoploid” peak. (Gong et al., 1994; Kajstura et al., 2007). The threshold of DNA detection was set at a constant level of $1/10^{th}$ to $1/20^{th}$ of the fluorescence value of intact G1 cells. This methodology is proposed by Darzynkiewicz and co-workers (Darzynkiewicz et al., 2001) to eliminate all particles with a DNA content of less than 10 or 5 % of that of G1 cells from the analysis which might not be of apoptotic origin. HepG2 cells were seeded in T25 culture flasks at a density of 1 $\times 10^6$ cells in 5 ml of culture medium. Exposure of the test substance MTBITC at a final concentration of 20 µM for 1-24 h was carried out at exponential growth. After test substance treatment, HepG2 cells were harvested by trypsination, washed twice with PBS and subsequently fixed with 2 ml of 70 % ice cold ethanol for 24 h at 4°C. After fixation, the cells were again washed with PBS two times, the cell pellet was subsequently resuspended in PI master mix (PBS, 40 µg/ml propidium iodide, 100 µg/ml Rnase (Dnase free)) at a final density of 0.5×10^6 cells/ml and incubated for 30 min at 37 °C before analysis by flow cytometry in an FL-2 histogram. Quantification of the “sub-G1” DNA peak was done with the software Modifit© LT, UK.

4.3.5 Measurement of single stranded, formamide denatured apoptotic DNA (ssDNA assay)

It was shown in earlier studies that the staining of ssDNA with a monoclonal antibody is a sensitive and specific marker for the identification of apoptosis in adherent cells and is especially suitable to identify early stages of apoptosis (Frankfurt and Krishan, 2001a; Zhao et al., 2003). The monoclonal antibody used in this assay reacts with a homopolymer of deoxythimidine and requires a large stretch of at least 25-30 bases in length to bind to ssDNA. Therefore, the antibody does not react with single-stranded DNA ends, which is a great advantage compared to e. g. the TUNEL assay. Because it is this detection of ssDNA ends, present in necrotic cells, which is responsible for the non-specificity of the TUNEL assay. Additionally, under the applied gentle denaturation conditions i.e. heating to 75°C of formamide-treated samples, DNA denaturation neither occurs in necrotic nor in viable cells with DNA breaks, but only in the apoptotic cells (Allera et al., 1997). Changes in DNA-histone interactions in condensed chromatin of apoptotic nuclei are likely to be responsible for this effect. Whereas the phosphorylation of H3 results in tight chromatin condensation in mitotic nuclei, the deacetylation of H3 and H4 during apoptotic chromatin condensation decreases the affinity of histones to DNA, which is then readily denatured under these contitions (Frankfurt and Krishan, 2001b).

The assay was carried out as described by the manufacturer with slight modifications. Briefly, 1 x 10^4 cells were seeded into a 96-well plate and exposed to the test substance at exponential growth. After centrifugation of the plate (1000 g, 5 min. 4°C), the medium was removed and the cells fixed with 200 µl of 80 % methanol (30 min at RT) in the wells. The cells were attached to the plate surface by thorough drying at 37°C and the apoptotic DNA denatured by the addition of 50 µl of formamide for 10 min at RT and subsequent heating to 75°C for 20 min. The plate was cooled down, the formamide removed and the cells washed with PBS three times before adding 200 µl of 5 % nonfat dry milk for blocking of unspecific binding sites for 1 h at 37°C. The blocking solution was then substituted by 100 µl of antibody solution consisting of a mixture of primary antibody and secondary enzyme-conjugated antibody and incubated for another 30 min. Before the addition of ABTS solution for colour development, the cells were washed three times with the supplied washing solution for 30 s, each. The reaction was terminated by addition of an equal volume of stop solution (sulphuric acid) and the absorption detected at 405 nm with a reference of 690 nm in an ELISA reader. Confirmation of the specificity of the monoclonal antibody binding was achieved by digesting DNA of untreated HepG2 cells with S1

nuclease (10 U/µl, 30 min, 37°C) in a single stranded conformation. For an internal assay positive control, wells were coated with 100 µl of solution containing 0.3 µg/ml of ssDNA. The assay was carried out three times in triplicate.

4.4 Measurement of the cell cycle distribution of HepG2 cells

DNA content analysis also provides information about the cell cycle phase of the non-apoptotic cells and can be applied to investigate the cell cycle specificity of apoptosis (Darzynkiewicz et al., 1997). The software Modifit© LT was likewise used here to deconvolute the DNA frequency histograms to estimate the proportions of cells in particular phases of the cell cycle. The cells were treated and prepared for analysis as described in chapter 4.3.3. An example of the software supported cell cycle analysis is given in figure 4.

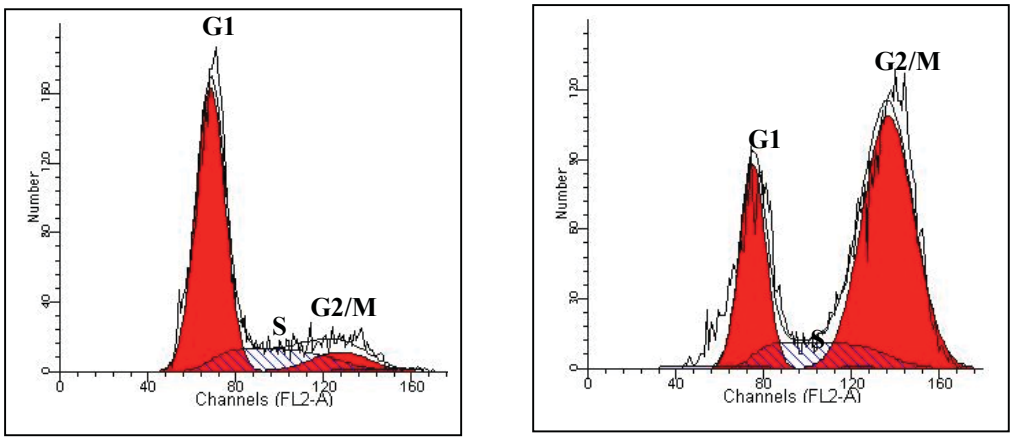

Figure 4: Cell cycle analysis of HepG2 cells. a) DMSO-treated and b) 20 µM MTBITC-treated cells analysed for their DNA content distribution after 24 h. The analysis was conducted with the software Modifit. A clear accumulation of cells at the G2/M phase can be seen after treatment with 20 µM MTBITC for 24 h.

4.5 Detection of DNA damage by the Comet assay

The single cell gel electrophoresis assay (SCGE; Comet assay) detects DNA damage and DNA repair on the single cell level by electrophoretic separation of DNA fragments (Singh et al., 1990; Tice et al., 1990). The cells are lysed and separated by an electrophoretic field. After electrophoresis and staining of the DNA with ethidium bromide, the migrated DNA resembles a comet tail, the non-migrated DNA the head, hence the naming. Depending on the experimental conditions, i.e. the pH, the comet assay detects single or double strand breaks as well as alkali labile sites and DNA crosslinks.

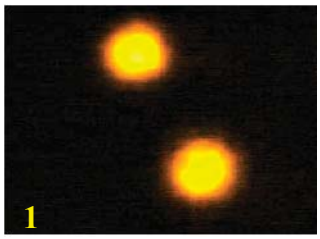

Figure 5: DNA migration of HepG2 cell in the Comet assay. 1) HepG2 cells after treatment with 0.1 % DMSO. The cells are round no DNA migration is visible after alkaline lysis, electrophoresis and fluorescence staining with ethidium bromide (magnification 400 x)

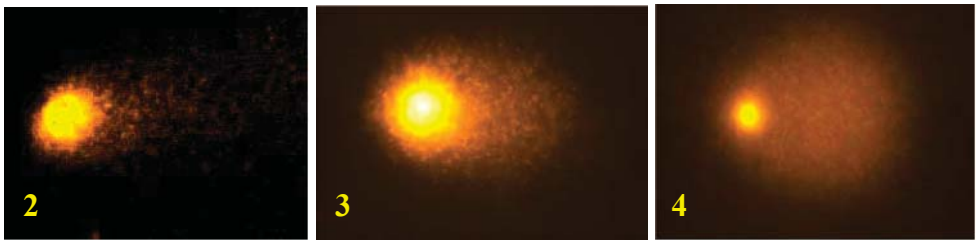

2 to 4) HepG2 cells after treatment with B(a)P in a concentration range of 25 µM, 50 µM or 100 µM for 24 h. Images were made after alkaline lysis, electrophoresis and fluorescence staining with ethidium bromide (magnification 400 x)

So far, a large number of DNA damaging agents have been evaluated with the comet assay (see for reference Fairbairn et al., 1995; Faust et al., 2004; Knasmuller et al., 2004; Mersch-Sundermann et al., 2004; Rojas et al., 1999; Tice and Strauss, 1995). The comet assay is highly sensitive and enables the detection of only a few hundred breaks per cell (Collins et al., 1997).

Fully frosted slides were cleaned with ethanol/aceton-solution (v/v 1: 1). Next, they, were covered with two layers of normal melting point (NMP) agarose (1st layer 1 %, 2nd layer 0.7) and solidified at 4°C for 15 min. 3 x 10^5 cells were seeded in a 12- well plate and exposed to the test substance at exponential growth for 1 h. After harvesting, the cells were

mixed with 100 µl of 0.5 % low melting point (LMP) agarose and layered on top of the slide. After solidification at 4°C, the cells were lysed at pH 10 for 1 h at 4°C, treated with unwinding buffer for 20 min and subsequently electrophoresed at pH 13 for 25 min at 300 mA, 25 V. After electrophoresis, the cells were incubated in neutralization buffer (pH 7.5) for 10 min and washed with distilled water. Directly before analysis, the cells were stained with 10 µg/ml ethidium bromide. Analysis was performed with a CCD camera, connected to a fluorescent microscope (excitation wavelength 254 nm) and an image analysis system (Optilas inc.); densitometric evaluation was carried out with the software Comet 5.5 (Optilas, Germany). The parameter olive tail moment (OTM) was used for the description of the results. It was calculated as follows:

$|m_K m_S|$ x $DNA_{Tail,}$ wheras $|m_K m_S|$ = Distance between mass-center of comet head to mass-center of comet tail.

4.6 Analysis of the mitochondrial membrane potential (MMP)

Disruption of the MMP precedes the gross morphological changes associated with apoptosis. It is reported that this effect comes before activation of the caspase cascade and phosphatidylserine transposition. But it presents a point just beyond final commitment. The MMP is generated by production of energy using the mitochondrial respiratory chain. This energy drives ATP synthesis and is stored as an electrochemical gradient consisting of a transmembrane electrical potential, negative inside of about 180-200 mV, and a proton gradient of about 1 unit. Loss of the MMP, which presents one part in the permeability transition process, involves redistribution of ions resulting in the loss of the net negative charge of the matrix.

For detection of changes in the MMP at the single cell level, the lipophilic cation 5,5',6,6'-tetrachloro-1,1',3,3'-tetraethylbenzimidazolcarbocyanine iodide (JC-1) was used. This probe enters selectively into mitochondria and is capable of changing reversibly the colour from green to orange, depending on the polarization of the mitochondrial membrane (over values of about 80-100 mV). Consequently, a decrease in the red/green fluorescence intensity ratio indicates mitochondrial depolarization.

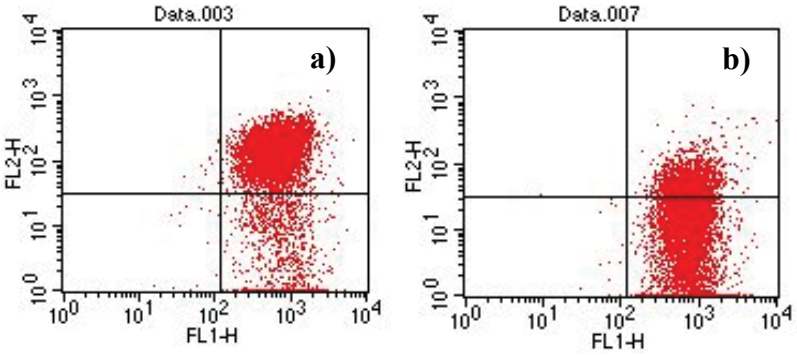

Figure 6: Analysis of the mitochondrial membrane potential. Scatter blot of a) polarized mitochondria (high FL1, high FL2) after treatment of HepG2 cells with 0.1 % DMSO and b) valinomycin-induced depolarization of mitochondria (higher FL1, lower FL2) in HepG2 cells, as revealed by staining with JC-1. The red/green fluorescent ratio decreases if the MMP drops.

After exposure to MTBITC, the cells were harvested by trypsination, washed twice with PBS and resuspended in 1 ml of culture medium prewarmed to 37°C supplemented with the probe JC-1 at a final concentration of 2.5 µg/ml. The pH of the samples was carefully checked to be at 7.4 since the formation of J-aggregates is very sensitive to this parameter. The samples were gently vortexed and incubated under cell culture conditions for 30 min. Afterwards, the cells were again washed two times with ice cold PBS. Then they were finally resuspended in 500 µl PBS and directly analysed by a FACSCalibur in FL-1 and FL-2 (BD, USA). A concentration of 10 µM valinomycin was used as positive control.

4.7 Detection of reactive oxygen species by DHR123

Altered activity of free-radical process in cell systems is associated with cell signalling and apoptosis induction. As shown in earlier studies, reactive oxygen species, including hydrogen peroxide (in the presence of peroxidase or cytochrome c) and peroxynitrite can be detected by dihydrorhodamine 123 (DHR123) (Henderson and Chappell, 1993; Kooy et al., 1994). DHR123 enters readily into most of the cells and is oxidized to the fluorescent product form rhodamine 123, a positively charged lipophilic compound, which is sequestered intracellularly (Johnson et al., 1980). Rhodamine 123 will preferentially accumulate within mitochondria to a marked degree with little loss to the extracellular space. It has been reported that DHR 123 establishes stable intracellular concentrations within 15 min and intracellular levels remain stable for at least 1 h as long as there is continued presence of probe in the extracellular medium (Royall and Ischiropoulos, 1993).

DHR123 was dissolved in DMSO at a concentration of 5 mM. The stock solution was purged, covered with a layer of N_2 and stored at –20°C in the dark until use. For the experiments, DHR123 was diluted in culture medium w/o phenol red to a final concentration of 5 µM. Before test substance-exposure, HepG2 cells were incubated with a final concentration of 5 µM DHR123 in culture medium w/o phenol red for 15 min in the dark and afterwards exposed to MTBITC. Fluorescent intensity due to the conversion of DHR123 to the fluorescent DHR was measured with an ELISA reader (Infinite M200, Tecan, Austria) at an excitation wavelength of 500 nm and an emission wavelength of 536 nm. HepG2 cells incubated with 5 µM DHR123 were used as background control to detect spontaneous oxidation of DHR123 to rhodamine 123. For correction of autofluorescence, every measurement was paralleled by a set of the same samples lacking DHR123 incubation. The assay was carried out three times in triplicate.

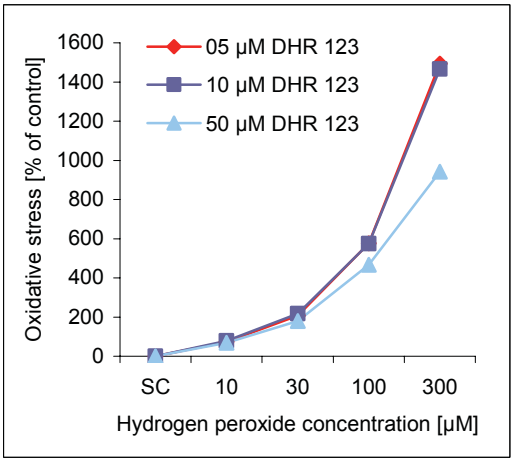

Figure 7: Production of reactive oxygen species (ROS) determined by the conversion of DHR123 to the fluorescent RH123. For experimental setup, HepG2 cells were incubated with DHR123 at different concentrations of 5 µM, 10 µM or 50 µM for 15 min and subsequently exposed to H_2O_2 in a concentration range of 10 to 300 µM for 1 hour. To determine the optimal concentration of DHR123, 5 to 50 µM of the reagent were added to the treated cells which were then analysed for the production of ROS. Fluorescence of hydrogen peroxide-treated HepG2 cells was measured with an ELISA reader (Ex: 500 nm, Em: 536 nm), SC = distilled water (N = 2).

4.8 Determination of the glutathione status

The tripeptide γ-glutamylcysteinylglycine or glutathione (GSH) is widely distributed in cells and has been shown to participate in a multitude of cellular functions. GSH serves as a nucleophilic co-substrate to glutathione transferases in the detoxification of xenobiotics and many of these functions are associated with protection against reactive intermediates, including free radicals and electrophiles. The maintenance of a suitable thiol-redox-balance with low-molecular weight and protein thiols is also crucial for cellular homeostasis.

Glutathione content of HepG2 cells was measured with a kit from Cayman, Germany. The assay is based on the reaction of the sulfhydryl group of GSH with 5.5′-dithiobis-2-nitrobenzoic acid (DTNB) to the yellow coloured 5-thio-2-nitrobenzoic acid (TNB). The rate of the TNB produced is thus directly proportional to the concentration of GSH in the samples. Since the oxidized form GSSG is easily reduced to GSH by the provided GSH reductase, the total glutathione content of the cells is measured. The samples were harvested by scraping with a rubber policeman and washed twice with PBS. After centrifugation (700 g, 5 min, 4°C) the supernatant was decanted and the cells resuspended in 300 µl PBS and subsequently lysed on ice by sonication (set to impulse, 50 sec). The lysate was centrifuged (10.000 g, 20 min. 4°C) and 250 µl of the GSH containing supernatant deproteinated with 10 % MPA reagent in a new eppendorf cup. Therefore, the sample was mixed with MPA 1:1, vortexed and incubated at RT for 5 min before centrifugation (5000 g, 5 min, 4°C). The supernatant was transferred to a new eppendorf cup and stored at –20°C until assaying. For assaying, all reagents were pre-warmed to RT before use. In order to increase the pH of the samples, 5 µl of TEAM reagent were added to 100 µl of sample and immediately vortexed. The provided GSSG standard was diluted as described in the manual to cover a concentration range of 0 to 8 µM GSH. 50 µl of the standards or the samples were transferred into a 96well plate and 150 µl of freshly prepared assay cocktail consisting of 102 µl MES buffer, 4 µl cofactor mix, 19 µl enzyme mix, 20.9 µl aqua dest. and 4 µl DTNB added to each sample. The plate was shaken in the ELISA reader for 30 sec and measured at 5 min intervals for 30 min at an absorbance of $A_{410\text{-}690\ nm}$. The results were calculated by comparison with the generated standard curve. A representative GSH standard curve is given in figure 8. The assay was carried out two times in triplicate.

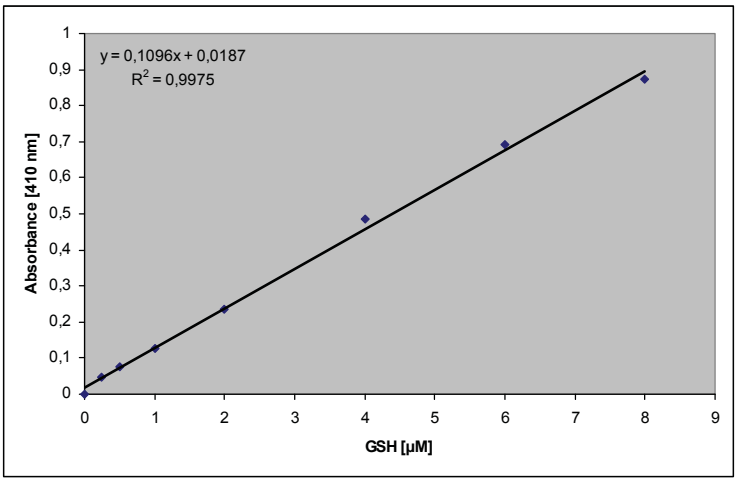

Figure 8: GSH standard curve covering a range of 0 to 8 µM.

4.9 Telomerase activity measurement by TRAP-ELISA

Telomerase activity was detected by a photometric enzyme immunoassay, commercially available from Roche. This assay utilizes the polymerase chain reaction (PCR)-based telomeric repeat amplification protocol (TRAP) and ELISA assay for semi-quantitative determination of telomerase activity (Wright et al., 1995). In the first step, telomerase adds telomeric repeates to the 3´end of a biotinylated telomerase substrate oligonucleotide. After terminating the telomerase activity, the extended products are amplified by PCR reaction using Taq polymerase. This extension generates a ladder of products with 6 base increments detectable with a 12 % PA-gel and staining with SYBRgold. During the ELISA assay, the labelled products are immobilized onto a streptavidin-coated microtiter plate via biotin-streptavidin-interaction and detected by an antibody conjugated to HRP. The amounts of TRAP products is determined by means of the HRP activity using the substrate 3,3`,5,5`-tetramethylbenzidine (TMB) and subsequent colour development. The assay was carried out according to the manufacturers´ instructions with slight modifications. The samples were harvested with a rubber policeman and lysed with 200 µl of the provided lysing buffer for 15 min on ice before centrifugation (16.000 g, 30 min., 4°C).

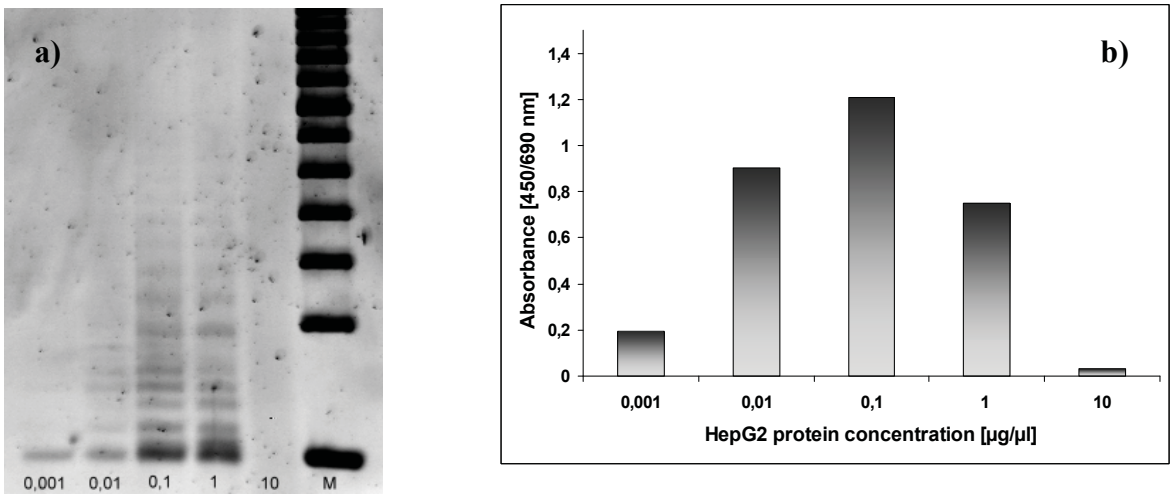

Figure 9: Titration of HepG2 protein concentration (0.001 to 10 µg) for telomerase detection by the TRAP assay, a) qualitative detection after gel electrophoretic separation of the PCR products by an 12 % AA gel and SYBRgold staining b) detection of telomerase activity by ELISA reaction at an absorbance of $A_{405 - 690}$ nm.

175 µl of the supernatant were transferred to a new eppendorf cup, shock frozen in liquid nitrogen and stored at –80 °C until use. 0.05 µg of sample were set to a volume of 25 µl with DEPC-treated distilled water and mixed with 25 µl of the provided reaction mixture containing the biotinylated telomerase substrate P1-TS, the optimized anchor-primer P2, nucleotides and Taq DNA polymerase. For background correction, an aliquot of each sample, containing the same amount of protein was treated with 0.1 µg/µl RNase (DNase free) and incubated at 37°C for 20 min. An equal volume of lysis solution served as reagent control. PCR settings were as follows:

Step	Time [s]	T [°C]	No of cycles
Primer elongation	1800	25	
Telomerase inactivation	300	94	
Amplification			
Denaturing	30	94	
Annealing	30	50	30
Synthesizing	90	72	
	600	72	
Storage		4	

For the qualitative analysis of telomerase activity, 30 µl of the PCR product were mixed with loading buffer and loaded onto a 12 % acrylamide gel in 1 x TBE buffer. The current

was set to 50 V for 30 min and then to 190 V for 3 h. After electrophoresis, the gel was stained with SYBRgold solution in 1 x TBE for 20 min and then detected under UV-light. 10 µg of a 50 bp DNA size marker were run in each gel. For ELISA detection, 2.5 µl of the amplification product were mixed with 10 µl of denaturation reagent and incubated at RT for 10 min. Then, 100 µl of hybridization solution was added and incubated for 2 h at 37°C at 300 rpm on a minishaker. The supernatant was removed, the wells were washed three times with 250 µl of washing buffer for 30 sec. each and 100 µl anti-DIG-HRP working solution was added to each sample for 30 min at RT while shaking. The solution was removed and the wells were washed 5 times with 250 µl of washing buffer for 30 sec. each before addition of 100 µl of TMB substrate to each well for colour development. The reaction was stopped after 2 min by 100 µl of stop reagent producing a change in colour from blue to yellow. The absorbance of the samples was detected at $A_{450\text{-}690nm}$ with an ELISA reader (Infinite M200, Tecan).

The TRAP-ELISA assay was optimized by titration of the protein concentration in the range of 0.001 µg to 10 µg to determine the linear range of the PCR reaction and to minimize the influence of PCR inhibitors. Figure 10 displays the results of the titration experiments. A concentration of 0.05 µg protein was used for all further experiments. Experimental setup was then carried out by the treatment of HepG2 cells with TMPyP4 in a concentration range of 30 to 300 µM for 24 h and processed as described in this chapter. The results of the experimental setup are summarized in figure 10.

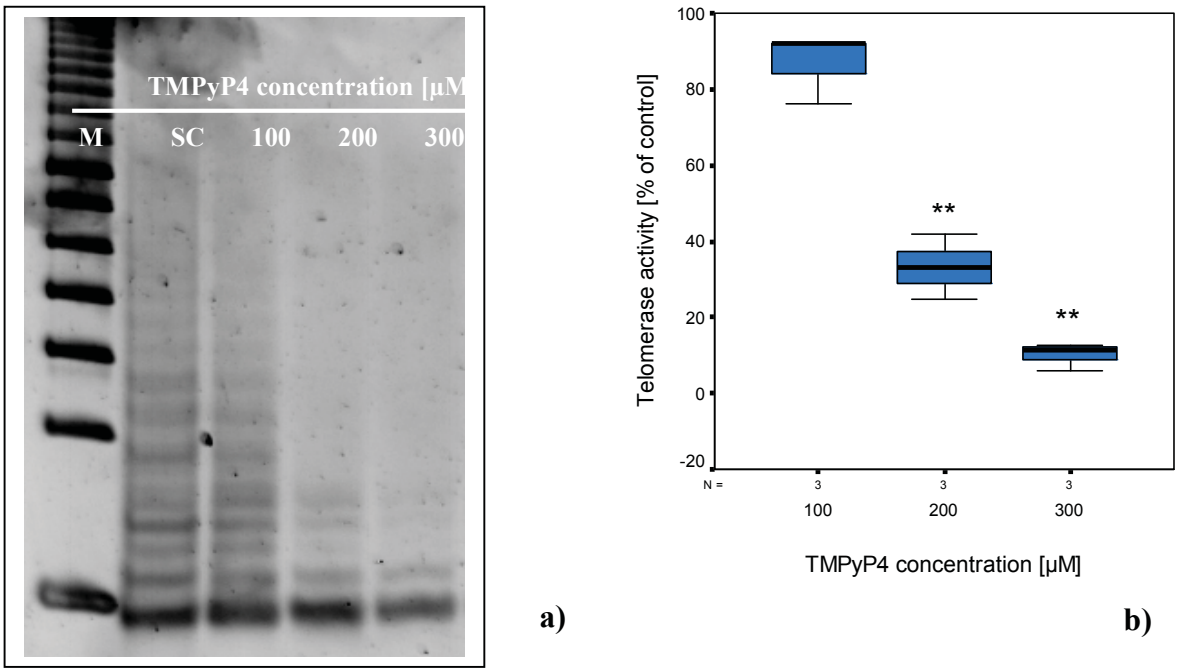

Figure 10: Experimental setup of telomerease measurement with TMPyP4. Suppression of telomerase activity by TMPyP4 was detected after 24 h-treatment of HepG2 cells in the TRAP assay. The cells were exposed to TMPyPy in a concentration of 100 to 300 µM and subsequently prepared as described above. a) qualitative detection after gel electrophoretic separation of the PCR products by an 12 % AA gel and SYBRgold staining b) detection of telomerase activity by ELISA reaction at an absorbance of $A_{405\text{-}690}$ nm. The experiments were performed three times. SC: solvent control = 0.1 % DMSO.

4.10 Telomere length assessment by flow-FISH

Telomere length was determined by flow-FISH methodology using the Telomere PNA kit/FITC from Dako, Denmark (Cat no. K5327). The assay is based on labeling telomeres by introduction of synthetic, fluorochrome-tagged peptide nucleic acid (PNA) probes that mimic the DNA sequences complimentary to the telomere sequence ($(CCCTAA)_3$). These PNA probes have been shown to be very reliable for FISH analysis of telomere length (Baerlocher et al., 2002; Lauzon et al., 2000; Law and Lau, 2001). Rufer et al. (Rufer et al., 1998) have established an empirically determined association between the approximate number of telomere repeats, PNA probe binding and fluorescence. However, for each flow cytometer, a calibration for the number of non-covalently bound PNA probes per telomere repeat has to be carried out to be linked directly to internal fluorescence value (Kapoor and Telford, 2004).

At the beginning and end of each measurement, the FACS system was calibrated and checked for linearity using molecules of equivalent soluble fluorochrome (MESF)

Quantum™ FITC beads (low) (Polyscience, Germany) to accurately quantify telomere length (i. e. number of telomere repeats) by correlating a specific fluorescence intensity value with an actual number of fluorochrome molecules which in consequence correlates with the number of PNA probes bound. Statistical analysis was carried out by the setting of markers, defining the „mean fluorescent intensity"(MFI) compared to the total event number with the software Cellquest pro (see figure 11). The MFI is a measure for the amount of bound fluorescence dye per particle. As an internal control the human T-cell CCRF-CEM leukaemia line was used (DSMZ, Germany), known for their long telomeres (Foley et al., 1965). This cell line was established from the peripheral blood of a 3-year old Caucasian girl with acute lymphoblasic leukaemia at relapse in 1964. The cells were grown in RPMI medium supplemented with 2 mM L-glutamine and 10 % FCS in a 5 % CO_2-atmosphere with 95 % humidity at 37°C.

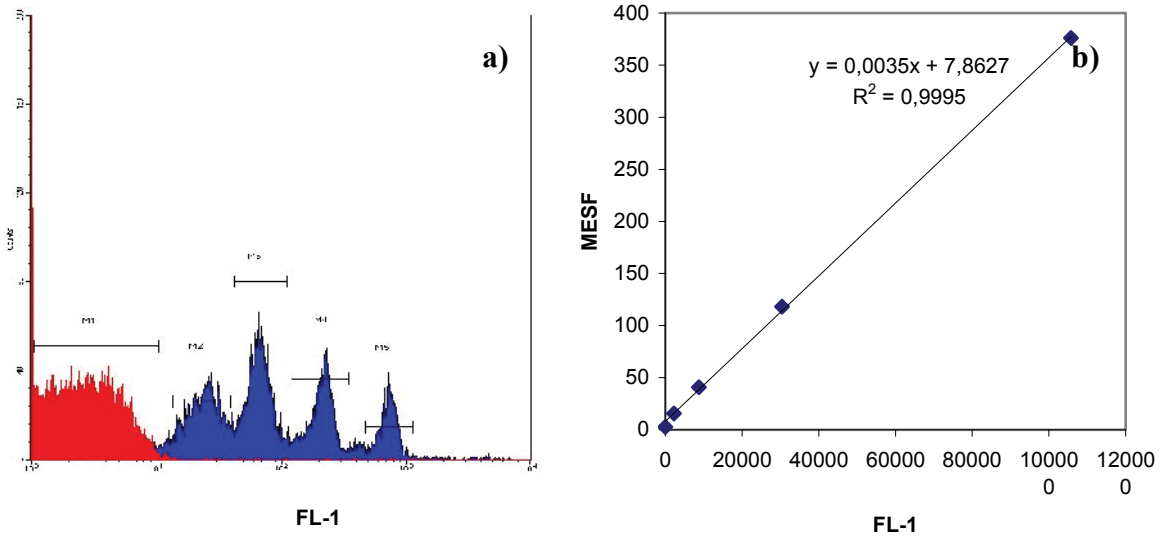

Figure 11: a) Analysis of the MESF beads in the FL1 channel and defining the mean fluorescence intensitiy (MFI) values for the background (red coloured peak) and the FITC-stained particles (blue coloured peaks) b) conversion of MFI to MESF values and generation of the calibration curve

The samples were harvested by trypsination and washed twice with PBS, containing 0.1 % FBS. A sample containing 1 x 10^6 HepG2 was incubated with 300 µl hybridization solution with telomere PNA probe at a final concentration of 0.3 µg/ml. For correction of auto-fluorescence, an aliquot of the same sample was incubated with hybridisation solution containing no probe. The samples were denatured at 82°C for 10 min and subsequently hybridized for 12 h in the dark at RT. The cells were then washed twice by adding 1 ml of the provided washing solution and incubation for 10 min at 40 °C. After the washing step,

the DNA was stained with 0.5 ml staining solution for 3 h at 4°C and the samples subsequently analyzed in a FACSCalibur (BD, USA). 2 x 10^6 CCRF-CEM cells were processed as described above and used as internal control. For selection of the single cell population the cells were analyzed in FL3-A and FL3-W. The selected cells were then displayed in FSC vs. FL3-H dot plot. For calculation of the relative telomere length (RTL) per genome equivalent, cells in the G0/1-phase of the cell cycle were identified (see figure 12). All fluorescence compensation was set to zero and the FITC detector was left at the same voltage as that used for the MESF beads.

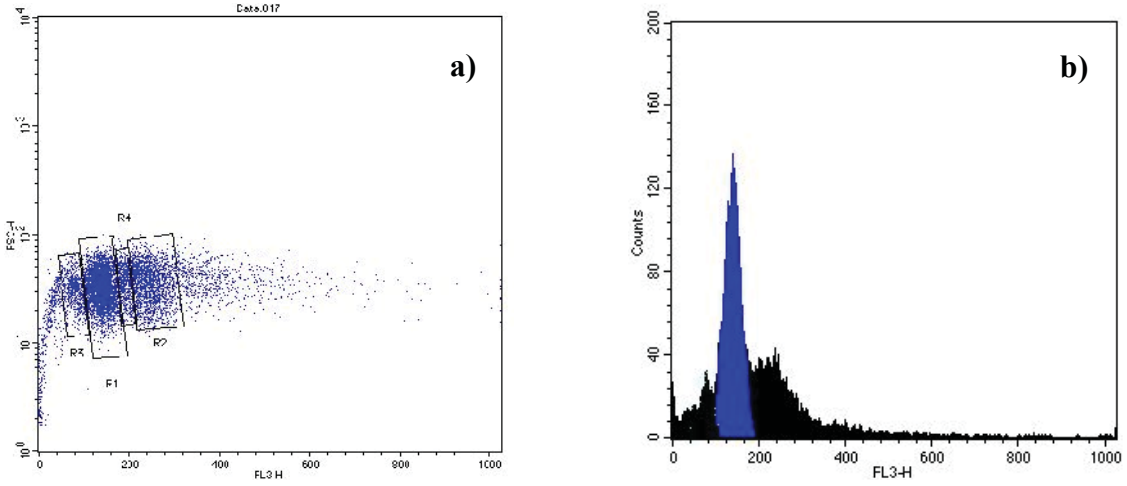

Figure 12: a) Scatter gating of the G0/1-phase (R1) in the analysis of the cell cycle distribution of HepG2 cells after PI staining. The forward-angle light scatter (FSC) is plotted against FL3 b) verification of the gated G0/1-phase cells (blue coloured peak) in a DNA histogram. Only G0/1-phase cells were used for further telomere length analysis.

The RTL value was calculated in relation to the telomere length of CCRF-CEM control cells by the following equation:

$$\text{RTL (\%)} = \frac{\text{(mean MESF sample cells with probe – mean MESF sample cells w/o probe)}}{\text{(mean MESF control cells with probe – mean MESF control cells w/o probe)}} \times 100$$

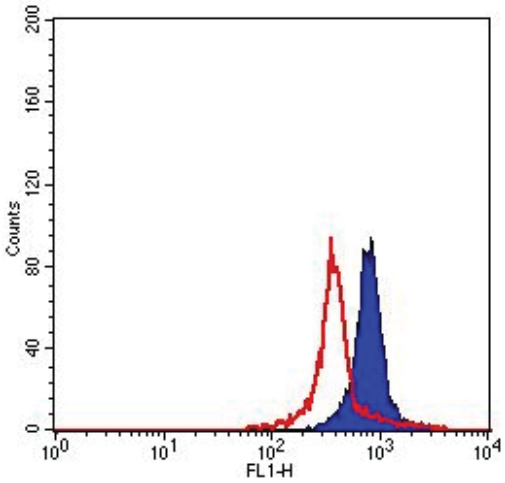

Figure 13: FITC histogram of G0/1-phase HepG2 cells hybridized to the telomere specific PNA probe (blue coloured peak) and the autofluorescence signal of PNA probe-negative HepG2 cells (red coloured line)

4.11 Protein analysis by immunoblotting

Proteins were analysed by immunoblotting, also referred to as western blotting after a modified protocol by Burnette (Burnette, 1981). This methodology uses sodium dodecyl sulfate polyacrylamide gel electrophoresis (SDS-PAGE) to separate native proteins by their molecular weight. Sampled proteins become covered in the negatively charged SDS and move to the positively charged electrode through the acrylamide mesh of the gel. Smaller proteins migrate faster through this mesh and the proteins are thus separated according to size. The so separated proteins are then transferred out of the gel onto a nitrocellulose membrane where they are probed using antibodies specific to the protein.

Treated samples were harvested with a rubber policeman and washed twice with cold PBS. After final washing, the cells were chemically lysed with 200 µl of Cellytic M for 30 min on ice, the cellular debris separated from the proteins by centrifugation (16.000 g, 30 min. 4°C) and 175 µl of the supernatant, containing the proteins, transferred to a new eppendorf cup. The aliquoted samples were shock frozen in liquid nitrogen and stored at –80°C until use. Protein concentration was determined after the modified method of Bradford (Bradford, 1976) as described in chapter 4.12. For immunoblotting, the samples were thawed on ice and 20 µg of protein mixed with ready made SDS-containing sample buffer, supplemented with DTT at a final concentration of 0.12 mM. Electrophoresis was performed according to the method of Laemmli (Laemmli, 1970). The samples were heated to 60 °C for 5 min and then cooled on ice for 5 min before loading onto a 10 % or 15 % discontinuous PA-gel dimensioned 9 x 6 cm. The current was first set to 1 V/cm for 30 min and then to 2 V/cm for 60 min. The gel was then transferred to a nitrocellulose membrane by semi-dry or wet blotting (0.7 mA/cm^2, 90 min.) and blocked with 5 % BSA

or milk powder in TBS/T for 24 h. After blocking, the membrane was incubated with 2 ml of primary antibody diluted in TBS/T containing 5% BSA for 1 to 24 h at 4°C, then washed three times with cold TBS/T for 5 min and subsequently incubated with a horseradish peroxidase (HRP)-labeled secondary antibody for 1 to 24 h. After antibody incubation, the membrane was washed again three times with cold TBS/T and detected with a chemiluminescent agent (2 ml of solution A, 0.6 µl hydrogen peroxide (30%) and 200 µl of solution B) producing luminescence in proportion to the amount of protein.

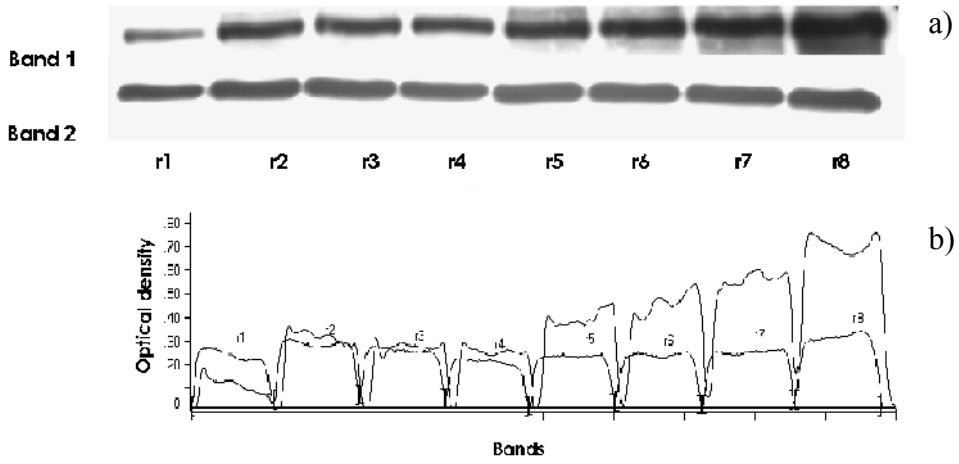

Figure14: Densitometric analysis of western blots. The chemiluminescent signal of the antibody-treated proteins (a) was captured by a CCD camera and quantified with a software from Intas, Germany (b). The relative staining-amount of the protein of interest (Band 1) was then normalized to b-actin (Band 2).

A digital image of the western blot was captured by a CCD camera and the image analysed by densitometry, evaluating the relative amounts of protein staining and quantifying the result in terms of optical density normalized to b-actin with software from Intas (Germany).

Size approximations were taken by comparing the stained bands to that of a protein standard loaded during electrophoresis. The process was repeated for the structural protein b-actin which should not change between samples. The amount of target protein could then be indexed to the structural protein to control between groups. This ensured correction for the amount of total protein on the membrane in case of errors or incomplete transfers.

Immunoblotting was used to determine the protein expression levels of the tumor supressor gene products p53 and p63, of the murine double minute MDM2, $p21^{WAF1}$and Bcl_{XL}. Furthermore the expression levels of the heat shock proteins HSP70 and HSP90 and of the

human telomerase reverse transcriptase hTERT were determined by this method. The specifications and dilution factors of the antibodies are given in chapter 3.5.

4.12 Determination of the protein concentration after Bradford

The protein concentration of the samples was determined by the method after Bradford et al. (1976) with modifications for microtiter application. This method is based on the shift in absorbance of Coomassie Brilliant Blue G-250 when bound to protein residues like arginine, tryptophan, tyrosine, histidine and phenylalanine, whereas the assay responds 8 times more to arginine residues. Coomassie Brilliant Blue G-250 binds to these residues in the anionic form, which has an absorbance maximum at 595 nm (blue). The free dye in solution is in the cationic form, which has an absorbance maximum at 470 nm (red). The extinction coefficient for the dye-protein complex is stable over 10 orders of magnitude (assessed in albumin). The dye reagent is stable for approximately one hour. Since the absorption spectra of the two forms overlap, the assay responds non-linearly in the standard curve over a wide concentration range. Therefore, the assay was modified after the method of Zor and Selinger (Zor and Selinger, 1996), who proposed the measurement of absorbance ratio 590/470 nm to determine the protein concentration. Bovine serum albumine (BSA) in a concentration range of 1 to 80 µg/ml was used to establish a standard curve.

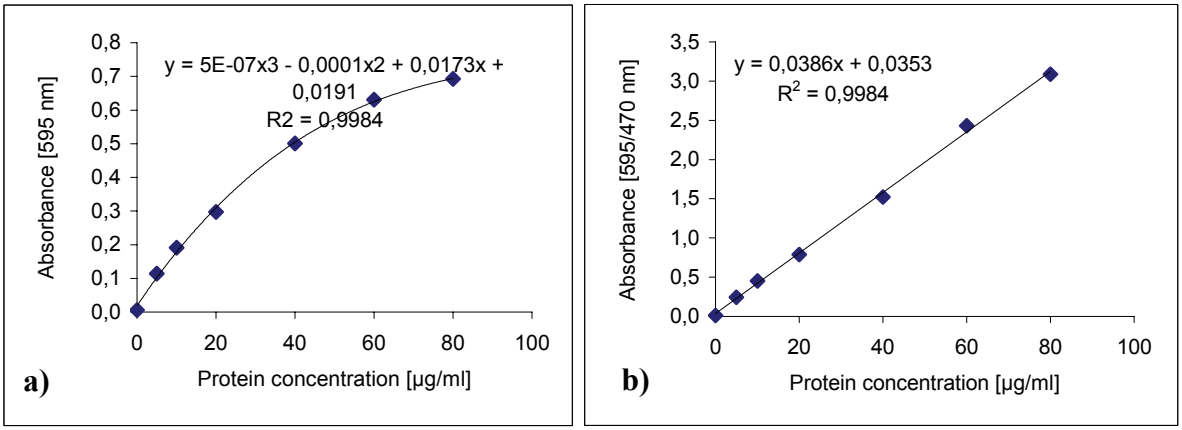

Figure 15: Measurement of protein concentration with a modified version of the Bradford assay. A calibration function generated in the Bradford assay with BSA in a concentration range between 0-80 µg/ml after a) measurement of the absorbance at 595 nm and b) calculation of the ratio A_{595} /A_{470} nm.

4.13 Chemical analysis by GC-MS/MS

The reactivity and volatility of ITCs is well known (Patai, 1977). The highly electrophilic central carbon atom of the N=C=S group reacts rapidly, and under mild conditions with oxygen-, sulfur-, or nitrogen centered nucleophiles to give rise to carbamates, thiocarbamates, or thiourea derivatives, respectively (Zhang and Talalay, 1994). To investigate the stability and kinetics of MTBITC under the conditions of the cell culture studies, and to learn more about the origin of the ITC-decomposition, a set of experiments was carried out and the ITC subsequently analysed by gas-chromatography.mass spectrometry (GC-MS/MS).

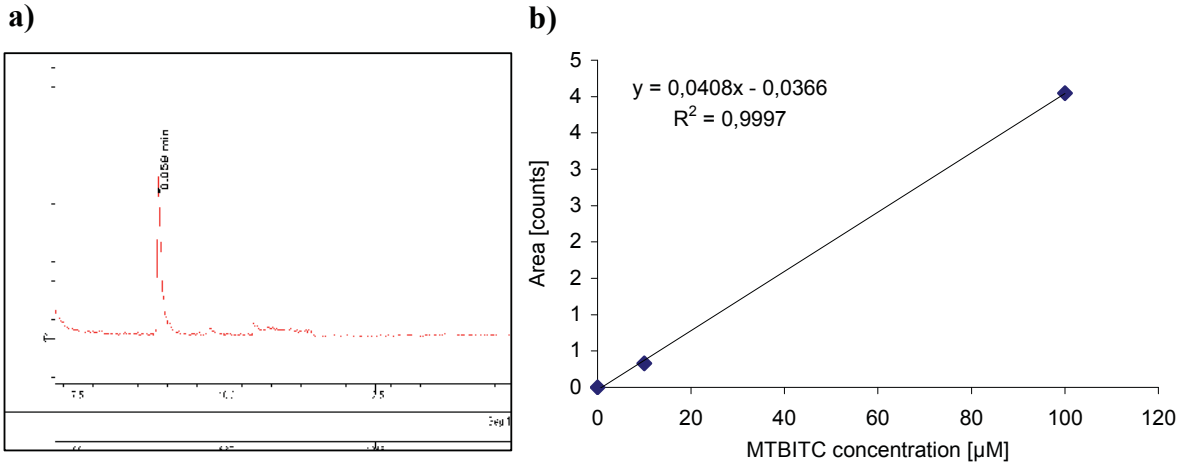

Figure 16: a) GC-MS/MS chromatochram of MTBITC. The retention time of MTBITC under the applied conditions was 8.859 minutes, **b) calibration curve for the GC-MS/MS measurements of MTBITC.** The calibration was performed in a concentration range of 0-100 µM MTBITC. MTBITC was therefore diluted in cyclohexane/ethylacetate (v/v).

T25 cell culture flasks containing

A. 1 x 10^6 adherent growing HepG2 cells in 5 ml culture medium and MTBITC at a final concentration of 20 µM were covered with a 0.22 µM-filter cap.

B. only 5 ml culture medium and MTBITC at a final concentration of 20 µM were covered with a 0.22 µM-filter cap.

C. 5 ml of distilled water and MTBITC at a final concentration of 20 µM were covered with a 0.22 µM-filter cap.

D. 5 ml of distilled water and MTBITC at a final concentration of 20 µM were sealed air- and liquid-tight with a sealing film (Nescofilm).

The flasks were then incubated at 37°C, in a 5 % CO_2- atmosphere and 95 % humidity for 0-24 h. After incubation, 2 ml of the liquid were removed from the flask and mixed vigorously with 1 ml of cyclohexane/ethylacetate (1:1) for 2 x 1 min. For phase separation, the suspension was centrifuged (5000 g, 10 min, 4°C) and the organic phase containing MTBITC transferred to a 15 ml falcon. The procedure was repeated and the second layer of organic phase added to the first one.

Chemical analysis and quantification of MTBITC was performed by a GC-MS/MS from Varian, Germany. The flow rate of the helium carrier gas was set to 1 ml/min. The temperature settings are shown in table 12.

Table 12: Temperature program of the varian GC capillary column, injector and transferline

Appliance	T [°C]	T increase [°C/min]	T hold [min]
capillary column	30		0.5
	90	5.0	5.0
	160	5.0	5.0
	280	30	10.0
Injector (injection volume = 1 µl)	210		
MS/MS transferline	210		

Mass spectra were obtained by electron ionisation at 70 eV, in single ion mode (SIM) at the mass 115 after 8.595 min. Quantification was performed with an external standard calibration function for each compound.

For quality control, the recovery rate of 10 to 100 µM MTBITC in the culture medium was determined in triplicate.

4.14 Statistical data analysis

Statistical analysis of the experimental data was performed with the software SPSS 11.0 for Windows. The samples were described by the mean value or median ± standard deviation (SD). All results were derived from at least two independent experiments. The data were analysed for significance of difference compared to control by the Students´ t-test.

V. RESULTS

5.1 MTBITC inhibits the proliferation of HepG2 cells

At the beginning of the study, a first characterization of MTBITC was achieved by detection of progress in cell proliferation after chemical- treatment with the WST-1 test, which measures the activity of mitochondrial succinate dehydrogenases of living cells. These experiments were conducted over a three-day time period in a concentration range of 1 to 30 µM MTBITC.

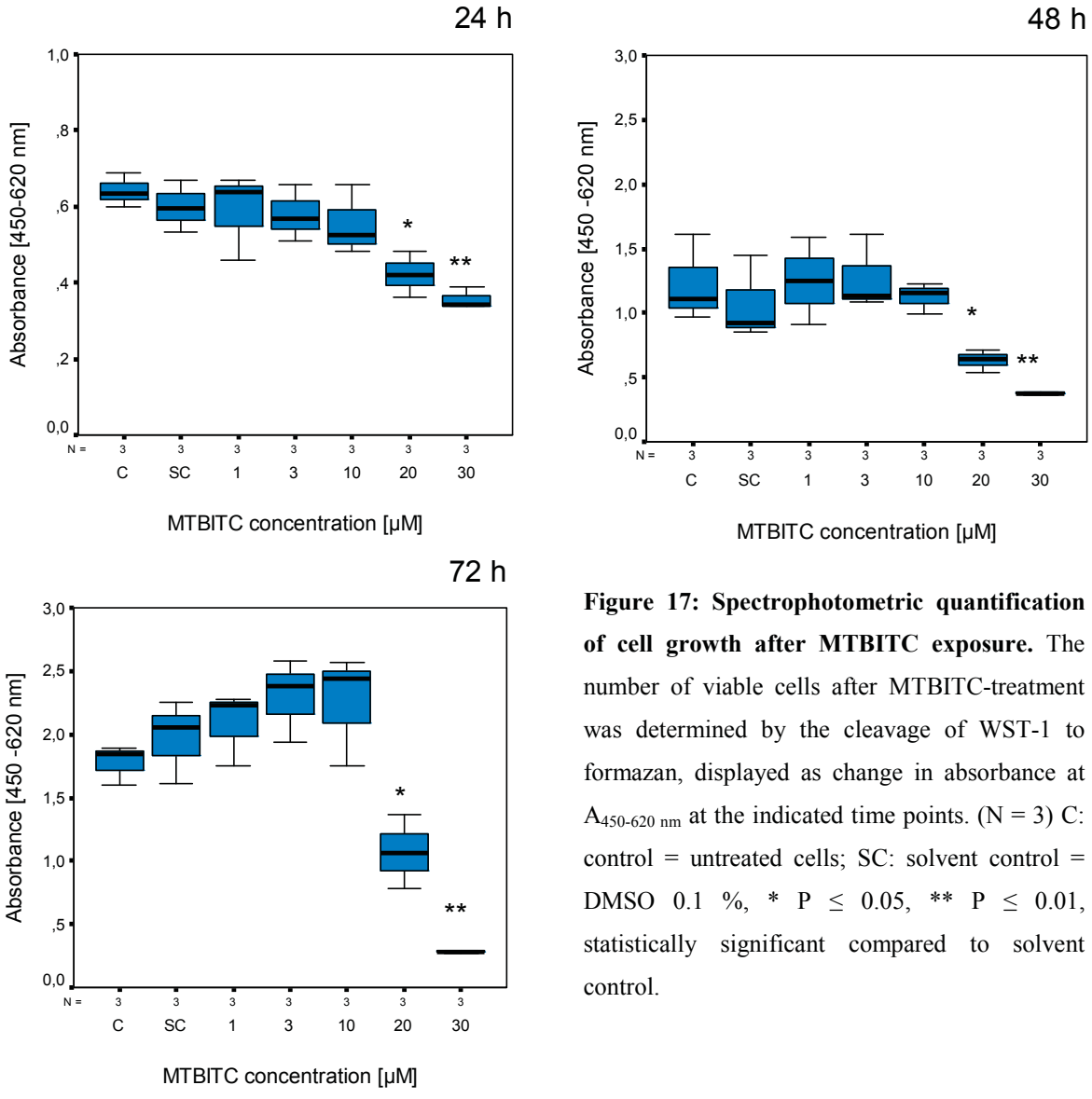

Figure 17: Spectrophotometric quantification of cell growth after MTBITC exposure. The number of viable cells after MTBITC-treatment was determined by the cleavage of WST-1 to formazan, displayed as change in absorbance at $A_{450\text{-}620\ nm}$ at the indicated time points. (N = 3) C: control = untreated cells; SC: solvent control = DMSO 0.1 %, * $P \leq 0.05$, ** $P \leq 0.01$, statistically significant compared to solvent control.

Figure 17 summarizes the results of three independent experiments. A concentration and time-dependent reduction in proliferation activity could be observed in cells treated with MTBITC exceeding 10 µM. After 24 h exposure of HepG2 cells to MTBITC in a concentration of 20 µM, a significant change in the proliferation activity of the cells compared to control cells could be observed. At this concentration, a proliferation reduction of HepG2 cells by 35 % was detectable (0.64 ± 0.05 vs. 0.42 ±0.61). This difference in proliferation activity compared to the control cells persisted after 48 h (1.22 ± 0.31 vs. 0.63 ± 0.92) and even after 72 h around 60 % of cells were still WST-1 positive (1.77 ± 0.15 vs. 1.07 ± 0.29). The treatment with MTBITC in a concentration range between 1 to 10 µM MTBITC for up to 72 h had no inhibitory effect on HepG2 cells, but a slight increase after 72 h could be detected in comparison to control cells (2.25 ± 0.44 vs. 1.77 ± 0.15). Exposure of cells towards 30 µM MTBITC for 24 h to 72 h resulted in a successive growth inhibition of 45 %, 70 % and 85 %, respectively.

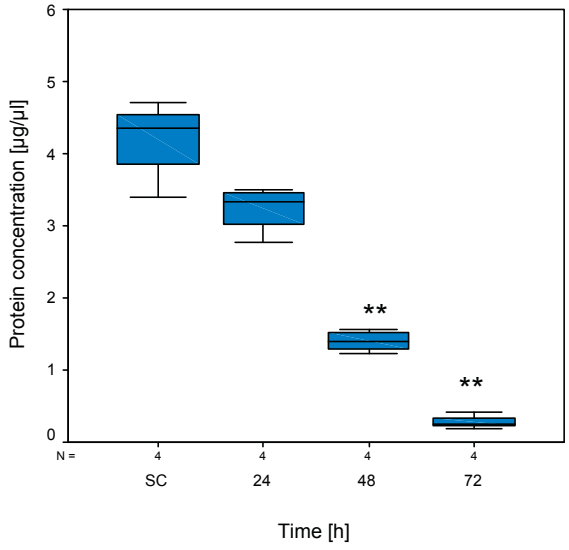

Figure 18: Quantification of the protein content of MTBITC-treated HepG2 cells by a modified version of Bradford. 2 x 10^6 cells were seeded into T25 culture flasks and exposed to 20 µM MTBITC at exponential growth. The protein concentration of lysates was determined after the indicated time points. (N = 4) SC: solvent control = lysate of HepG2 cells treated with 0.1 % DMSO for 72 h. * P ≤ 0.05, ** P ≤ 0.01, statistically significant compared to solvent control

Additionally to the WST-1 test, the protein content of HepG2 cells was determined as an indication for proliferation. The results are depicted in figure 18. The protein content of HepG2 cells exposed to 20 µM MTBITC was already reduced after 24 h to 76 % of control (3.23 ± 0.31 vs. 4.20 ± 0.56). After 48 and 72 h, the concentration was further reduced to 33 and 6 % of control (1.40 ± 0.15 and 0.28 ± 0.09, respectively).

5.2 Apoptosis is induced in a concentration- and time-dependent manner

The inhibitory effect of MTBITC on the proliferation of HepG2 cells was further characterized to determine whether the observed reduction in viability was of necrotic or apoptotic origin. Therefore, internucleosomal DNA fragmentation, representing one of the hallmarks of apoptosis was measured by two methodologies, the analysis of discrete "subG1" peaks on a DNA histogram by flow cytometry and the separation of fragmented DNA on an agarose gel. The results of these experiments are displayed in figures 19 and 20, respectively.

After 24-h exposure of HepG2 cells with MTBITC, DNA content analysis revealed a concentration-dependent increase in the formation of hypoploid DNA, which peaked at a concentration of 20 µM. At this concentration, the measurement of the "subG1" DNA content resulted in a 16.03 ± 1.52 % increase. Compared to that, exposure of the cells to the solvent control DMSO and to the positive control CPT led to an increase of 2.21 ± 0.25 % and 15.8 ± 2.65 % hypoploid events, respectively. A further increase in the concentration of MTBITC resulted in a reduction of the "subG1" DNA content, probably due to the accumulation of necrotic events.

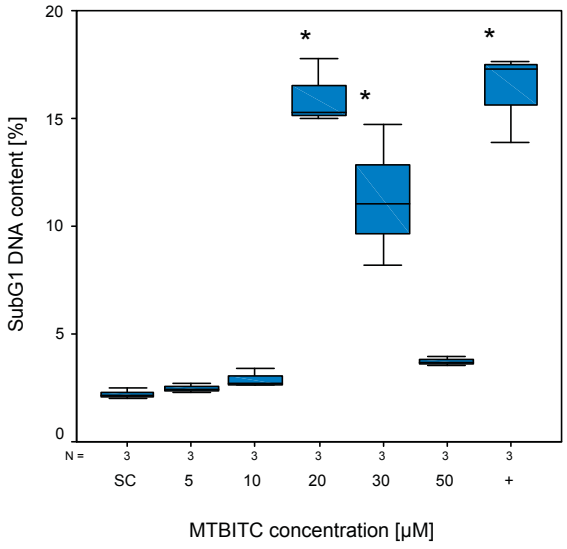

Figure 19:
Alteration in the "subG1" DNA content of HepG2 cells after exposure to MTBITC in a concentration range between 1 to 30 µM for 24 h. (N = 3) SC: solvent control = 0.1 % DMSO, +: positive control = 6 µM CPT. * $P \leq 0.05$, statistically significant compared to solvent control

The process of apoptosis induction after MTBITC treatment of HepG2 cells *over time* was tracked with the detection of the DNA fragmentation in the DNA laddering assay. 1 or 3 h post-treatment, no apoptotic DNA was present. However, after 6 h-incubation with 20 µM MTBITC distinct apoptotic changes could be observed. The amount of fragmented apoptotic DNA increased even further after 24 h-detection. No DNA fragmentation could

be seen with untreated or 0.1 % DMSO treated cells. No signs of necrotic events, visible as a smear in the agarose gel, were detected after exposure of HepG2 cells with 20 µM MTBITC for the indicated time-points.

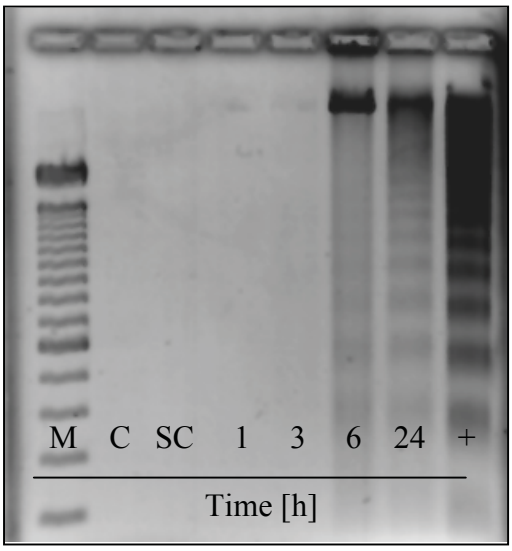

Figure 20:
Induction of internucleosomal DNA fragmentation after treatment of HepG2 cells for 1 to 24 h. The apoptotic DNA was separated by a 2 % agarose gel in an electric field and stained with ethidium bromide. M: 100 bp DNA size marker; C: untreated HepG2 cells; SC: solvent control = 0.1 % DMSO; +: positive control = 5.7 µM CPT. The experiments were carried out three times.

It is known that early during apoptosis only a small fraction of DNA is degraded to the size of internucleosomal fragments, while in more advanced stages nearly all the DNA is fragmented. Thus, the amount of low MW DNA varies manifold depending on the stage of apoptosis. As a consequence, the total content of low MW DNA does not provide information about the frequency of apoptotic cells. The “sub-G1” peak can represent, in addition to apoptotic cells, mechanically damaged cells or cellular debris. Moreover, cells in a late necrotic stage are also characterized by a loss of DNA and may therefore be stained similarly to apoptotic cells on a DNA histogram. To ascertain the present results and to quantify the amount of MTBITC-induced apoptotic cells, in addition, specific detection of single stranded apoptotic DNA with a monoclonal antibody was conducted. These results are shown in figure 21.

In accordance to the DNA fragmentation analysis, no apoptosis could be detected after 1 or 3 h-exposure of HepG2 cells to 20 µM MTBITC with the ssDNA assay. A time-dependent increase could be observed beginning after 6 h-treatment of cells with MTBITC. After that time, a 1.6-fold increase in absorbance at 405 nm was detected, due to the staining of single stranded apoptotic DNA compared with the control (0.44 ± 0.69 vs. 0.3 ± 0.03) . 24 h after the addition of 20 µM MTBITC to HepG2 cells, 46 % of the DNA of treated cells were stained with the Mab compared to control. Interestingly, 1 and 3 h after treatment begin, the apoptotic signal was slightly suppressed compared to the control.

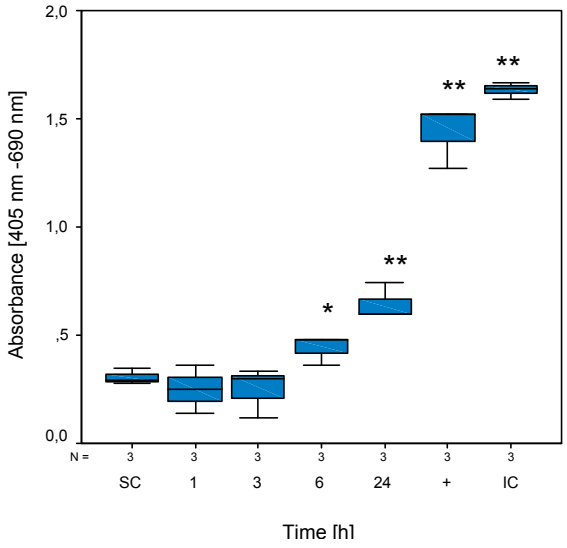

Figure 21: Formation of formamide denatured, single stranded apoptotic DNA in HepG2 cells. The cells were treated with MTBITC in a concentration of 20 µM for the indicated time points and apoptotic DNA stained with a Mab specific for ssDNA. (N = 3) SC: solvent control = 0.1 % DMSO; +: positive control = 6 µM CPT; IC: intern positive control = single stranded DNA. S1 Nuclease denatured HepG2 cells were used to confirm the specificity of the MAb binding. Absorbance of these cells was ≤ 0.2 in all three experiments. * P ≤ 0.05 and ** P ≤ 0.01, statistically significant compared to solvent control

5.3 The cell cycle progression is halted by MTBITC

Besides apoptosis induction, the decrease in cell proliferation detected with the WST1 assay after MTBITC-treatment could be a consequence of a cell cycle arresting influence of the ITC on the hepatoma cell line. Therefore, in the next step, the effect of MTBITC on cell cycle progression was analysed using flow cytometry. Results derived from three independent experiments are depicted in figure 22. A time-dependent arrest at the G2/M phase of the cell cycle was apparent at 6 h after MTBITC-treatment. At that time, 22.28 ± 3.45 % of MTBITC-treated HepG2 cells were arrested in the G2/M phase compared to 6.11 0.63 % of control cells. After 24 h, the amount of cells in the G2/M population increased from 10.31 ± 0.38 % of control cells to 59.42 ± 2.05 % of MTBITC-treated cells. The increase in the cell population at the G2/M phase was accompanied by a decrease in the cell population at the G1 phase of the cell cycle.

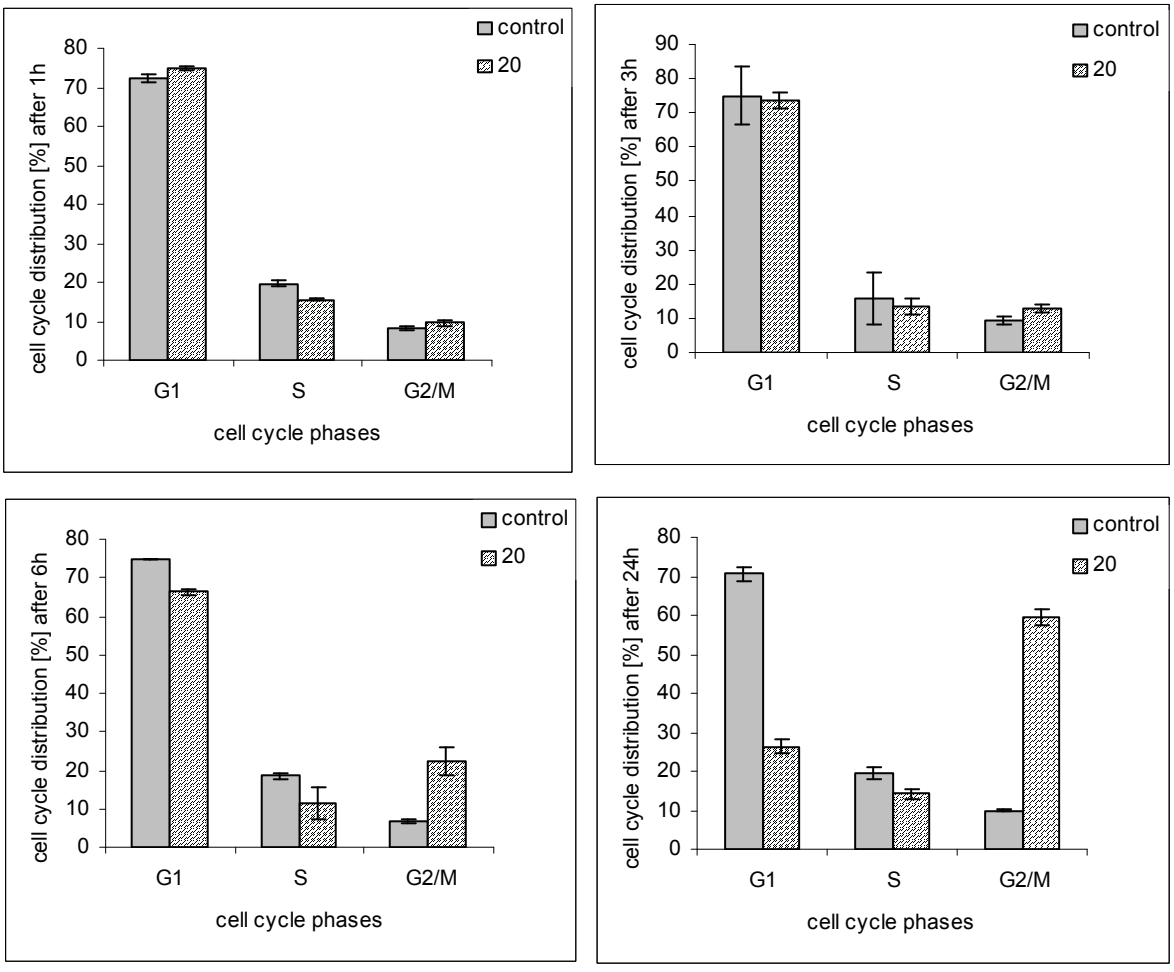

Figure 22: Analysis of cell cycle distribution after treatment of HepG2 cells with 20 µM MTBITC for 1 to 24 h by flow cytometry and PI staining of DNA. Cell cycle analysis was carried out with the software Modifit. (N = 3) Control: HepG2 cells, treated with 0.1 % DMSO.

5.4 p21^{WAF1} is increased by MTBITC-treatment

Eucaryotic cell cycle progression is regulated by sequential activation of cyclin-dependent kinases (cdks). p21^{WAF1} is ubiquitously expressed in mammalian cells and a well characterized cyclin-dependent kinase inhbitor that functions as a negative modulator of cell cycle progression (Gartel and Radhakrishnan, 2005). It is also a major target for transactivation by the tumor suppressor p53 and plays a cruical role in mediating growth arrest when cells are exposed to DNA damaging agents. To elucidate the mechanism of MTBITC-induced cell cycle arrest, lysates from control and MTBITC-treated HepG2 cells were subjected to western blotting using an antibody specific for p21^{WAF1}. The results of densitometric scanning and a representative immunoblot for the effect of MTBITC on the expression level of p21^{WAF1} are shown in figure 23. The expression of p21^{WAF1} was comparable to the control after 1 h of treatment with MTBITC. After 3 h, a 10 %-increase in the expression of p21^{WAF1} could be detected compared to the control; 6 h after treatment begin the protein level of p21^{WAF1} was elevated by 30 % compared to the control, which further increased to 50 % after 24 h and stabilized thereafter.

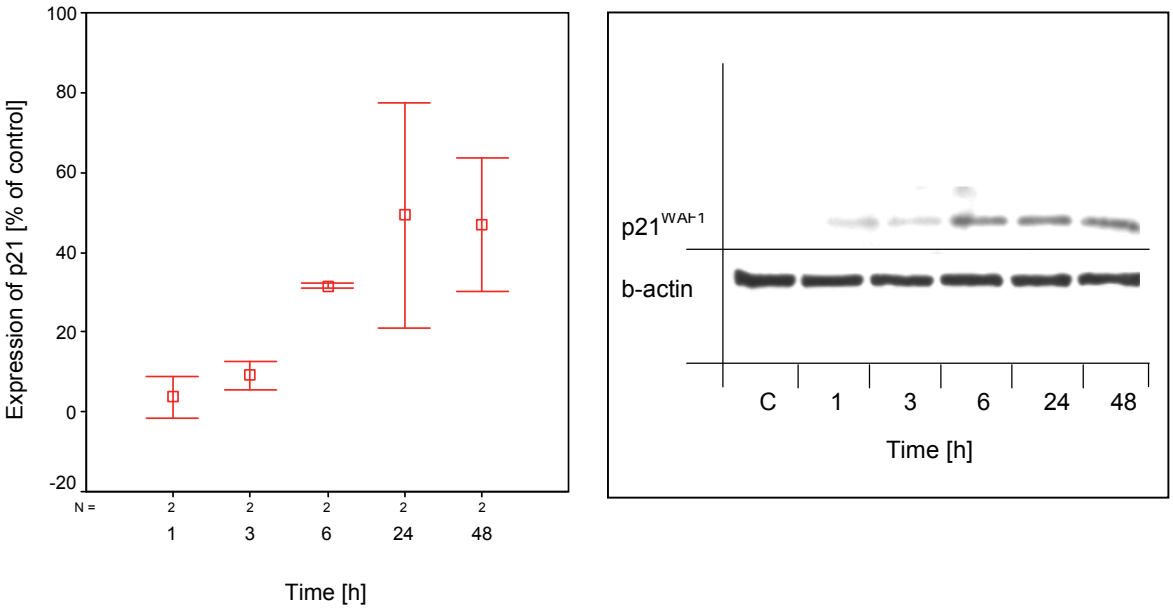

Figure 23: Time-dependent activation of p21^{WAF1} after exposure of HepG2 cells towards 20 µM MTBITC for 1 to 48 h. Cells were processed for immunoblot analysis and antibody probed. Lysate from HepG2 cells exposed to 0.1 % DMSO for 48 h were included as control. Left side: results of densitomentric scanning of the immunoreactive bands corresponding to p21^{WAF1}. The figure presents the mean of two independent immunoblot-experiments, normalized to b-actin ± SD. The results are expressed relative to the control, which was set to zero. Right side: representative blot of HepG2 protein lysate after p21^{WAF1} or b-actin antibody incubation.

5.5 MTBITC directly modifies the MMP

The loss of the MMP precedes the gross morphological changes associated with apoptosis. However, it represents a point just beyond final commitment. To explore the possible mechanism by which MTBITC induced apoptosis in HepG2 cells, the effect of the ITC on the mitochondrial membrane potential was investigated in time course experiments by flow cytometric analysis with the fluorescent probe JC-1. Representative scattergrams for red (indicator of an intact mitochondrial membrane potential) and green (indicator of mitochondrial collapse) fluorescence in HepG2 cells are shown in figure 24. In DMSO-treated control cells, mitochondria exhibited red fluorescence, due to accumulation of J-aggregates, indicating an intact mitochondrial membrane potential (figure 24.a). MTBITC-treatment disrupted the mitochondrial membrane potential in a concentration-dependent manner, as revealed by an increase in green fluorescence resulting from cytosolic accumulation of monomeric JC-1 (figures 24. b to d). Disruption of the MMP of HepG2 cells by MTBITC-treatment was not evident for 6 h. As shown in figure 25, exposure for 3 h did not alter the MMP, after 6 h however, a concentration-dependent disruption of the MMP was initialized, which dramatically amplified after 24 h. Compared to the control, 6 h-treatment of cells with 20 µM and 30 µM led to a reduction in the MMP of about 20 % and 45 %, respectively. After 24 h, the treatment of cells with 20 µM and 30 µM MTBITC resulted in a complete loss of the MMP. But even 3 µM MTBITC had a depolarizing effect on the mitochondria after 24 h.

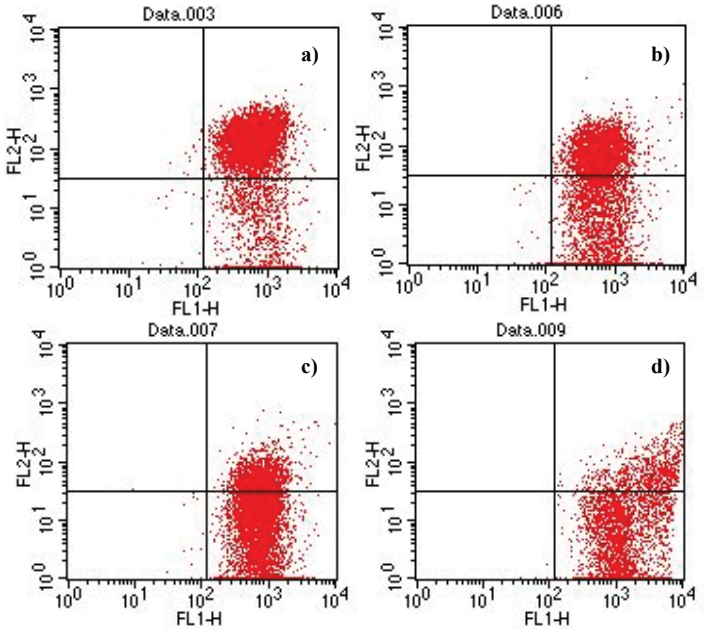

Figure 24:
Scattergrams of the MMP collapse after exposure of HepG2 cells to MTBITC. The pictures on the right side show the events detected in the FL-1 vs. FL-2 channel, after staining of cells with 2.5µg/ml JC-1 for 30 min. a) control cells, b) HepG2 cells treated with 20 µM MTBITC for 6 h, c) HepG2 cells treated with 20 µM MTBITC for 24 h, d) HepG2 cells treated with the positive control 10 µM valinomycin for 24 h.

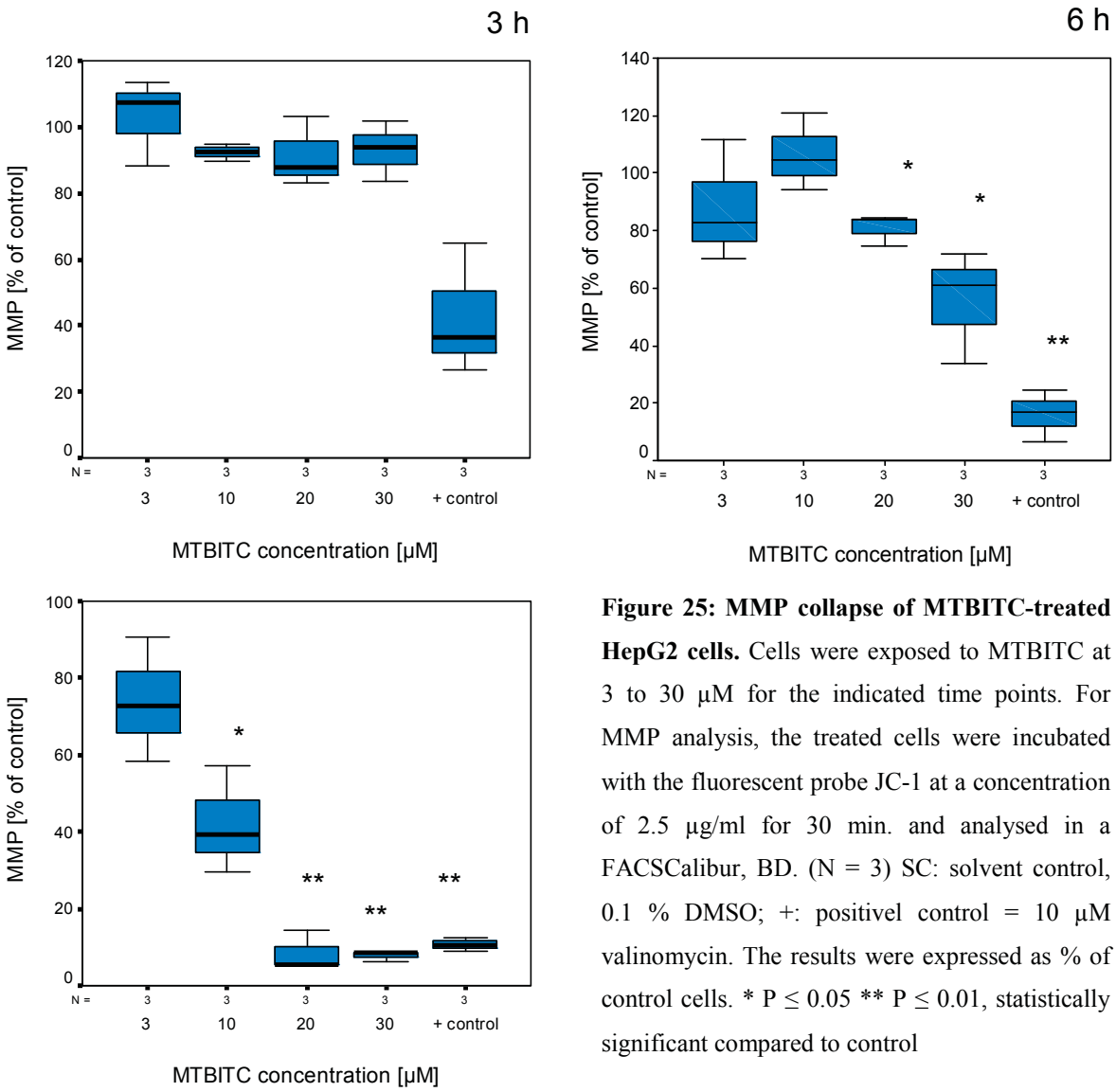

Figure 25: MMP collapse of MTBITC-treated HepG2 cells. Cells were exposed to MTBITC at 3 to 30 µM for the indicated time points. For MMP analysis, the treated cells were incubated with the fluorescent probe JC-1 at a concentration of 2.5 µg/ml for 30 min. and analysed in a FACSCalibur, BD. (N = 3) SC: solvent control, 0.1 % DMSO; +: positivel control = 10 µM valinomycin. The results were expressed as % of control cells. * $P \leq 0.05$ ** $P \leq 0.01$, statistically significant compared to control

5.6 The anti-apoptotic protein BCl_{xL} is suppressed

It has been shown in a variety of cellular systems that members of the Bcl-2 family function as gatekeepers of the cell death process. The anti-apoptotic multi-domain Bcl-2 protein Bcl_{xL} interacts and inhibits the function of pro-apoptotic Bcl-2 proteins. Furthermore, the disruption of the MMP is often accompanied by the suppression of anti-apoptotic proteins of the Bcl-2 family, which were found to be predominantly localized at the outer mitochondrial membrane. To confirm the involvement of mitochondria in MTBITC-induced cell death and to gain insight into the underlying mechanism of apoptosis induction by MTBITC, its effects on the expression level of $Bcl\text{-}_{xL}$ was determined by immunoblotting. To ensure equal loading of proteins in all samples, b-actin control was used. Figure 26 shows the results of the densitometric analysis. A slight increase in Bcl_{xL} protein expression of 15 % was observed after 1 h-treatment with MTBITC, which corresponds to the slight reduction in the apoptotic signal earlier observed in the ssDNA assay. Treatment of HepG2 cells with 20 µM MTBITC for ≥ 3 h resulted in a time-dependent suppression of the Bcl_{xL} protein. After 6 h, the level of Bcl_{xL} was decreased to 40 % of control and stabilized thereafter at this level.

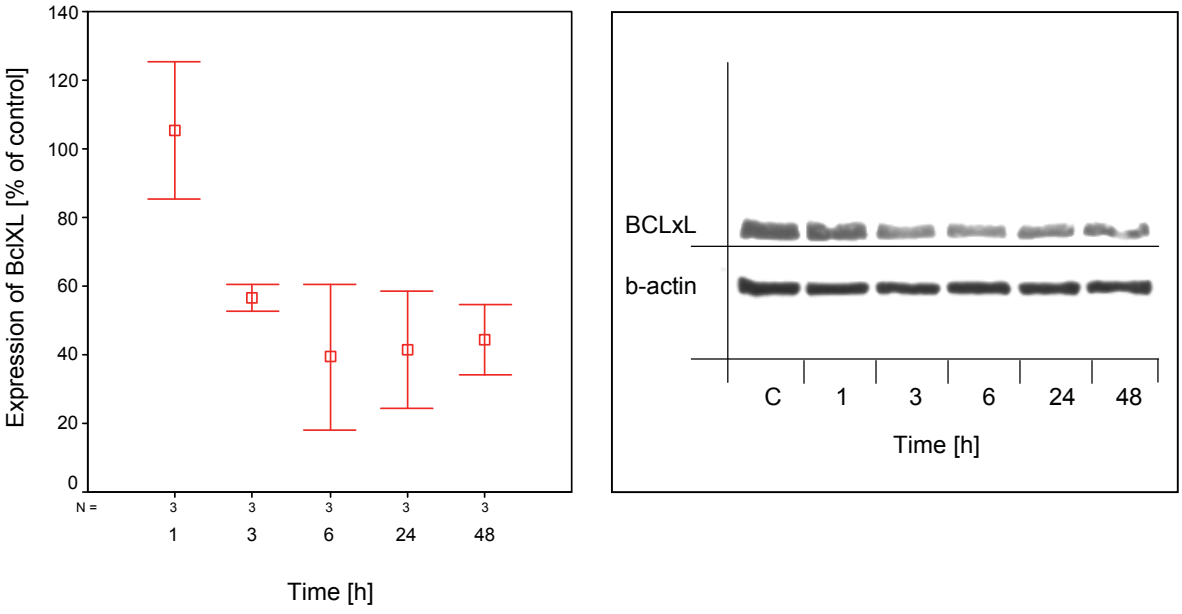

Figure 26: Time-dependent suppression of BCl_{XL} after exposure of HepG2 cells to 20 µM MTBITC for 1 to 48 h. Cells were processed for immunoblot analysis and antibody probed. Lysate from HepG2 cells exposed to 0.1 % DMSO for 48 h were included as control. Left side: results of densitomentric scanning of the immunoreactive bands corresponding to BCl_{XL}. The figure presents the mean of three independent immunoblot-experiments, normalized to b-actin ± SD. The results are expressed relative to the control. Right side: representative blot of HepG2 protein lysate after BCl_{XL} or b-actin antibody incubation.

5.7 The GSH level of HepG2 cells is dichotomous modulated

Glutathione (GSH) is the major intracellular antioxidant and an important cofactor of the detoxifying metabolism. ITCs readily and strongly bind to GSH due to their electrophilic N=C=S-group, a mechanism which is made responsible for the fast accumulation of ITC within the cell (Zhang, 2000). It was already reported by Hall et al. (Hall, 1999) that GSH depletion renders cells more susceptible to oxidative stress, which in consequence may trigger the induction of programmed cell death. On the other hand, ITC have been shown to induce g-glutamylcsteine synthetase (GCS), the limiting enzyme of GSH synthesis (Scharf et al., 2003). Therefore, the influence of MTBITC on the GSH status of HepG2 cells was investigated. The summarized results of two independent experiments are presented in figure 28, expressed as GSH concentration relative to the control.

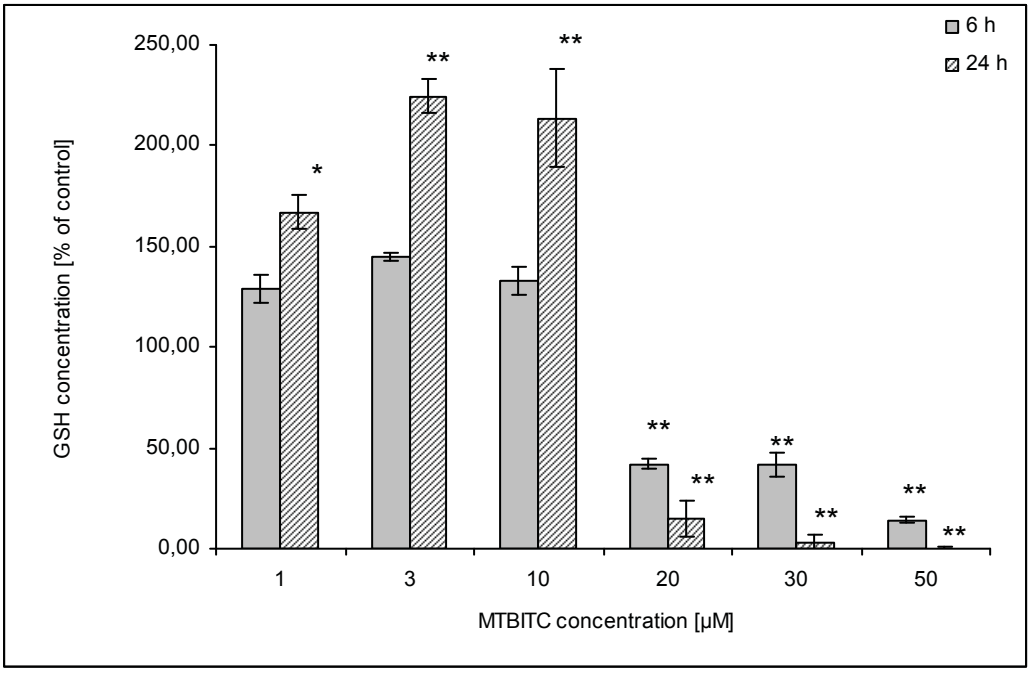

Figure 27: Modulation of the GSH level of HepG2 cells after treatment with MTBITC in a concentration range between 1-50 µM for 6 or 24 h. GSH level was spectrophotometrically determined by a kit from Cayman, Germany, based on the reaction of the sulfhydryl group of GSH with 5,5´-dithiobis-2-nitrobenzoic acid (DTNB) to the yellow coloured 5-thio-2-nitrobenzoic acid (TNB). The results are expressed as GSH concentration relative to the control (N=2) ± standard deviation. Control: 0,1 % DMSO * $P \leq 0.05$ ** $P \leq 0.01$, statistically significant compared to control

Not surprisingly, after 6 h-treatment of HepG2 cells in a concentration range of 1 to 10 µM, the GSH level concentration-dependently increased. This effect was even further elevated after 24 h. Concentrations leading cells into programmed death, i.e. exposure to ≥

20 µM MTBITC, however resulted in a massive GSH depletion, which was already evident after 6 h and resulted in a total depletion of the major cellular oxidative defence after 24 h. After 6 h and 24 h, the GSH level was decreased to 41 ± 2.54 % and 15 ± 8.99 % respectively in cells exposed to 20 µM MTBITC, compared to the control. This dichotomous behaviour of MTBITC is in accordance with the increase in the proliferation rate of HepG2 cells treated with lower concentration of MTBITC for a prolonged time on the one hand and a loss in vitality and MMP collapse in the higher concentration on the other hand.

5.8 ROS production is a late event in MTBITC-induced apoptosis

To confirm the production of oxidative stress due to the depletion of GSH, in a next step the production of reactive oxygen species by the exposure of MTBITC to HepG2 cells was investigated. This was done by measurement of the intracellular conversion of DHR123 to the fluorescent RH123, mediated by ROS. Short-term exposure of HepG2 human liver cells to 20 µM MTBITC for only 1 h significantly reduced the production of ROS compared to control cells. But after 3 h-treatment with the ITC, a concentration-dependent oxidation of DHR123 was monitored. This formation of ROS further increased after 6 h, at which time point 20 µM MTBITC produced a 10 %-increase of ROS compared to the control.

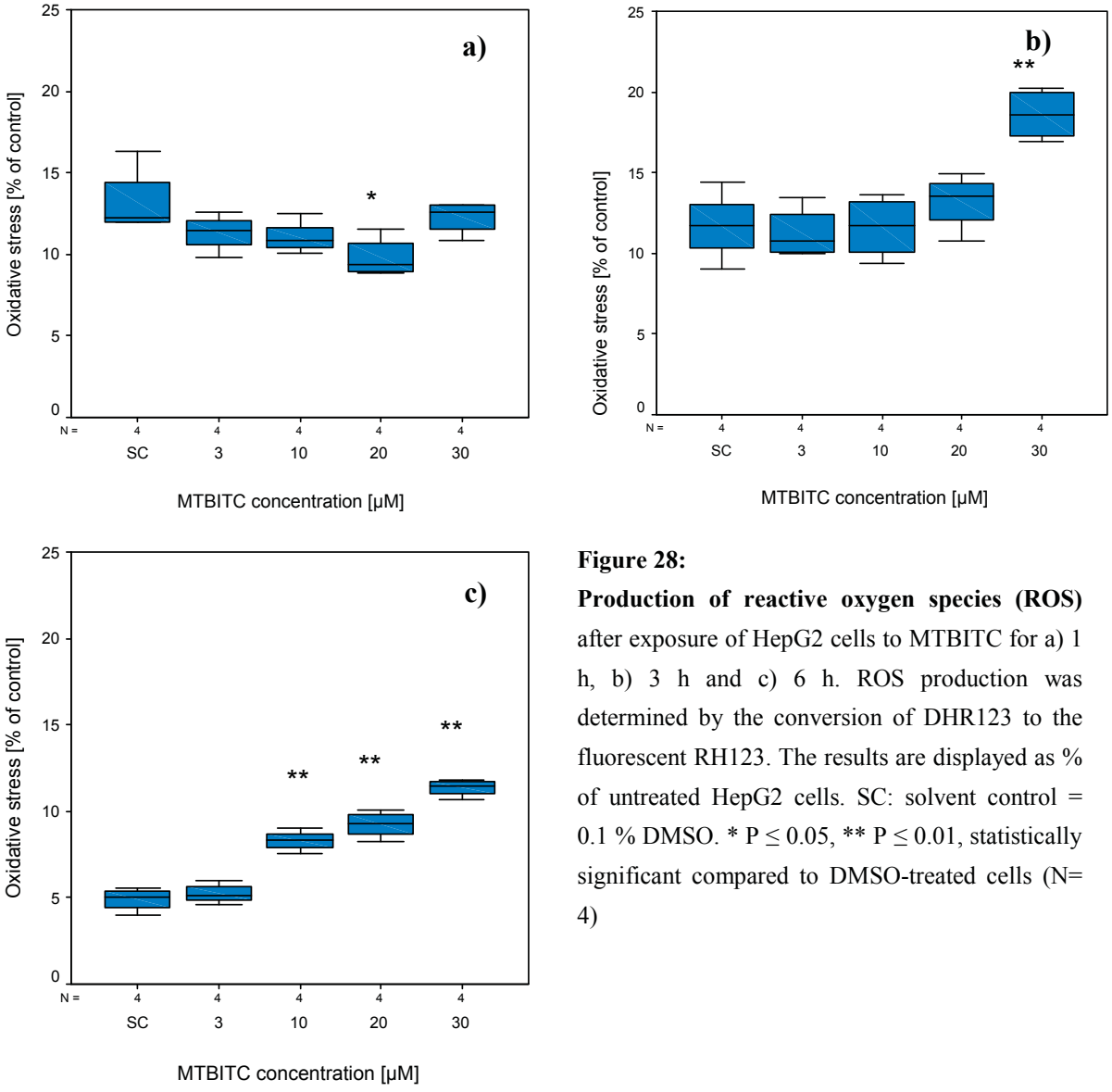

Figure 28:
Production of reactive oxygen species (ROS) after exposure of HepG2 cells to MTBITC for a) 1 h, b) 3 h and c) 6 h. ROS production was determined by the conversion of DHR123 to the fluorescent RH123. The results are displayed as % of untreated HepG2 cells. SC: solvent control = 0.1 % DMSO. * $P \leq 0.05$, ** $P \leq 0.01$, statistically significant compared to DMSO-treated cells (N= 4)

5.9 The p53 family is involved in MTBITC-mediated growth suppression

To determine whether the induction of cell cycle arrest and apoptosis in HepG2 cells was truly mediated by p53 expression, cells were treated with MTBITC in different concentrations from 1 to 24 h and analysed for their p53 protein expression level. Since the participation of $p21^{WAF1}$ was already clear, this could also provide further information about the involvement of a p53-dependent or independent regulation of $p21^{WAF1}$. As shown in figure 29a, exposure of HepG2 cells to MTBITC for 1 h led to a concentration-dependent increase in the expression level of p53. Exposure of cells to 20 µM MTBITC led to a 220 % increase in p53 protein level compared to DMSO-treated cells. 30 µM, which showed rather strong cytotoxic effects in the viability studies, did over-express p53, but this effect was rather short-lived compared to treatment of cells with 20 µM, as shown in figure 29 b. Stabilization of the p53 protein above control levels persisted for ≥ 6 h in HepG2 cells exposed to 20 µM MTBITC; a degradation of this tumor suppressor gene product was not detected until 24 h after treatment-begin (figure 29 c).

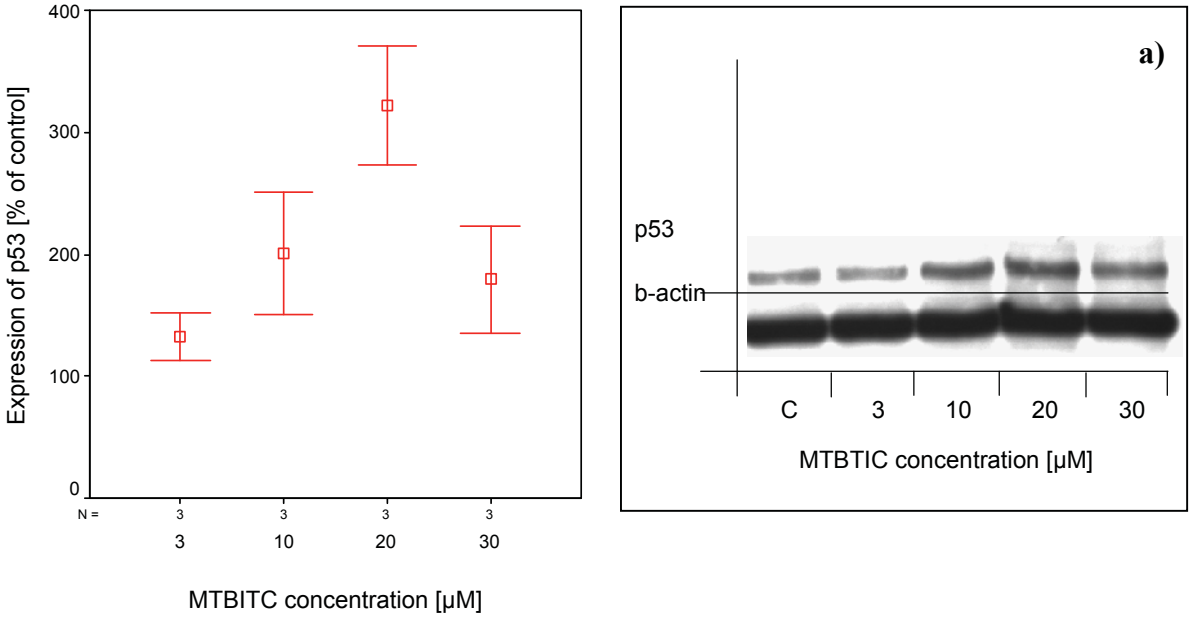

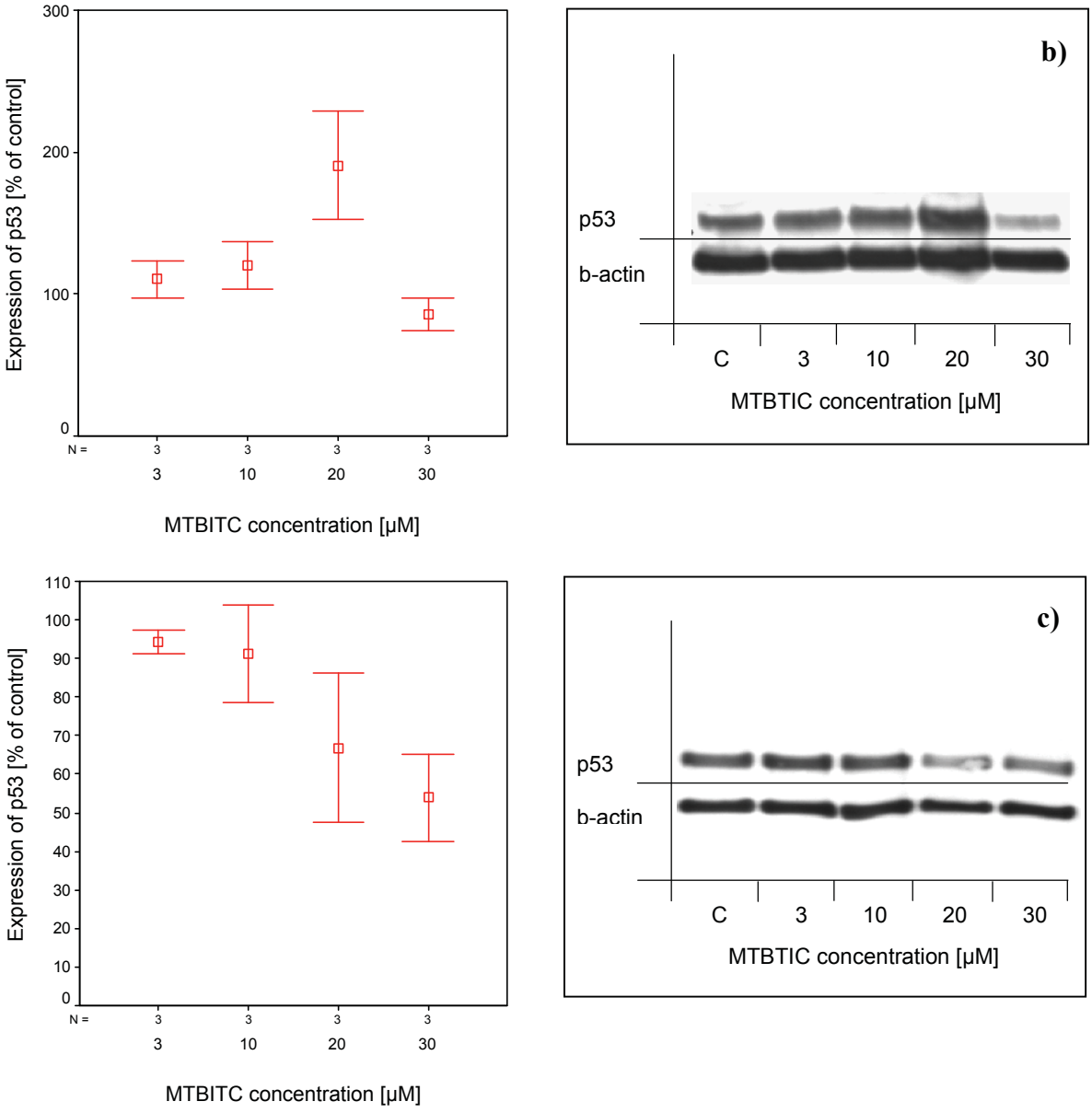

Figure 29: Concentration and time-dependent regulation of p53 in HepG2 cells after exposure to MTBITC for a) 1 h, b) 6 h and c) 24 h. Lysate from HepG2 cells exposed to 0.1 % DMSO for 1 to 24 h were included as control. Left side: results of densitomentric scanning of the immunoreactive bands corresponding to p53. The figures present the mean of three independent immunoblot-experiments, normalized to b-actin ± SD. The results are expressed relative to the control. Right side: representative blot of HepG2 protein lysate after p53 or b-actin antibody incubation.

p63 shares similar transcriptional functions with p53, including its potential for inducing apoptosis and growth suppression, although with varying efficiency (Gressner et al., 2005). With respect to this similarity between p53 and p63, the influence of MTBITC-treatment on the modulation of p63 was additionally investigated by western blotting. In control cells, no p63 protein could be detected with the applied methodology, as displayed in figure 30. A time-dependent increase of p63 protein content could be observed after 1 h-treatment of HepG2 cells with 20 µM MTBITC. The protein level initially stabilized at 100 % above the control for the first 6 hours. A further increase in p63 protein content to 230 % of the control could be seen 6 h after exposure–begin, and after 24 h and 48 h was even further elevated to 420 % and 510 % of the control.

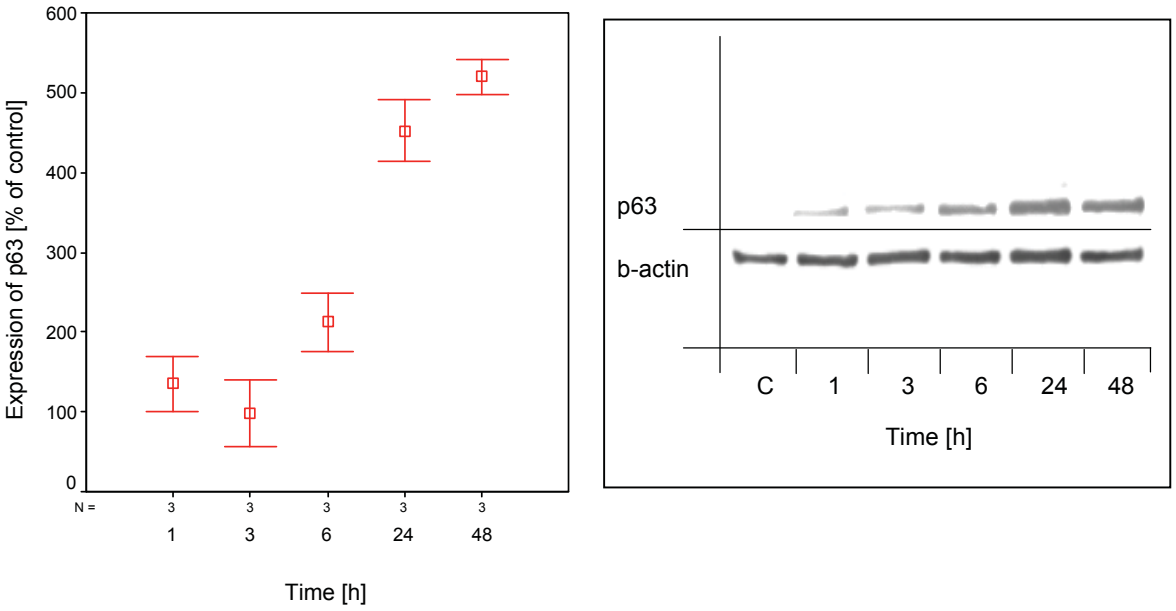

Figure 30: Time-dependent stabilization of p63 after exposure of HepG2 cells with MTBITC at a concentration of 20 µM for 1-48 h. Lysate from HepG2 cells exposed to 0.1 % DMSO for 48 h were included as control. Left side: results of densitomentric scanning of the immunoreactive bands corresponding to p63. The figure presents the mean of three independent immunoblot-experiments, normalized to b-actin ± SD. The results are expressed relative to the control which was set to zero. Right side: representative blot of HepG2 protein lysate after p63 or b-actin antibody incubation.

5.10 Overexpression of the murine double minute (MDM2) oncogene

In a next step, the observed degradation of p53 after 24 h-treatment with MTBITC was further examined by measuring the protein level of MDM2. It is known that due to its ubiquitin ligase properties, MDM2 renders p53 to proteosomal degradation and is therefore regarded as one of the most critical cellular antagonists of p53. Its role in p63 regulation, however, is not well-defined. As shown in figure 31, MDM2 was undetectable in control cells, whereas a time-dependent increase in MDM2 protein level could be detected in HepG2 cells exposed to 20 µM MTBITC. After 6-h treatment of HepG2 cells with MTBITC, a clear increase in MDM2 protein content to 170 % above the control could be observed, which peaked after 24 h with a 1000-fold increase compared to DMSO-treated HepG2 cells. These observations are perfectly in accordance to the chance in p53 protein expression and explain its observed time-dependent variation very well.

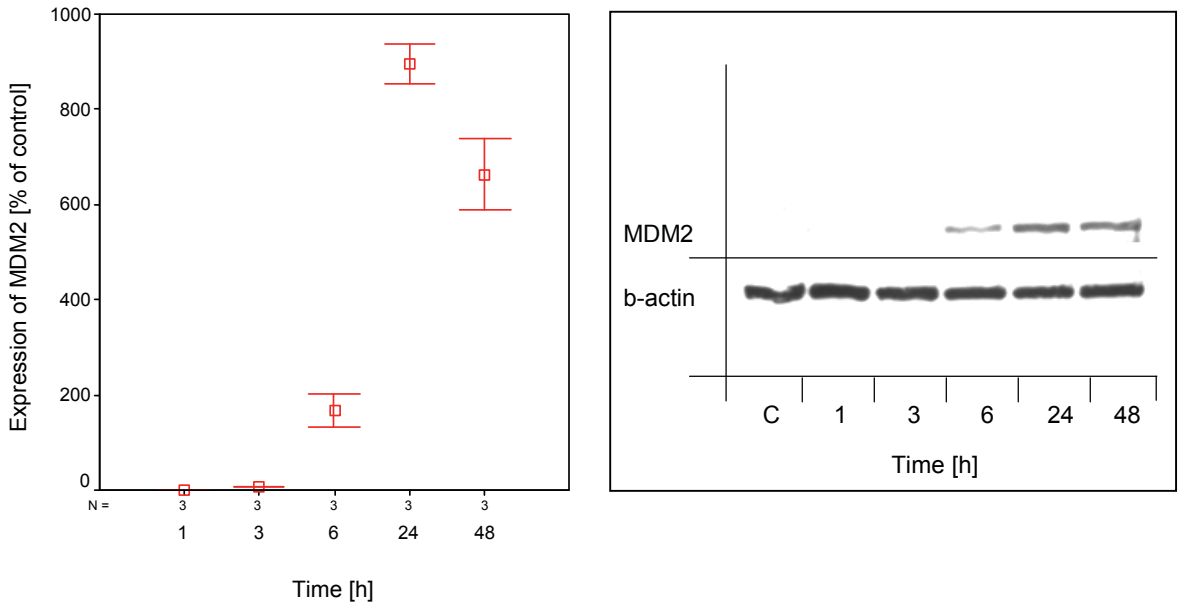

Figure 31: Time-dependent activation of MDM2 after exposure of HepG2 cells to MTBITC at a concentration of 20 µM for 1-48 h. Lysate from HepG2 cells exposed to 0.1 % DMSO for 48 h were included as control. Left side: results of densitomentric scanning of the immunoreactive bands corresponding to MDM2. The figure presents the mean of three independent immunoblot-experiments, normalized to b-actin ± SD. The results are expressed relative to the control. Right side: representative blot of HepG2 protein lysate after MDM2 or b-actin antibody incubation.

5.11 MTBITC induces DNA migration in the Comet assay

DNA strand breaks have been shown to be the initial signal in the DNA damaging signalling pathway of apoptosis induction and may act upstream of p53. In order to test whether DNA damage precedes MTBITC-mediated p53 stabilization and induction of the programmed cell death, HepG2 cells were exposed for 1 h to 20 µM MTBITC and subsequently analysed in the alkaline version of the SCGE assay. As shown in figure 32, MTBITC was found to significantly increase the level of strand breaks, expressed as OTM, 2.3-fold above the control level (2.1 ± 0.2 vs. 0.9 ± 0.1). The positive control 100 µM B(a)P induced an OTM of 2.6 ± 0.2. These results correspond to the early activation of the p53 family and make a good point in understanding the MTBITC-mediated effects of HepG2 cells observed so far.

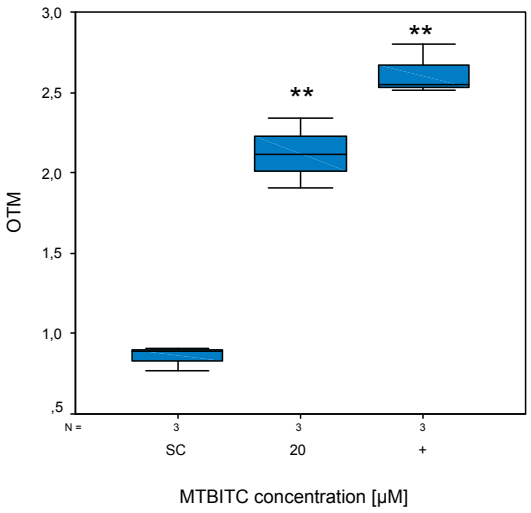

Figure 32: DNA damage induced by 20 µM MTBITC after 1 h exposure of HepG2 cells. Treated cells were separated in an electrophoretic field under alkaline conditions and the DNA stained with 10 µg/ml ethidium bromide. Analysis was carried out with the software COMET 5.0 from Optilas, Germany. SC: solvent control = 0.1 % DMSO, +: positive control = 100 µM B(a)P; OTM: olive tail moment; ** $P \leq 0.01$, statistically significant compared to control (N=3)

5.12 Telomerase and telomerase activity are suppressed by MTBITC

Having proved the MTBITC-dependent over-expression of p53 family members in HepG2 cells, the effect of the ITC on telomerase and telomerase activity was investigated in order to test the generated hypothesis. At first, the expression level of the catalytic subunit hTERT was determined by immunoblotting. The results of the hTERT expression level are summarized in figure 33. The analysis of hTERT revealed a continuous degradation of the protein, beginning 3 h after MTBITC-exposure of HepG2 cells. 24 h after treatment-begin, the protein was suppressed by 50 % compared to control cells. No further degradation of hTERT was evident after 48h.

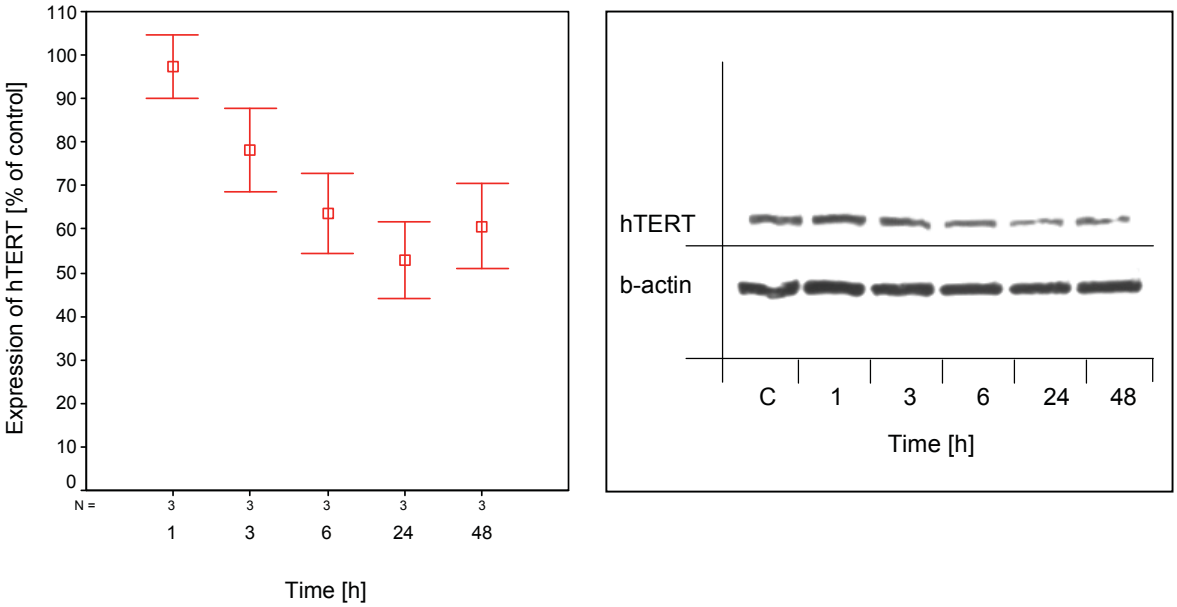

Figure 33: Time-dependent suppression of hTERT after exposure of HepG2 cells to MTBITC at a concentration of 20 µM for 1-48 h. Lysate from HepG2 cells exposed to 0.1 % DMSO for 48 h were included as control. Left side: results of densitomentric scanning of the immunoreactive bands corresponding to hTERT. The figure presents the mean of three independent immunoblot-experiments, normalized to b-actin ± SD. The results are expressed relative to the control. Right side: representative blot of HepG2 protein lysate after hTERT or b-actin antibody incubation.

Since the telomerase-limiting protein hTERT was found to be time-dependently suppressed, the results were verified by analysis of the holenzyme activity in the TRAP-ELISA assay. Therefore, HepG2 cells were again treated with a fixed concentration of 20 µM MTBITC for the same time points, additionally extended to a 72 h-exposure experiment. The results are depicted as the typical telomerase ladder consisting of 6 bp DNA increments derived by the TRAP reaction (figure 34 a). Additionally in figure 34 b

are the summarized results generated by ELISA-detection of the same PCR products. No suppression of the enzyme activity could be seen for 24 h, which corresponds to the long half-life of the enzyme. 24 h after treatment-begin of HepG2 cells to 20 µM MTBITC, a decrease in telomerase activity by 10 % compared to control was detected, which subsequently was further reduced to 50 % after 72 h. The treatment of cells with the positive control TMPyP4 resulted in an 85 % loss of telomerase activity within the first 24 h compared to control.

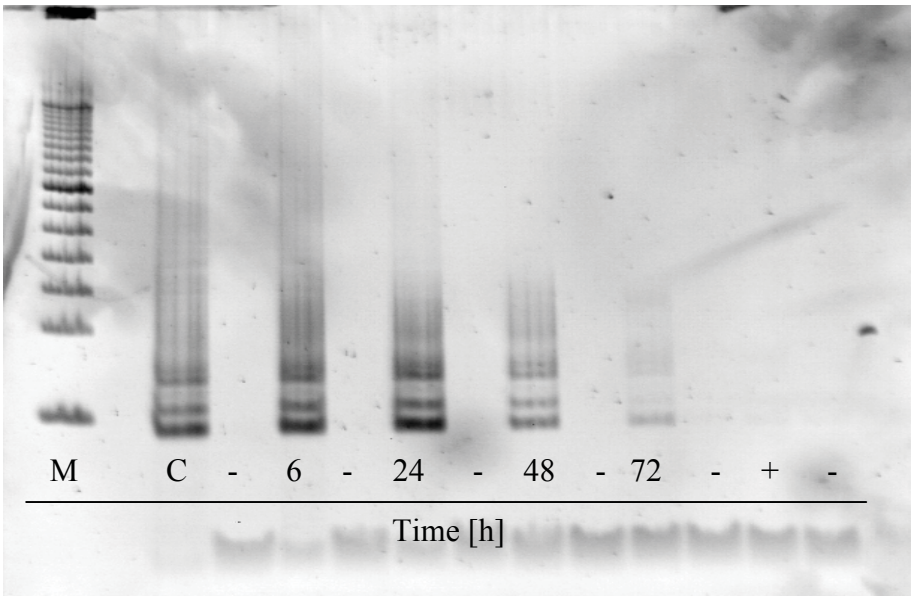

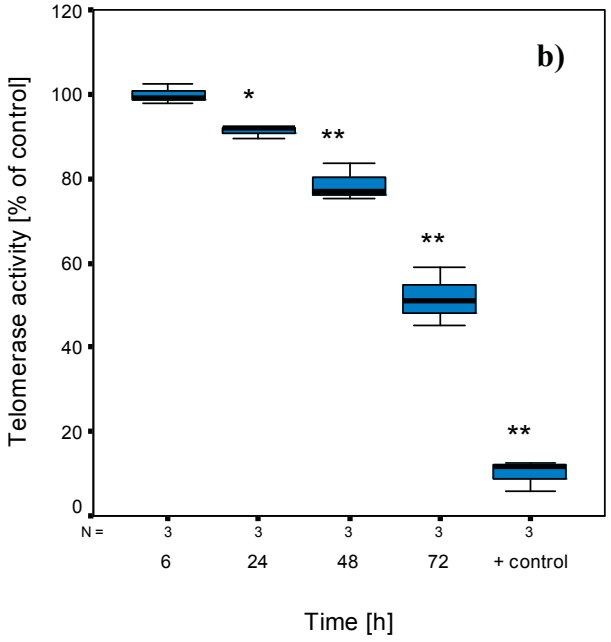

Figure 34: Suppression of telomerase activity in HepG2 cells after treatment with 20 µM MTBITC. Cells were treated with MTBITC for the indicated time points. 0.05 µg protein extract of HepG2 cells were then used for TRAP-ELISA analysis. Preparations of HepG2 cells treated with 0.1 % DMSO for 72 h were included as control. RNase-treated preparations of the samples were used to correct for background. a) 6 bp DNA increments derived by the TRAP reaction. Rows labelled (-) indicate the corresponding Rnase treated sample M: 100 bp DNA marker; C: solvent control = 0.1 % DMSO; + control: positive control = 300 µM TMPyP4. b) summarized results of three independent experiments generated by ELISA-detection of the PCR products. * $P \leq 0.05$ and ** $P \leq 0.01$, statistically significant compared to solvent control

5.13 MTBITC-treatment increases the level of HSP proteins

The HSP90 chaperon complex plays a crucial role in the folding of the telomerase enzyme to its active state. But this complex is also important for a functional stabilization of p53 during the suicidal death of cells. Therefore, the expression levels of HSP90 and HSP70 were determined in immunoblotting experiments. In figures 35 and 36, the results of MTBITC-treatment on HSP-expression level in HepG2 cells are displayed. A time-dependent increase in HSP90 accumulation was detected, beginning after 1h-treatment of cells with MTBITC. Compared to control, densitometic analysis showed a 3-fold over-expression of HSP90 in HepG2 cells harvested after 24 h of exposure to MTBITC.

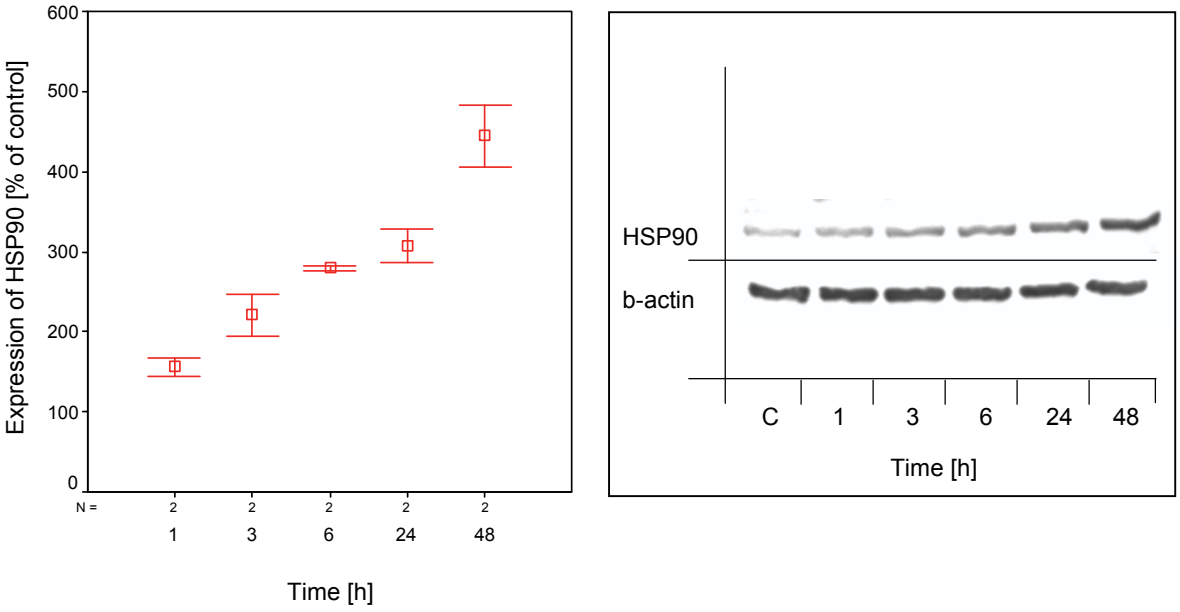

Figure 35: Time-dependent over-expression of HSP90 after exposure of HepG2 cells with MTBITC at a concentration of 20 µM for 1-48 h. Lysate from HepG2 cells exposed to 0.1 % DMSO for 48 h were included as control. Left side: results of densitomentric scanning of the immunoreactive bands corresponding to HSP90. The figure presents the mean of two independent immunoblot-experiments, normalized to b-actin ± SD. The results are expressed relative to the control. Right side: representative blot of HepG2 protein lysate after HSP90 or b-actin antibody incubation.

Similarly to the regulation of HSP90, a time-dependent increase in HSP70 was detected in MTBITC-treated cells; however, over-expression of HSP70 did not occur until 6 h-exposure of cells. For example, 24-h exposure of HepG2 cells resulted in a 170 %-increase in HSP70 expression above control. After 48 h, the densitometric analysis revealed a 220 % elevation of protein level compared to control HepG2 cells.

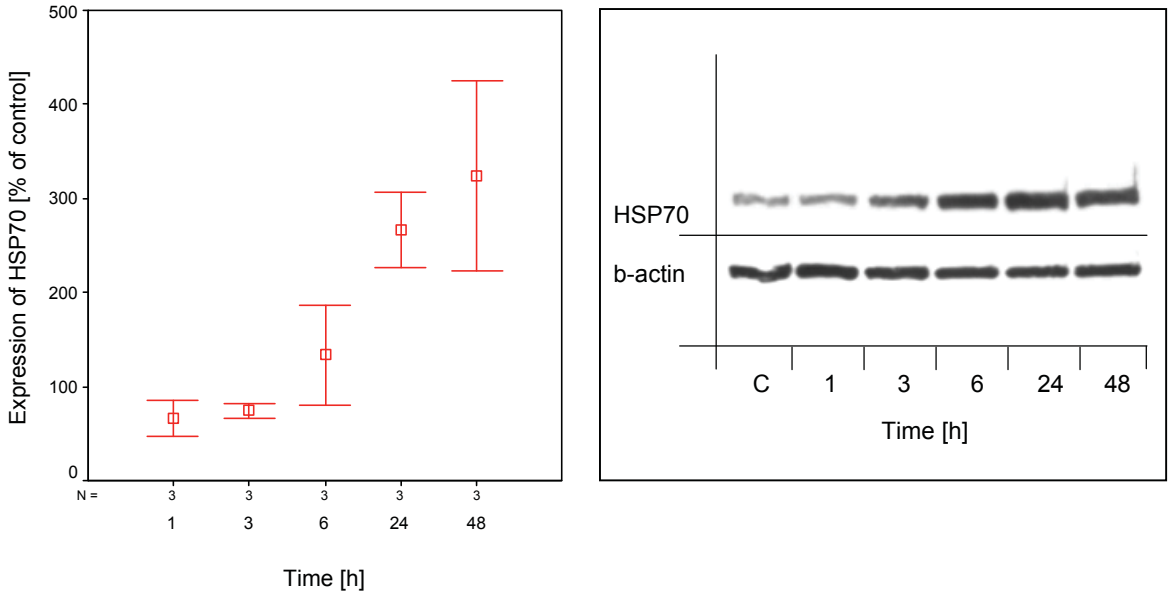

Figure 36: Time-dependent over-expression of HSP70 after exposure of HepG2 cells with MTBITC at a concentration of 20 µM for 1-48 h. Lysate from HepG2 cells exposed to 0.1 % DMSO for 48 h were included as control. Left side: results of densitomentric scanning of the immunoreactive bands corresponding to HSP70. The figure presents the mean of three independent immunoblot-experiments, normalized to b-actin ± SD. The results are expressed relative to the control. Right side: representative blot of HepG2 protein lysate after HSP70 or b-actin antibody incubation.

5.14 The telomere length of HepG2 cells is not rapidly decreased by MTBITC-treatment

By probing the telomeric sequences of HepG2 cells with fluorochrome-tagged PNA probes and subsequent flow cytometric analysis, the length of HepG2 telomeres was assessed after MTBITC-treatment. This was particularly interesting, since it has been shown that rapid decrease in telomeric repeat sequences due to the uncapping of telomeres can precede apoptosis induction, or can be triggered due to apoptotic signals. But as presented in figure 37, no significant alteration in the length of HepG2 telomeres could be observed within the full period of 48 h-treatment with MTBITC in a concentration of 20 µM.

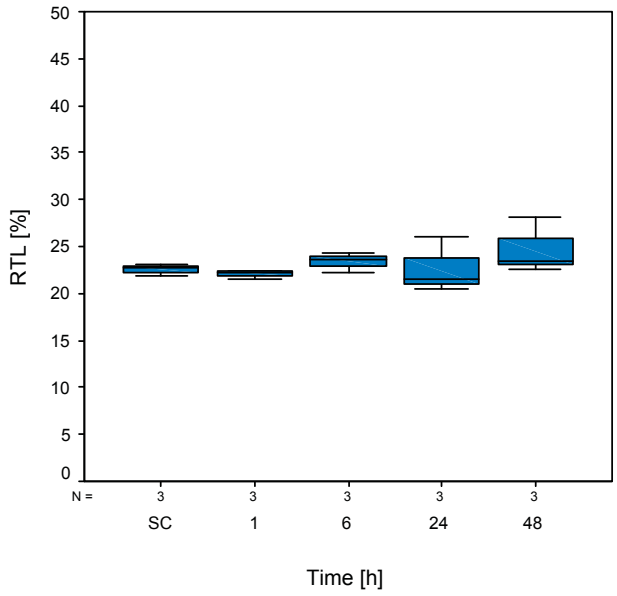

Figure 37: Relative telomeric length (RTL) of HepG2 cells treated with 20 µM MTBITC for the indicated time points. Telomere length is expressed relative to the length of CCRF-CEM cells. The results are derived from three independent experiments. SC: solvent control = 0.1 % DMSO

5.15 MTBITC degrades rapidly in the experimental system

To investigate the stability and degradation kinetics of MTBITC under the conditions of the cell culture studies, a set of experiments was carried out and the ITC subsequently analysed by GC-MS/MS. In all the experiments, MTBITC was applied at a final concentration of 10 µM, so that the results were comparable to the experiments already conducted with the cell culture. A rapid decrease of MTBITC could be observed within the first hour in culture flasks containing HepG2 cells adherent growing in culture medium (figure 38). During that time, a loss of 50 % MTBITC was detected in the extracted medium. After 6 h, only 25 % MTBITC remained in the medium and within 24 h MTBITC was no longer detectable.

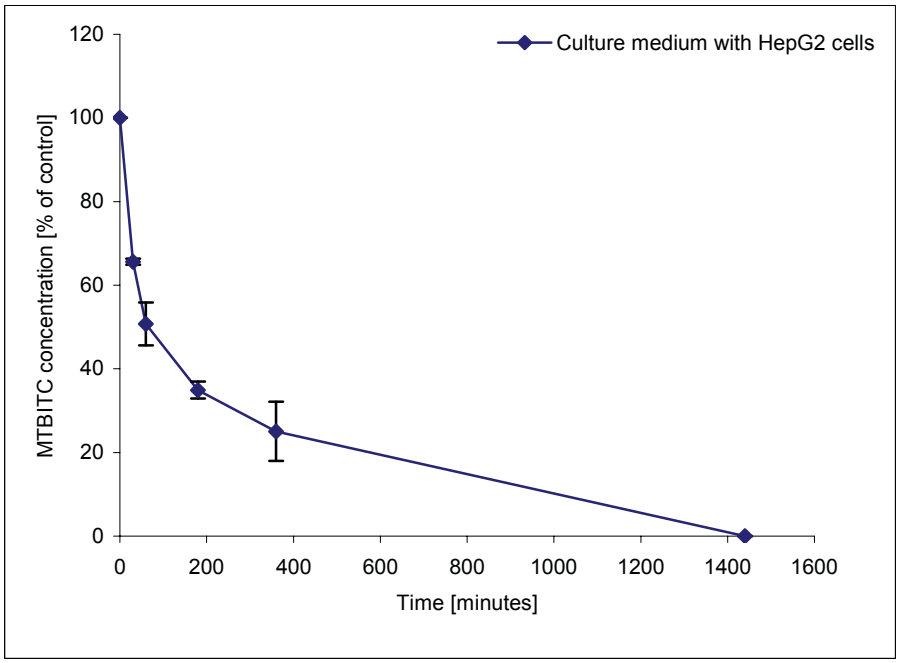

Figure 38: Degradation kinetics of 10 µM MTBITC in filter capped culture flasks containing 1 x 10^6 adherent growing HepG2 cells in 5 ml culture medium. The change in concentration over time was detected by GC-MS/MS analysis. The figure depicts the mean of three independent experiments ± SD, expressed relative to the control.

The experiment was repeated with the design differing only in the absence of HepG2 cells. As shown in figure 39, the kinetic of MTBITC degradation was similar to that derived with HepG2 cells. After 1 h, 50 % of the ITC was also degraded. 5 h later, 30 % was left in the medium and after 24 h, MTBITC was depleted by 100 %.

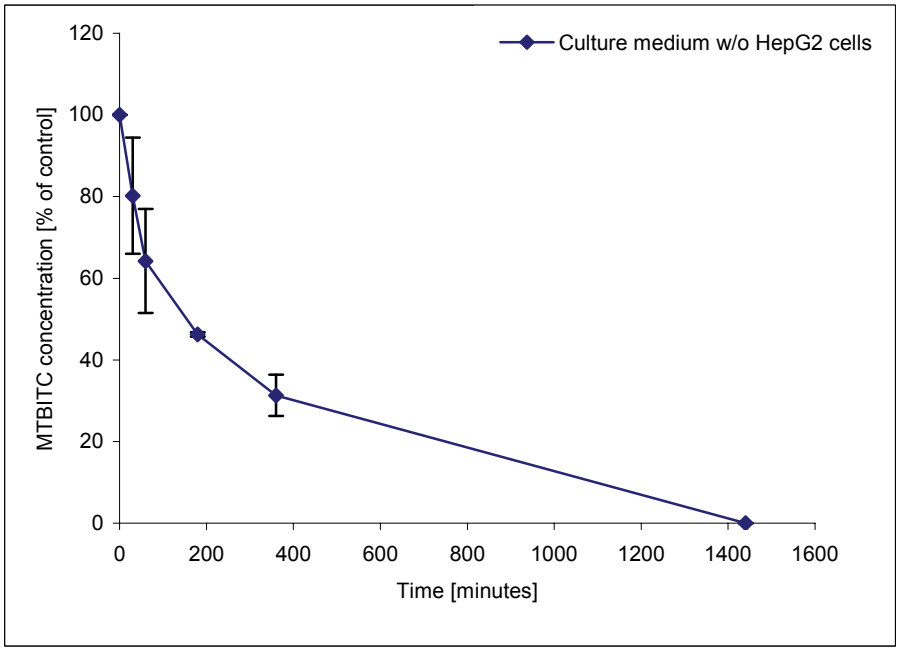

Figure 39: Degradation kinetics of 10 µM MTBITC in filter capped culture flasks containing 5 ml culture medium. The change in concentration over time was detected by GC-MS/MS analysis. The figure depicts the mean of two independent experiments ± SD, expressed relative to the control.

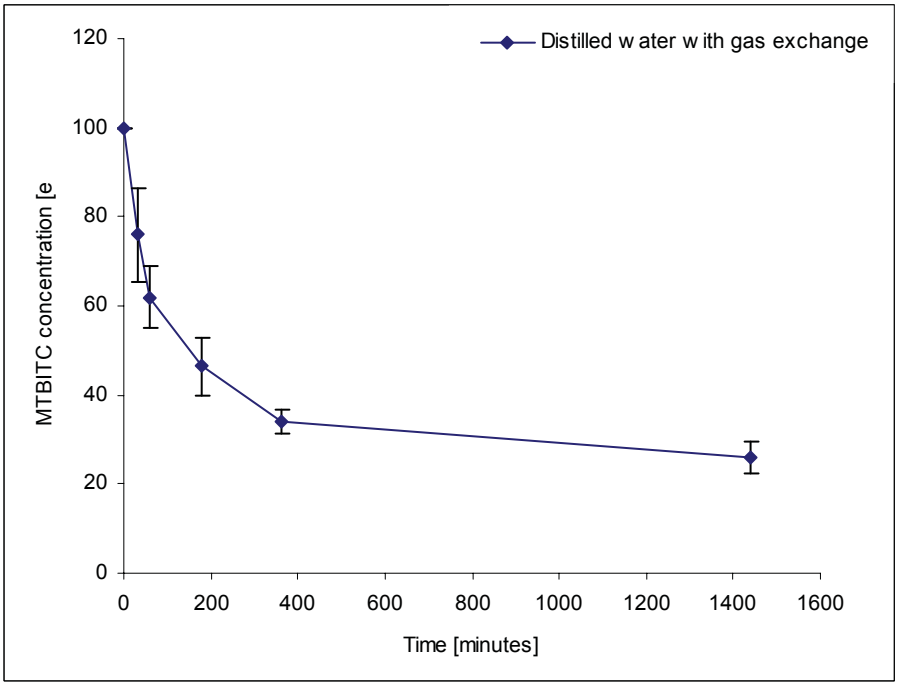

Figure 40: Degradation kinetics of 10 µM MTBITC in filter capped culture flasks containing 5 ml distilled water. The change in concentration over time was detected by GC-MS/MS analysis. The figure depicts the mean of two independent experiments ± SD, expressed relative to the control.

Analysis of MTBITC in the culture flasks containing distilled water instead of culture medium (figure 40) revealed that MTBITC was also degraded in the water in a time-dependent manner, but the decrease of the ITC was 40 % and 70 % after 1 and 6 h, respectively. 24 h after experiment begin, 25 % of the ITC was still detectable.

In the last set of experiments, MTBITC was added to distilled water in tightly sealed culture flasks. The results are presented in figure 41. The prevention of gas exchange managed to maintain 10 % more MTBITC in the distilled water compared to unsealed culture flasks. Although the rapid decrease within the first hour was identical (40 %) to the previous experiments, but after 6h 50 % still remained in the distilled water.

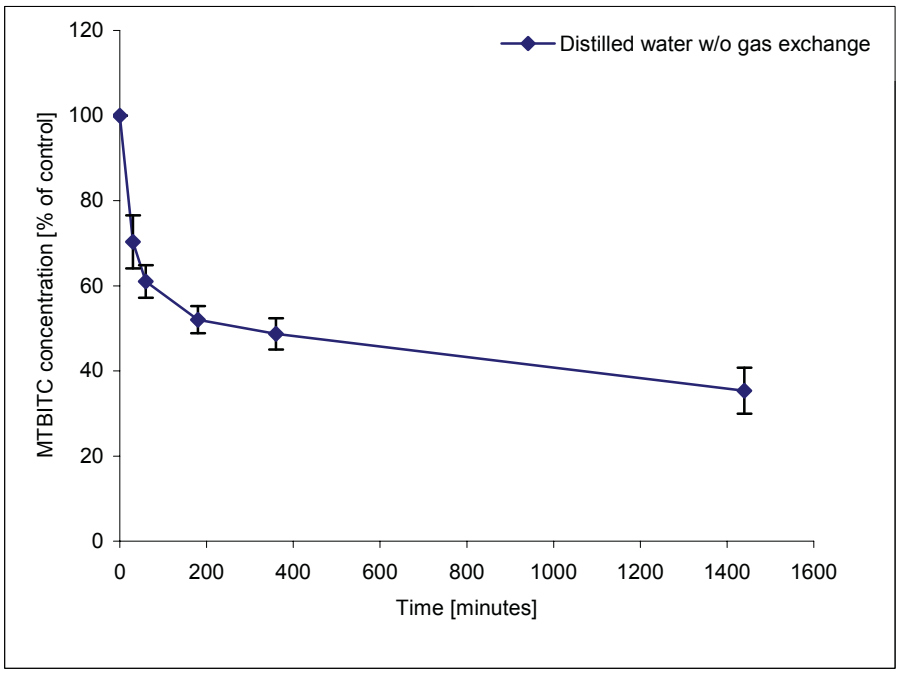

Figure 41: Degradation kinetics of 10 µM MTBITC in culture flasks containing 5 ml distilled water without gas exchange. To inhibit the gas exchange with the surrounding air, the culture flasks were tightly covered with parafilm. The change in concentration over time was detected by GC-MS/MS analysis. The figure depicts the mean of three independent experiments ± SD, expressed relative to the control.

5.16 Only early removal of MTBITC saves the cells from apoptosis

Early stages of p53-induced apoptosis may be reversible, as shown by Geske et al. (Geske et al., 2000) possibly due to the activation of DNA repair. However, the disruption of the MMP, is regarded to be an early, albeit already irreversible stage of apoptosis. If early stages of p53-induced apoptosis in MTBITC-treated HepG2 cells are indeed reversible through DNA repair, it is of interest to determine when the point of no return occurs in the cell system after MTBITC-exposure. These experiments were especially important, since it has been shown in human and in animal studies that the ITC decomposition rate is very high. Maximum levels are only present in these systems for rather a short time.

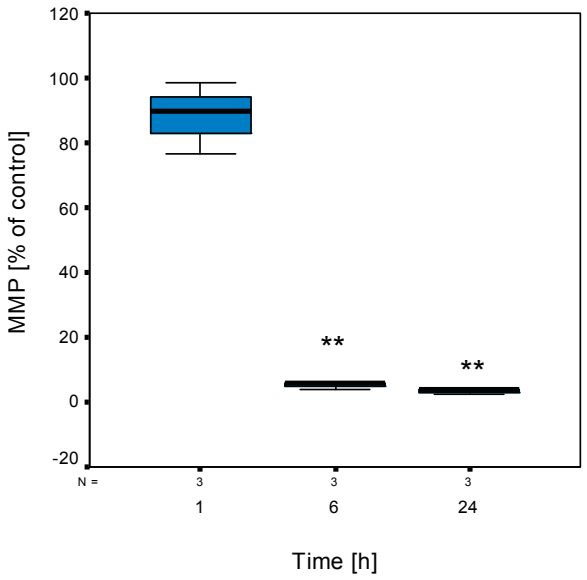

Figure 35: Determination of "the point of no-return": HepG2 cells were exposed to 20 µM MTBITC which was removed by washing after 1 or 6 h. The MMP was assessed after 24 h. HepG2 cells exposed to 20 µM MTBITC for the whole length of 24 h were used as reference control. The results are expressed relative to 0.1 % DMSO-treated cells. * $P \leq 0.05$, ** $P \leq 0.01$, statistically significant compared to control (N = 3)

Experiments were carried out to define the time point at which MTBITC-treatment of p53-induced HepG2 cells had to be terminated to prevent the cells from apoptosis induction. Cells were treated for 1 h (the point at which only p53-induction was detectable) or 6 h (the point at which p53-induction plus MMP disruption were detectable) with 20 µM MTBITC, which was then thoroughly washed out and harvested at the time point 24 hours. The exposure of cells towards 0.1 % DMSO or 20 µM MTBITC for the whole period of 24 h were used as controls. Figure 35 depicts the results of the effect on the MMP of HepG2 cells, derived from three independent experiments, presented relative to the control. Figure 36 displays the electrophoretic separation of internucleosomal DNA fragments of HepG2 cells as a parameter for apoptosis induction. Interestingly, the privation of MTBITC after 1 h saved the cells from a mitochondrial depolarization, which also prevented them from undergoing apoptosis. The "point of no return," beyond which MTBITC-exposure resulted

in irreversible progression to the loss of the MMP, occurred after exposure to 20 µM MTBITC for 6 h. At that point, the MMP was left to 5.34 % ± 1.17 compared to control cells. In relation to that, the MMP of HepG2 cells treated with MTBITC for the whole 24 h was diminished to 3.52 ± 1.08.

In the DNA laddering assay, a distinct DNA fragmentation could be seen with cells treated with the positive control 6 µM CPT. No fragmentation could be observed in DNA derived from control or 1 h MTBITC-treated cells. 6-h treatment with MTBITC caused a weak but yet visible DNA ladder which intensified after the full length of 24 h-treatment with the ITC.

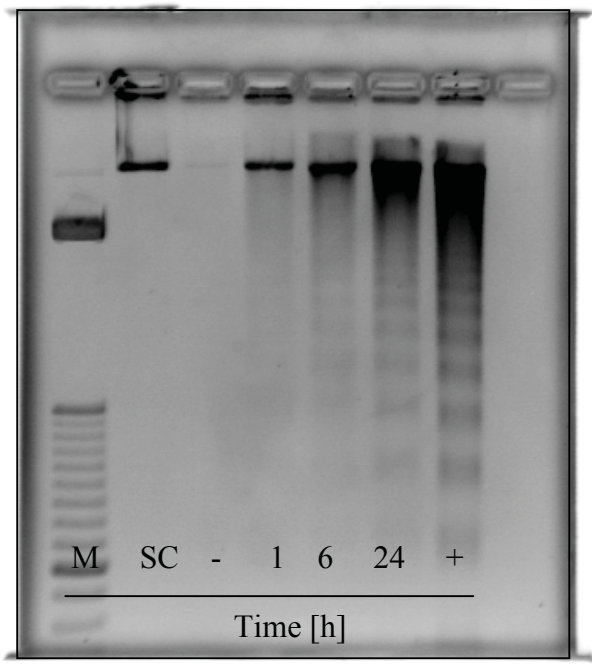

Figure 36: Internucleosomal DNA fragmentation as parameter for apoptosis induction for the determination of "the point of no-return": HepG2 cells were exposed to 20 µM MTBITC which was removed by washing after 1 or 6 h. Electrophoretic DNA separation was then assessed at the time point 24 h. HepG2 cells exposed to 20 µM MTBITC for the whole length of 24 h were used as reference control. M: size marker; SC: solvent control = 0.1 % DMSO; +: positive control = 6 µM CPT (N = 3).

VI. DISCUSSION

6.1 DNA damage is an initial event in MTBITC-mediated growth inhibition

At the beginning of the study, the WST-1 assay and the analysis of protein content showed a concentration-dependent reduction in proliferation of HepG2 cells after MTBITC-exposure. This was in accordance with other studies, which also reported inhibitory effects of ITCs on the growth of cancer cells in culture at µM-concentrations comparable with those at hand. For example, SFN, the structure analogue of MTBITC, inhibited the growth of colon cancer HT29 cells by 50 % at a concentration of 15 µM (Gamet-Payrastre et al., 1998). Phenylethyl ITC (PEITC) also reduced the proliferation of HepG2 cells with an IC_{50} value of 17 µM (Xiao et al., 2003). Therefore, it is interesting to note that at these concentrations the ITCs did not influence the growth of non-cancer cells, which were also tested in the reported studies. The reason for this difference in response to ITC-treatment is probably based on the elevated stress level necessary for cancer cells to maintain their normal metabolic activity. Additional stress therefore results in a threshold crossing, which initializes the suicide program of the cancer cell.

One of the earliest events in MTBITC-induced growth inhibition was probably a damaging effect on the DNA of HepG2 cells. This was already detected in the comet assay after 1 h-exposure of HepG2 cells to MTBITC. It is proposed, that due to its electrophilic properties, MTBITC reacts readily with the nucleophilic sites of the DNA to cause damage. Although it has been proposed that ITCs can undergo spontaneous hydrolysis, leading to the formation of superoxide and H_2O_2, it is not very likely that ROS production is responsible for the genotoxic effect at this early stage since no increased level in oxidative stress could be detected at that time. Although, it should be noted that only the production of peroxides could be detected with DHR123. The fact that almost 50 % of MTBITC were degraded within only one hour also accounts for the high intra-system reactivity of the ITC. It can also be excluded that the increase in DNA migration after MTBITC-treatment at that time is due to apoptotic changes in the cells as has been proposed by Choucroun and his group (Choucroun et al., 2001) since there were no indications in the apoptosis specific assays. In an earlier study, Kassie et al. also reported DNA breaking effects of benzyl ITC and phenylethyl ITC in a HepG2 cell line with concentrations of ≥ 5 µM (Kassie et al., 2003). However, the assay was terminated after 24 h-treatment of the cells with the ITCs. At that time point, the suicide program of the cells must have already been in progress and it cannot be excluded that their results were not at least influenced by apoptotic degradation

of DNA. It is known that the extent of DNA damage can also regulate the outcome. Low levels of DNA damage induce cell-cycle arrest, allowing the DNA damage to be repaired, and more extensive damage leads to the activation of the apoptotic process. It has been shown by our group that HepG2 cells can repair MTBITC-induced DNA damage to a certain extent (own data) and this might also be the reason for abrogation of apoptotic signs onto early removal of MTBITC (discussed later in this chapter); but at prolonged exposure towards MTBITC beyond this time, the DNA repair capabilities are obviously not sufficient to completely avoid the initialization of the apoptotic process.

6.2 MTBITC-induced apoptosis and G2/M arrest are downstream events of p53/p21^{WAF1}

Apoptosis is a genetically controlled mechanism of cell death that is essential for cell population homeostasis and for the elimination of unwanted, i.e. damaged cells. In the presence of un-repaired chromosomal alterations, cells are prevented from entering into mitosis by the activation of certain checkpoints that ensure orderly and timely completion of such defects; however, in the case of severe damage, cell cycle arrest leads to apoptosis. It has been suggested that pathways to induce cell cycle arrest and apoptosis are simultaneously activated, but apoptosis is dominant to cell cycle arrest in cells competent to die (Shen and White, 2001). In the present study, MTBITC-induced apoptosis in HepG2 cells could be observed by internucleosomal DNA fragmentation, flow cytometry analysis and the detection of single stranded apoptotic DNA. In all three assays, clear apoptotic events were present after 6 h-exposure to 20 µM MTBITC. Other studies have shown that although the group of ITCs are rather similar in structure, the time point of detectable apoptotic changes varies as well as the necessary concentration for its induction. In comparison to the results in the present study, HepG2 cells treated with 20 µM PEITC were TUNEL- and "SubG1-content" negative after 6 h, but stained positive after 12 h. However, caspase-3-like activity already significantly increased after 1 h (Rose et al., 2003). At a concentration of 20 µM, PEITC did not affect the cell cycle of HepG2 cells in their study; a G2/M phase-arrest could only be detected at 5 and 10 µM. This arrest was as early as 6 h and non-persistent at 5 µM, but irreversible at 10 µM PEITC-treatment. In the present study, 60 % of the HepG2 cells were caused to arrest by MTBITC at the G2/M phase of the cell cycle within the first 24 h, beginning at the same time as typical apoptotic features became evident and persisting for at least 24 h. This conforms to the observed reduction in the metabolic activity of HepG2 cells after 24 h, which remained static over a

prolonged time. Also, light-microscopic survey of the cells exposed to MTBITC for 48 h and 72 h (data not shown) did no show any further increase in detached, apoptotic cells, but a hold-up in cell number. All this would argue for a continuing arrest of more than 24 h. However, since no analysis of DNA content distribution was conducted for more than 24 h, it is for speculation whether the cells remained arrested or were also subsided to apoptotic death later on.

The decision between promoting cell cycle arrest versus apoptosis partially relies on the p53 protein level. Wild-type p53 is a sequence specific transcription factor mediating downstream effects such as cell cycle arrest or apoptosis in response to a variety of stress signals, including DNA damage, oncogene activation and hypoxia (Oren, 2003). Whereas high levels of p53 correlate with apoptosis, low level expression of the protein leads to cell cycle arrest. Furthermore, the proportion of arrested cells depends on cell type, growth conditions and the checkpoint controls operative in the cell (Niculescu et al., 1998). In the present study, increased expression of p53 and its family member p63 was observed in HepG2 cells after MTBITC-treatment in a time-dependent manner. This corresponds to a study recently published by Fimorgnari and co-workers, who reported an increase in p53 protein expression after 8 h of MTBITC-treatment in a concentration of 10 µM. This p53 stabilization was followed by a prolonged arrest of Jurkat cells at the G2 phase (Fimognari et al., 2004b). In the present study, the stabilized expression of p53 is reckoned to be a direct response to the chromosomal damage observed at the same time in the comet assay. It has been shown, that DNA single strand breaks lead to the DNA binding and consecutive stabilization of p53, which controls a G2 checkpoint upstream of $p21^{WAF1}$(Bunz et al., 1998). Shortly after the stabilization of p53, an increase in $p21^{WAF1}$ protein expression was observed in the study at hand, which was clearly stabilized 6 h after chemical treatment. $p21^{WAF1}$ is mainly reported as a mediator for the arrest of cells at the G1 phase, but it has also been shown to inhibit proliferation at the G2/M phase. Especially after DNA damage, $p21^{WAF1}$ is essential to sustain the G2 checkpoint in human cells (Gartel and Radhakrishnan, 2005). After 24 h-exposure of HepG2 cells to MTBITC, p53 was suppressed, probably by the activation of MDM2. It is known that high levels of MDM2 by increased p53 activity generates an auto-regulatory loop that leads to rapid turnover of the p53 protein, allowing induced p53 to act during a short time window before it is withdrawn to its normal cellular levels (Haupt et al., 1997; Kubbutat et al., 1997).

On the contrary, p63 was not degraded after MDM2 activation. Recent studies indicate the importance of the interaction between p63 and p53 in controlling the function of p53

during cellular death. It has been proposed that DNA damage not only recruits p53, but also p63, initializing the mitochondrial mediated-death pathway (Gressner et al., 2005). Although the members of the p53 family share a lot of gene regions, p63 is not destabilized by MDM2. p63 is able to physically interact with MDM2 in that way, increasing the steady-state level of intracellular p63 and enhancing its transcriptional activity (Calabro et al., 2002). Calabro and co-workers proposed that MDM2 expression could support p63-specific transcriptional function, while at the same time reducing interference by p53. These observations are consistent with the present findings that after MTBITC-treatment, p63 is immediately activated but then remains on a basal expression level. However, the level dramatically increases with the activation of MDM2 after 6 h, indicating for an MDM2-mediated stabilization of p63 rather than degradation.

p63 protein has already been shown to contribute to chemical-induced apoptosis, but this is the first time the involvement of p63 in ITC-induced apoptosis is reported in a study. The exact role and relevance of p63 in ITC-mediated cell death has yet to be determined in further studies. Like p53, p63 may simultaneously recruit genes, acting additively or synergistically in the ITC-mediated suicidal death. This protein might be especially interesting due to its prolonged activation and further stabilisation by MDM2 during the growth suppression of the hepatoma cells.

6.3 Glutathione depletion and the production of ROS in HepG2 cells

The loss of GSH may impair cellular antioxidant defences, resulting in the accumulation of ROS (Tirmenstein et al., 2000). These are generated as by-products of normal cellular function, mainly mitochondrial respiration or cytochrome P450, but are also found as downstream mediators of enhanced p53 expression in the apoptotic process (Johnson et al., 1996; Li et al., 1999). Hall proposed oxidative stress as a trigger of the apoptotic process, whereas GSH depletion renders cells more susceptible to oxidative damage (Hall, 1999). This, in consequence, may initialize signal transduction for the induction of programmed cell death.

In the present study, significant depletion of GSH occurred after 6 h-exposure to MTBITC in a concentration of ≥ 20 µM. This GSH depletion was persistent over at least 24 h and not temporarily as reported by Ye and Zhang (Ye and Zhang, 2001). As stated above, MTBITC is assumed to react with nucleophiles, especially those that contain a sulphur moiety like GSH. It has been reported that ITCs readily and strongly bind to GSH, a mechanism which is made responsible for the fast accumulation of ITCs within the cell.

Zhang reported a 200-fold total intracellular accumulation of SF or BITC as GSH-conjugates in murine Hepa1c1c7 cells compared to the extra-cellular level within 30 min. This accumulation resulted in a depletion of intracellular GSH by 50 % (Zhang, 2001). Similar effects were reported by other authors (Zhang, 2000). The loss of GSH may then allow critical protein thiol groups, e. g. the inner mitochondrial adenine nucleotide translocase (ANT), to be alkylated, which in turn results in the formation of oxidative stress (Hudson et al., 2005; Kim et al., 2003; Xu and Thornalley, 2001). Hepatic mitochondria are especially vulnerable to the accumulation of ROS since they lack the H_2O_2-metabolizing enzyme catalase. This concurs with the present study, where a significant amount of ROS (i.e. predominantly peroxides), could be observed in parallel to the exhaustion of the GSH supplies and the beginning collapse of the MMP. Taking into account that the detected oxidative stress generation was a) significant, but rather weakly elevated compared to other studies and b) detectable at the same time of early apoptotic events, it is likely, that the monitored oxidative stress was due to leaking from damaged mitochondria rather than preceding the apoptotic cascade as suggested by Hall. It is also possible that the rise in peroxide level contributes as p53 downstream effector, as proposed earlier (Tirmenstein et al., 2000), although it should be mentioned that in their study, ROS were generated concomitantly with increased levels of p53 and the onset of apoptosis. In contrast, the peroxide production significantly elevated not until 6 h-treatment of HepG2 cells in the study at hand, despite a p53-stabilization after 1 h.

It also remains to be determined whether superoxides (*O) account for apoptosis initialisation by MTBITC as has been reported for PEITC in HepG2 cells (Rose et al., 2003). Significant *O production was reported in their study to occur as early as 1 h in PEITC-treated HepG2 cells. In contrast to the present study, the authors did not detect increased peroxide generation during PEITC-exposure, however their measurement ranged only from 0.25 to 3 h after treatment begin, which might have been too short for the peroxide detection. On the other hand, it should be taken into consideration that *O are rapidly converted by enzymes like e.g. superoxide dismutase (SOD) to H_2O_2 which is more stable than *O. Therefore, extensive *O-production would have been expected to be indirectly detectable with the H2DCFDA assay, applied in their study or DHR123 used in the present study. In PC-3 cells, for example, PEITC already induced both peroxide and *O-production after 1 h, whereas apoptosis induction was not detectable before 4 h, indicating an upstream-function of ROS in these cells (Xiao et al., 2006)

6.4 The intrinsic mitochondrial-dependent pathway contributes mainly to MTBITC-induced apoptosis

Dissipation of the mitochondrial membrane potential is a general feature of apoptosis, irrespective of the cell type and of the apoptosis inducer. Whenever a pharmacological or genetic manipulation succeeds in preventing apoptosis, it also abolishes the MMP disruption that usually precedes cytolysis. The MMP collapse constitutes an early event of apoptosis; nonetheless, it marks an already irreversible stage of the apoptotic process. Massive loss in mitochondrial integrity caused by ITCs has been reported by several authors. For example, Rose and co-workers (Rose et al., 2005) reported severe mitochondrial damage after exposure of HepG2 cells to 20 µM PEITC for only 15 min. In these studies it was proposed that the collapse of the MMP was due to the massive production of ROS by ITCs, exerting downstream signalling onto the mitochondria. Interestingly, a severe loss in the mitochondrial membrane integrity was not observed in the present study until 6 h of exposure of HepG2 cells to 20 µM MTBITC. The beginning collapse of the MMP was accompanied by the suppression of Bcl_{XL}, which exerts critical anti-apoptotic function by stabilizing the outer mitochondrial membrane and preventing the release of death factors (Huang and Strasser, 2000). As already discussed above, peroxide production was a late event in the present study and is considered to originate from within the mitochondria. But the confirmation of Bcl_{XL}-suppression allows to suggest yet a further possibility of cell death signalling besides the already discussed: it has been shown earlier, that over-expression of Bcl_{XL} suppresses p53-dependent cell death. Additionally, recent evidence has proposed the existence of a transcription-independent pathway of p53-mediated apoptosis. In this process, a fraction of the p53 molecules that accumulate in damaged cells translocates to mitochondria, and this translocation is sufficient for p53 to induce permeabilization of the outer mitochondrial membrane through formation of complexes with the protective proteins Bcl_{XL} and Bcl_2, resulting in the release of cytochorme c into the cytosol (Mihara et al., 2003; Mihara and Moll, 2003). So, whether the collapse of the MMP by MTBITC could be mediated indirectly through ROS or directly by p53 must be elucidated more closely in future research.

6.5 MTBITC successfully suppressed telomerase in HepG2 cells

For a long time, the approaches in telomerase research and its suppression as a potential new way in selective chemotherapy of cancer only focused on the theory that abrogation of its enzyme activity leads to the successive shortening of telomeres, finally resulting in

cellular crisis and senescence. So reports dealing with the suppression of telomerase in the presence of reduced cell viability were eyed critically and simply labeled “cytotoxic effects caused by chemical treatment”. For example, in a study by Holt et al. a 5-fold decrease in telomerase-activity after treatment of HT1080 and SW480 cells with the G2/M blocker doxorubicin was reported (Holt et al., 1997). However, this was accompanied by a large amount of cell death after 12 to 16 h. Nocodazole-treated cells also showed a 2.5-fold decrease in telomerase activity compared to control cells, but also contained 2-fold less protein per cell than the control population. Faraoni et al. evaluated the general applicability of telomerase activity measurement as a marker of chemotherapy failure in telomerase-positive tumor cells (Faraoni et al., 1997). The authors showed a clear correlation between the decline of telomerase activity and the antineoplastic agent-induced growth impairment of tumor cells. However, in their experiments, 50 % of the tumor cells were already suppressed by chemical treatment after 24 h, approaching 100 % suppression another 48 h later. Only very recently, it was concluded that telomerase regulation was not simply a matter of the enzymatic activity but that the catalytic subunit hTERT affects cell cycle regulation. Although conflicting information is available about the connection between the cell cycle of cancer cells and telomerase, some studies demonstrated that telomerase activity was constant during progression through the cell cycle stages of several immortal cultured cells and generally correlates with growth rate (Holt et al., 1997); others show an increase during the S phase of artificially arrested cells (Zhu et al., 1996). It seems, the analysis of telomerase depends upon the nature of cell-cycle perturbation, cell type and experimental design. Akiyama and co-workers investigated the influence of the anti-proliferative agent interferon α (IFN-α) on telomerase and its constituents (Akiyama et al., 1999). These investigations were performed by a halt of cell cycle progression, rather than progression from the resting state. They found telomerase activity and hTERT expression independent from the cell cycle of untreated Daudi cells but after IFN-α – treatment, a suppression of the enzyme activity in the cells accumulated at the G1 phase.

The role of hTERT in the regulation of the cell cycle and its importance in the vulnerability to drug-induced apoptosis is not well understood. But, it has been shown by Biroccio et al. that the ability of hTERT-positive human melanoma cells to recover from drug-induced damage was attributable to the restoration of cell cycle progression (Biroccio et al., 2003). In contrast to hTERT negative cells which were arrested irreversible at the G2/M phase of the cell cycle after chemical-treatment, hTERT-positive cells were saved of this G2/M block. The reconstitution of hTERT in these melanoma cells resulted in a decreased

number of total chromosomal end-to-end fusions rendering cells less sensitive to chemical induced apoptotic death. The persistence of structural chromosomal lesions was evident only in hTERT negative cells, treated with drugs.

In HepG2 cells, a suppression of hTERT protein by 50 % compared to control could be detected 24 h after exposure to MTBITC. At this time point, a maximal number of arrested cells at the G2/M phase and all typical features of apoptosis were observed. Telomerase enzyme activity was also significantly suppressed after 24 h, detected by the TRAP assay. These changes occurred without any detectable rapid shortening in telomere length of HepG2 cells. This corresponds to a study by Cao et al., who proposed a pro-survival, anti-apoptotic role of hTERT aside from its telomere elongating function in PMC42 breast cancer cells (Cao et al., 2002). In their study, down-regulation of hTERT resulted in apoptosis induction without telomere-shortening. Other authors also reported anti-apoptotic properties of hTERT, proposing a telomere capping function of telomerase, independently from the telomere elongation function (Blackburn, 2000). It seems that in MTBITC-treated HepG2 cells, the telomerase catalytic subunit also regulates cell survival besides its enzymatic role and that hTERT suppression might indeed be initialized by the activation of p53, as hypothesized. The downstream effect of p53-transactivation of the p21-promotor represents the negative modulator of the cell cycle, preventing progression past the G2/M checkpoint. It was reported by Lai and co-workers (Lai et al., 2007) that the activation of $p21^{WAF1}$ leads to the repression of the hTERT promotor, thereby effectively shutting down the cell cycle. In their study, hTERT exerted effects on its upstream regulators, p53 and p21, thereby partially regulating itself. Additionally, it has been shown that over-expression of $p21^{WAF1}$ induces the suppression of hTERT in human squamous cell carcinoma (Henderson et al., 2000) and glioma cells (Harada et al., 2000) which both abnormally express telomerase. This is in accordance to the present study, where the suppression of hTERT occurred after the activation of $p21^{WAF1}$, suggesting an indirect path of telomerase regulation besides the earlier proposed SP1 squelching for hTERT promoter repression (Xu et al., 2000). This telomerase suppression, mediated by the p53/p21/E2F pathway was already reported by Shats and his group (Shats et al., 2004).

Since MTBITC-induced apoptosis was mediated by the mitochondrial-death pathway, a migration of hTERT from the nucleus to the mitochondria could additionally play a role in MTBITC-mediated cell death. hTERT could thereby amplify the oxidative load in the mitochondria and result in increased damage to the mitochondrial DNA. This mechanism was proposed by Haendeler et al., who showed that H_2O_2 triggers the nuclear export of

hTERT, which dramatically increased the sensitivity of cells towards ROS-dependent apoptosis in their study (Haendeler et al., 2003). It will be a challenge for future research to elucidate these possible mechanistic pathways of hTERT regulation in growth inhibition by ITCs.

6.6 The HSP90 complex might stabilize the telomerase holenzyme

The time lag between the treatment begin of HepG2 cells with MTBITC and an observable suppression of telomerase is consistent with the reported long half-life of the functionally active enzyme (Holt et al., 1997). Telomerase activity appears to be highly stable with a half-life of > 24 h in a variety of cell lines. A number of studies reported a 12 to 48 h lasting delay between the downregulation of hTERT mRNA and the decrease in telomerase activity. For example, Shats et al. observed a significant p53-dependent reduction of hTERT mRNA 18 h post-treatment using real-time quantitative RT-PCR (Shats et al., 2004). A decline in the enzyme activity, however, did not occur before 48 h. It is proposed that in the present study an improved assembly of the remaining hTERT protein to the functionally active enzyme by the HSP complex resulted in a delayed activity decay and provided for an increased half-life of the telomerase enzyme, as so proposed by Akalin and co-workers (Akalin et al., 2001). Immunoblot-analysis revealed a strong, prolonging increase in the heat shock proteins HSP90 and HSP70 after MTBITC-treatment. The HSP90 chaperone complex, including p23, HSP90 and HSP70 is known to facilitate the folding of several reverse transcriptases. By forming conformation-dependent high-order chaperone complexes, HSP90 regulates the half-lives of its client proteins (Johnson et al., 1998). It was proposed earlier by Holt et al. that this complex is strongly required to allow functional association of the telomerase enzyme both *in vitro* and *in vivo* (Holt et al., 1999). The authors showed that HSP90 binds to hTERT, the blocking of this interaction inhibited the assembly of telomerase. Furthermore, after the addition of purified chaperones in an *in vitro* P69 prostate cell reconstitution system, telomerase activity dramatically increased, suggesting a significant proportion of telomerase being unfolded or unassembled in cells, possibly due to inadequate chaperone expression (Akalin et al., 2001).

6.7 Despite its rapid degradation, MTBITC could exert sufficient therapeutic effects

Disposal kinetics of ITCs have already been performed in animals (Ioannou et al., 1984) and humans (Ji and Morris, 2003). Also, the metabolic conversion of several ITCs have

been elucidated in cell culture systems or in animals (Zhang, 2000) . However, as yet, no efforts have been made to determine the kinetics of ITCs in the *in vitro* models at hand. To investigate the stability and kinetics of MTBITC under the conditions of the cell culture studies, and to learn more about the origin of the ITC-decomposition, a set of experiments was carried out and the ITC subsequently analysed by GC-MS/MS. The present kinetic studies of MTBITC in the cell culture system showed that the ITC degraded within the first hour by 50 % and was totally absent (i. e. below the detection limit) after 24 h. At first, the metabolic conversion of MTBITC by the hepatoma cells was thought to be solely responsible since the analysis covered only the ITC and not the metabolites. Zhang et al. showed that ITCs are rapidly converted to their thio-derivatives *in vitro* and *in vivo* (Zhang, 2000). However, the next set of experiments, repeated in the same line but without cells, revealed that only around 10 % could be attributed to the metabolic activity of HepG2 cells. The reactivity and volatility of ITCs was already noted above. ITCs react rapidly, and under mild conditions with oxygen-, sulfur-, or nitrogen centered nucleophiles to give rise to carbamates, thiocarbamates, or thiourea derivatives, respectively (Zhang and Talalay, 1994). Ohta and his group showed that allyl ITC is highly unstable in aqueous solution, its decomposition by the nucleophilic attack of water or even more of hydroxide ions against the ITC group being rapid (Ohta et al., 1995). A study by Sommerlade and co-workers dealing with the behaviour of ITC in atmospheric surroundings demonstrated that ITCs react intensely with OH radicals to form a variety of different conversion products, which are mainly isocyanates and sulfur dioxide (Sommerlade et al., 2006). Jiang and his group (Jiang et al., 2006) confirmed later the fact that the reaction between ITC and hydroxyl/water was endothermic, thus *in vitro* experiments, normally carried out at 37°C, always present extreme unfavorable conditions for the ITC. MTBITC differs structurally only slightly from allyl ITC, therefore, the vast amount of MTBITC degradation is possibly due to its reactivity with the surrounding aqueous material. Additionally, the autolysis of MTBITC to its isocyanate-derivative could also account for the observations. Loss by simple diffusion of the volatile MTBITC out of the culture flask is therefore thought to constitute for around 10 % of the total. About 25 % might be attributed to the reaction of MTBITC with thiol-containing amino acids (e.g. methionine) or larger proteins in the culture medium. Albumin for instance, which is also supplemented to the culture medium, has been proposed to be the main transporting molecule of ITCs within the blood system (Holst and Williamson, 2004) and a docking of MTBITC to such a protein in the medium would indeed result in a decreased extraction result.

These findings are all the more intriguing considering the rapid loss in MTBITC on the one hand, and the strong cytostatic effect of the ITC on the other. This suggests that irrespective of the intense degradation kinetics of MTBITC, the anti-proliferative activity and the potency in apoptosis induction is not markedly affected by it.

It has been suggested that early stages of p53-induced apoptosis may be reversible upon removal of the apoptosis stimulus due to DNA repair initialization (Geske et al., 2000). The reversibility of MTBITC-induced death of HepG2 hepatoma cells was tested at the initiation phase (DNA damage after 1 h) and at the commitment/degradation phase (beginning MMP collapse after 6 h) which showed that the apoptotic process may only indeed be reversible or at least weakened at the very early stages upon a removal of MTBITC. It was also shown in a study by Zhang et al. that exposure to ITCs for only a short time of one or three hours was sufficient to irreversibly inhibit cell growth (Zhang et al., 2003). *In vivo*, ITCs are metabolised and excreted within 24 h with a blood plasma peak concentration during the first 2 to 6 h. Thus, although the ITC is only present at maximum concentrations in a living system for a rather short time, this might be sufficient to exert its therapeutic effects.

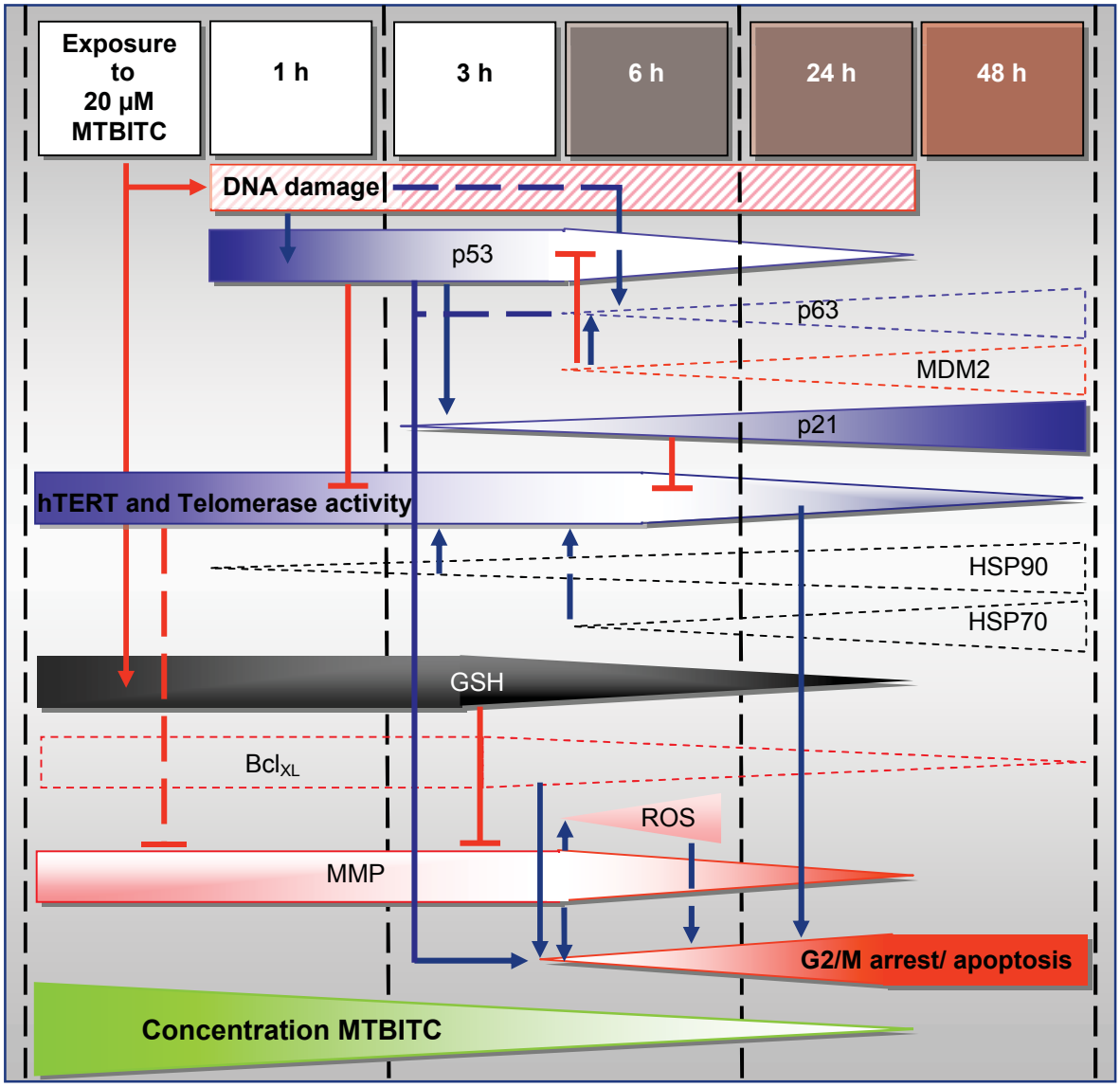

Figure 42: Time scheme of the events detected in HepG2 cells after exposure to MTBITC for 1 to 48 h and proposed signalling pathways. → indicate the initial interaction of MTBITC with GSH or the DNA. → was used to indicate an activating event. ⊥ was set for a proposed blocking/destabilizing mechanism.

6.8 Conclusions

This study presents for the first time the suppression of telomerase in malignant cells mediated by ITCs. MTBITC-treatment of HepG2 cells could successfully down-regulate telomerase, either through transcriptional suppression of hTERT by p53 or through an indirect $p21^{WAF1}$-dependent pathway. The present findings support the idea of an existing extra-telomeric, cell cycle regulation function of hTERT in HepG2 cells. Thus, DNA damage induced by MTBITC is proposed to present the initial event leading to p53-activated cell cycle arrest and apoptosis induction in these cells. Whether p63 promotes stabilization of p53 and which contribution p63 generally makes in hTERT suppression has to be further explored. The role of telomerase in ITC-mediated growth suppression of malignant cells will now have to be elucidated more closely and its general contribution in ITC-mediated apoptosis induction and cell proliferation clarified. This information may help for a better understanding of the role of telomerase and could be valuable in improving the effectiveness of future therapeutic interventions.

6.9 Future perspectives

In an actual study in our lab, MTBITC and several other structure analogues have been shown to exert also positive results in the micronucleus (MN) test, carried out with HepG2 cells. The MN test is a biomarker of chromosomal instability, whereas the detected MNs are due to the exclusion of chromosomes or chromosomal fragments from daughter nuclei (Fenech, 2005). The results of the present study raise the question, whether this genotoxicity observed with the MN test in HepG2 cells after the ITC-treatment is at least partly due to the detection of end-to-end fusions, initialized by the suppression of hTERT, which consequently resulted in the loss of telomere capping. As already stated, HepG2 cells possess only short telomeres and are therefore very susceptible for chromosomal alterations. This becomes especially apparent in the MN test, where it has been shown, that HepG2 cells exert a rather high rate in the spontaneous formation of micronuclei, compared to other cell lines. For this reason, it would be intriguing to find out, if the increased frequency of MNs observed after cell-treatment with ITCs, origins from the exclusion of telomeric sequences. This would shed a new light on the meaning of positive results in the MN test derived from experiments with ITCs.

VII. LIST OF REFERENCES

Aden D.P., Fogel A., Plotkin S., Damjanov I., Knowles B.B. 1979. Controlled synthesis of HBsAg in a differentiated human liver carcinoma-derived cell line. Nature 282(5739):615-616.

Akalin A., Elmore L.W., Forsythe H.L., Amaker B.A., McCollum E.D., Nelson P.S., Ware J.L., Holt S.E. 2001. A novel mechanism for chaperone-mediated telomerase regulation during prostate cancer progression. Cancer Res 61(12):4791-4796.

Akiyama M., Horiguchi-Yamada J., Saito S., Hoshi Y., Yamada O., Mizoguchi H., Yamada H. 1999. Cytostatic concentrations of anticancer agents do not affect telomerase activity of leukaemic cells in vitro. Eur J Cancer 35(2):309-315.

Allera C., Lazzarini G., Patrone E., Alberti I., Barboro P., Sanna P., Melchiori A., Parodi S., Balbi C. 1997. The condensation of chromatin in apoptotic thymocytes shows a specific structural change. J Biol Chem 272(16):10817-10822.

Baerlocher G.M., Mak J., Tien T., Lansdorp P.M. 2002. Telomere length measurement by fluorescence in situ hybridization and flow cytometry: tips and pitfalls. Cytometry 47(2):89-99.

Berridge M., Tan A., McCoy C., Wang R. 1996. The biochemical and cellular basis of the cell proliferation assays that use tetrazolium salts. Biochemica 4:14-19.

Bianchini F., Vainio H. 2004. Isothiocyanates in cancer prevention. Drug Metab Rev 36(3-4):655-667.

Biroccio A., Gabellini C., Amodei S., Benassi B., Del Bufalo D., Elli R., Antonelli A., D'Incalci M., Zupi G. 2003. Telomere dysfunction increases cisplatin and ecteinascidin-743 sensitivity of melanoma cells. Mol Pharmacol 63(3):632-638.

Blackburn E.H. 2000. Telomere states and cell fates. Nature 408(6808):53-56.

Bodnar A.G., Ouellette M., Frolkis M., Holt S.E., Chiu C.P., Morin G.B., Harley C.B., Shay J.W., Lichtsteiner S., Wright W.E. 1998. Extension of life-span by introduction of telomerase into normal human cells. Science 279(5349):349-352.

Bradford M.M. 1976. A rapid and sensitive method for the quantitation of microgram quantities of protein utilizing the principle of protein-dye binding. Anal Biochem 72:248-254.

Bressac B., Galvin K.M., Liang T.J., Isselbacher K.J., Wands J.R., Ozturk M. 1990. Abnormal structure and expression of p53 gene in human hepatocellular carcinoma. Proc Natl Acad Sci U S A 87(5):1973-1977.

Bryan T.M., Sperger J.M., Chapman K.B., Cech T.R. 1998. Telomerase reverse transcriptase genes identified in Tetrahymena thermophila and Oxytricha trifallax. Proc Natl Acad Sci U S A 95(15):8479-8484.

Bunz F., Dutriaux A., Lengauer C., Waldman T., Zhou S., Brown J.P., Sedivy J.M., Kinzler K.W., Vogelstein B. 1998. Requirement for p53 and p21 to sustain G2 arrest after DNA damage. Science 282(5393):1497-1501.

Burnette W.N. 1981. "Western blotting": electrophoretic transfer of proteins from sodium dodecyl sulfate--polyacrylamide gels to unmodified nitrocellulose and radiographic detection with antibody and radioiodinated protein A. Anal Biochem 112(2):195-203.

Buttery R., Guadagni D., Ling L., Seifert R., Lipton W. 1976. Additional Volatile Components of Cabbage, Broccoli, and Cauliflower. J Agric Food Chem 24(4):829-832.

Calabro V., Mansueto G., Parisi T., Vivo M., Calogero R.A., La Mantia G. 2002. The human MDM2 oncoprotein increases the transcriptional activity and the protein level of the p53 homolog p63. J Biol Chem 277(4):2674-2681.

Cao Y., Li H., Deb S., Liu J.P. 2002. TERT regulates cell survival independent of telomerase enzymatic activity. Oncogene 21(20):3130-3138.

Capranico G., Ferri F., Fogli M.V., Russo A., Lotito L., Baranello L. 2007. The effects of camptothecin on RNA polymerase II transcription: roles of DNA topoisomerase I. Biochimie 89(4):482-489.

Chang J.T., Chen Y.L., Yang H.T., Chen C.Y., Cheng A.J. 2002. Differential regulation of telomerase activity by six telomerase subunits. Eur J Biochem 269(14):3442-3450.

Choucroun P., Gillet D., Dorange G., Sawicki B., Dewitte J.D. 2001. Comet assay and early apoptosis. Mutat Res 478(1-2):89-96.

Collins A.R., Dobson V.L., Dusinska M., Kennedy G., Stetina R. 1997. The comet assay: what can it really tell us? Mutat Res 375(2):183-193.

Conaway C.C., Yang Y.M., Chung F.L. 2002. Isothiocyanates as cancer chemopreventive agents: their biological activities and metabolism in rodents and humans. Curr Drug Metab 3(3):233-255.

Cong Y.S., Wen J., Bacchetti S. 1999. The human telomerase catalytic subunit hTERT: organization of the gene and characterization of the promoter. Hum Mol Genet 8(1):137-142.

Darzynkiewicz Z., Bedner E., Traganos F. 2001. Difficulties and pitfalls in analysis of apoptosis. Methods Cell Biol 63:527-546.

Darzynkiewicz Z., Juan G., Li X., Gorczyca W., Murakami T., Traganos F. 1997. Cytometry in cell necrobiology: analysis of apoptosis and accidental cell death (necrosis). Cytometry 27(1):1-20.

Doostdar H., Grant M.H., Melvin W.T., Wolf C.R., Burke M.D. 1993. The effects of inducing agents on cytochrome P450 and UDP-glucuronyltransferase activities in human HEPG2 hepatoma cells. Biochem Pharmacol 46(4):629-635.

Ducrest A.L., Szutorisz H., Lingner J., Nabholz M. 2002. Regulation of the human telomerase reverse transcriptase gene. Oncogene 21(4):541-552.

Fahey J.W., Zalcmann A.T., Talalay P. 2001. The chemical diversity and distribution of glucosinolates and isothiocyanates among plants. Phytochemistry 56(1):5-51.

Fairbairn D.W., Olive P.L., O'Neill K.L. 1995. The comet assay: a comprehensive review. Mutat Res 339(1):37-59.

Faraoni I., Turriziani M., Masci G., De Vecchis L., Shay J.W., Bonmassar E., Graziani G. 1997. Decline in telomerase activity as a measure of tumor cell killing by antineoplastic agents in vitro. Clin Cancer Res 3(4):579-585.

Faust F., Kassie F., Knasmuller S., Boedecker R.H., Mann M., Mersch-Sundermann V. 2004. The use of the alkaline comet assay with lymphocytes in human biomonitoring studies. Mutat Res 566(3):209-229.

Fenech M. 2005. In vitro micronucleus technique to predict chemosensitivity. Methods Mol Med 111:3-32.

Feng J., Funk W.D., Wang S.S., Weinrich S.L., Avilion A.A., Chiu C.P., Adams R.R., Chang E., Allsopp R.C., Yu J., et al. 1995. The RNA component of human telomerase. Science 269(5228):1236-1241.

Fimognari C., Nusse M., Berti F., Iori R., Cantelli-Forti G., Hrelia P. 2004a. Isothiocyanates as novel cytotoxic and cytostatic agents: molecular pathway on human transformed and non-transformed cells. Biochem Pharmacol 68(6):1133-1138.

Fimognari C., Nusse M., Iori R., Cantelli-Forti G., Hrelia P. 2004b. The new isothiocyanate 4-(methylthio)butylisothiocyanate selectively affects cell-cycle

progression and apoptosis induction of human leukemia cells. Invest New Drugs 22(2):119-129.

Foley G.E., Lazarus H., Farber S., Uzman B.G., Boone B.A., McCarthy R.E. 1965. Continuous Culture of Human Lymphoblasts from Peripheral Blood of a Child with Acute Leukemia. Cancer 18:522-529.

Forsythe H.L., Jarvis J.L., Turner J.W., Elmore L.W., Holt S.E. 2001. Stable association of hsp90 and p23, but Not hsp70, with active human telomerase. J Biol Chem 276(19):15571-15574.

Frankfurt O.S., Krishan A. 2001a. Enzyme-linked immunosorbent assay (ELISA) for the specific detection of apoptotic cells and its application to rapid drug screening. J Immunol Methods 253(1-2):133-144.

Frankfurt O.S., Krishan A. 2001b. Identification of apoptotic cells by formamide-induced dna denaturation in condensed chromatin. J Histochem Cytochem 49(3):369-378.

Furuta M., Nozawa K., Takemura M., Izuta S., Murate T., Tsuchiya M., Yoshida K., Taka N., Nimura Y., Yoshida S. 2003. A novel platinum compound inhibits telomerase activity in vitro and reduces telomere length in a human hepatoma cell line. Int J Cancer 104(6):709-715.

Gamet-Payrastre L., Lumeau S., Gasc N., Cassar G., Rollin P., Tulliez J. 1998. Selective cytostatic and cytotoxic effects of glucosinolates hydrolysis products on human colon cancer cells in vitro. Anticancer Drugs 9(2):141-148.

Gartel A.L., Radhakrishnan S.K. 2005. Lost in transcription: p21 repression, mechanisms, and consequences. Cancer Res 65(10):3980-3985.

Geske F.J., Nelson A.C., Lieberman R., Strange R., Sun T., Gerschenson L.E. 2000. DNA repair is activated in early stages of p53-induced apoptosis. Cell Death Differ 7(4):393-401.

Golstein P., Ojcius D.M., Young J.D. 1991. Cell death mechanisms and the immune system. Immunol Rev 121:29-65.

Gong J., Traganos F., Darzynkiewicz Z. 1994. A selective procedure for DNA extraction from apoptotic cells applicable for gel electrophoresis and flow cytometry. Anal Biochem 218(2):314-319.

Grand C.L., Han H., Munoz R.M., Weitman S., Von Hoff D.D., Hurley L.H., Bearss D.J. 2002. The cationic porphyrin TMPyP4 down-regulates c-MYC and human telomerase reverse transcriptase expression and inhibits tumor growth in vivo. Mol Cancer Ther 1(8):565-573.

Gressner O., Schilling T., Lorenz K., Schulze Schleithoff E., Koch A., Schulze-Bergkamen H., Lena A.M., Candi E., Terrinoni A., Catani M.V., Oren M., Melino G., Krammer P.H., Stremmel W., Muller M. 2005. TAp63alpha induces apoptosis by activating signaling via death receptors and mitochondria. Embo J 24(13):2458-2471.

Griffith J.D., Comeau L., Rosenfield S., Stansel R.M., Bianchi A., Moss H., de Lange T. 1999. Mammalian telomeres end in a large duplex loop. Cell 97(4):503-514.

Haendeler J., Hoffmann J., Brandes R.P., Zeiher A.M., Dimmeler S. 2003. Hydrogen peroxide triggers nuclear export of telomerase reverse transcriptase via Src kinase family-dependent phosphorylation of tyrosine 707. Mol Cell Biol 23(13):4598-4610.

Hall A.G. 1999. Review: The role of glutathione in the regulation of apoptosis. Eur J Clin Invest 29(3):238-245.

Harada K., Kurisu K., Sadatomo T., Tahara H., Tahara E., Ide T., Tahara E. 2000. Growth inhibition of human glioma cells by transfection-induced P21 and its effects on telomerase activity. J Neurooncol 47(1):39-46.

Harris K.E., Jeffery E.H. 2007. Sulforaphane and erucin increase MRP1 and MRP2 in human carcinoma cell lines. J Nutr Biochem.

Haupt Y., Maya R., Kazaz A., Oren M. 1997. Mdm2 promotes the rapid degradation of p53. Nature 387(6630):296-299.

Hecht S.S. 1999. Chemoprevention of cancer by isothiocyanates, modifiers of carcinogen metabolism. J Nutr 129(3):768S-774S.

Henderson L.M., Chappell J.B. 1993. Dihydrorhodamine 123: a fluorescent probe for superoxide generation? Eur J Biochem 217(3):973-980.

Henderson Y.C., Breau R.L., Liu T.J., Clayman G.L. 2000. Telomerase activity in head and neck tumors after introduction of wild-type p53, p21, p16, and E2F-1 genes by means of recombinant adenovirus. Head Neck 22(4):347-354.

Hewitt N.J., Hewitt P. 2004. Phase I and II enzyme characterization of two sources of HepG2 cell lines. Xenobiotica 34(3):243-256.

Holst B., Williamson G. 2004. A critical review of the bioavailability of glucosinolates and related compounds. Nat Prod Rep 21(3):425-447.

Holt S.E., Aisner D.L., Baur J., Tesmer V.M., Dy M., Ouellette M., Trager J.B., Morin G.B., Toft D.O., Shay J.W., Wright W.E., White M.A. 1999. Functional requirement of p23 and Hsp90 in telomerase complexes. Genes Dev 13(7):817-826.

Holt S.E., Aisner D.L., Shay J.W., Wright W.E. 1997. Lack of cell cycle regulation of telomerase activity in human cells. Proc Natl Acad Sci U S A 94(20):10687-10692.

Hosono S., Lee C.S., Chou M.J., Yang C.S., Shih C.H. 1991. Molecular analysis of the p53 alleles in primary hepatocellular carcinomas and cell lines. Oncogene 6(2):237-243.

Huang C., Ma W.Y., Li J., Hecht S.S., Dong Z. 1998. Essential role of p53 in phenethyl isothiocyanate-induced apoptosis. Cancer Res 58(18):4102-4106.

Huang D.C., Strasser A. 2000. BH3-Only proteins-essential initiators of apoptotic cell death. Cell 103(6):839-842.

Hudson T.S., Stoner G.D., Morse M.A., Young H., Mallery S.R. 2005. Comparison of phenethyl and 6-phenylhexyl isothiocyanate-induced toxicity in rat esophageal cell lines with and without glutathione depletion. Toxicol Lett 155(3):427-436.

Ioannou Y.M., Burka L.T., Matthews H.B. 1984. Allyl isothiocyanate: comparative disposition in rats and mice. Toxicol Appl Pharmacol 75(2):173-181.

Iwakuma T., Lozano G. 2003. MDM2, an introduction. Mol Cancer Res 1(14):993-1000.

Ji Y., Morris M.E. 2003. Determination of phenethyl isothiocyanate in human plasma and urine by ammonia derivatization and liquid chromatography-tandem mass spectrometry. Anal Biochem 323(1):39-47.

Jiang Z.-T., Zhang Q.-F., Tian H.-L., Li R. 2006. The reaction of allyl isothiocyanate with hydroxyl/water and b-cyclodextrin using ultraviolet spectrometry. Food Technol Biotechnol 44(3):423-427.

Johnson B.D., Schumacher R.J., Ross E.D., Toft D.O. 1998. Hop modulates Hsp70/Hsp90 interactions in protein folding. J Biol Chem 273(6):3679-3686.

Johnson L.V., Walsh M.L., Chen L.B. 1980. Localization of mitochondria in living cells with rhodamine 123. Proc Natl Acad Sci U S A 77(2):990-994.

Johnson T.M., Yu Z.X., Ferrans V.J., Lowenstein R.A., Finkel T. 1996. Reactive oxygen species are downstream mediators of p53-dependent apoptosis. Proc Natl Acad Sci U S A 93(21):11848-11852.

Kajstura M., Halicka H.D., Pryjma J., Darzynkiewicz Z. 2007. Discontinuous fragmentation of nuclear DNA during apoptosis revealed by discrete "sub-G1" peaks on DNA content histograms. Cytometry A 71(3):125-131.

Kanaya T., Kyo S., Hamada K., Takakura M., Kitagawa Y., Harada H., Inoue M. 2000. Adenoviral expression of p53 represses telomerase activity through down-regulation of human telomerase reverse transcriptase transcription. Clin Cancer Res 6(4):1239-1247.

Kapoor V., Telford W.G. 2004. Telomere length measurement by fluorescence in situ hybridization and flow cytometry. Methods Mol Biol 263:385-398.

Kassahun K., Davis M., Hu P., Martin B., Baillie T. 1997. Biotransformation of the naturally occurring isothiocyanate sulforaphane in the rat: identification of phase I metabolites and glutathione conjugates. Chem Res Toxicol 10(11):1228-1233.

Kassie F., Laky B., Gminski R., Mersch-Sundermann V., Scharf G., Lhoste E., Kansmuller S. 2003. Effects of garden and water cress juices and their constituents, benzyl and phenethyl isothiocyanates, towards benzo(a)pyrene-induced DNA damage: a model study with the single cell gel electrophoresis/Hep G2 assay. Chem Biol Interact 142(3):285-296.

Keum Y.S., Jeong W.S., Kong A.N. 2004. Chemoprevention by isothiocyanates and their underlying molecular signaling mechanisms. Mutat Res 555(1-2):191-202.

Kim B.R., Hu R., Keum Y.S., Hebbar V., Shen G., Nair S.S., Kong A.N. 2003. Effects of glutathione on antioxidant response element-mediated gene expression and apoptosis elicited by sulforaphane. Cancer Res 63(21):7520-7525.

Kim N.W., Piatyszek M.A., Prowse K.R., Harley C.B., West M.D., Ho P.L., Coviello G.M., Wright W.E., Weinrich S.L., Shay J.W. 1994. Specific association of human telomerase activity with immortal cells and cancer. Science 266(5193):2011-2015.

Knasmuller S., Mersch-Sundermann V., Kevekordes S., Darroudi F., Huber W.W., Hoelzl C., Bichler J., Majer B.J. 2004. Use of human-derived liver cell lines for the detection of environmental and dietary genotoxicants; current state of knowledge. Toxicology 198(1-3):315-328.

Knasmuller S., Parzefall W., Sanyal R., Ecker S., Schwab C., Uhl M., Mersch-Sundermann V., Williamson G., Hietsch G., Langer T., Darroudi F., Natarajan A.T. 1998. Use of metabolically competent human hepatoma cells for the detection of mutagens and antimutagens. Mutat Res 402(1-2):185-202.

Knowles B.B., Howe C.C., Aden D.P. 1980. Human hepatocellular carcinoma cell lines secrete the major plasma proteins and hepatitis B surface antigen. Science 209(4455):497-499.

Kooy N.W., Royall J.A., Ischiropoulos H., Beckman J.S. 1994. Peroxynitrite-mediated oxidation of dihydrorhodamine 123. Free Radic Biol Med 16(2):149-156.

Kuang Y.F., Chen Y.H. 2004. Induction of apoptosis in a non-small cell human lung cancer cell line by isothiocyanates is associated with P53 and P21. Food Chem Toxicol 42(10):1711-1718.

Kubbutat M.H., Jones S.N., Vousden K.H. 1997. Regulation of p53 stability by Mdm2. Nature 387(6630):299-303.

Kullak-Ublick G.A., Beuers U., Paumgartner G. 1996. Molecular and functional characterization of bile acid transport in human hepatoblastoma HepG2 cells. Hepatology 23(5):1053-1060.

Laemmli U.K. 1970. Cleavage of structural proteins during the assembly of the head of bacteriophage T4. Nature 227(5259):680-685.

Lai S.R., Cunningham A.P., Huynh V.Q., Andrews L.G., Tollefsbol T.O. 2007. Evidence of extra-telomeric effects of hTERT and its regulation involving a feedback loop. Exp Cell Res 313(2):322-330.

Lauzon W., Sanchez Dardon J., Cameron D.W., Badley A.D. 2000. Flow cytometric measurement of telomere length. Cytometry 42(3):159-164.

Law H., Lau Y. 2001. Validation and development of quantitative flow cytometry-based fluorescence in situ hybridization for intercenter comparison of telomere length measurement. Cytometry 43(2):150-153.

Li P.F., Dietz R., von Harsdorf R. 1999. p53 regulates mitochondrial membrane potential through reactive oxygen species and induces cytochrome c-independent apoptosis blocked by Bcl-2. Embo J 18(21):6027-6036.

Lin S.Y., Elledge S.J. 2003. Multiple tumor suppressor pathways negatively regulate telomerase. Cell 113(7):881-889.

Mersch-Sundermann V., Knasmuller S., Wu X.J., Darroudi F., Kassie F. 2004. Use of a human-derived liver cell line for the detection of cytoprotective, antigenotoxic and cogenotoxic agents. Toxicology 198(1-3):329-340.

Mihara M., Erster S., Zaika A., Petrenko O., Chittenden T., Pancoska P., Moll U.M. 2003. p53 has a direct apoptogenic role at the mitochondria. Mol Cell 11(3):577-590.

Mihara M., Moll U.M. 2003. Detection of mitochondrial localization of p53. Methods Mol Biol 234:203-209.

Niculescu A.B., 3rd, Chen X., Smeets M., Hengst L., Prives C., Reed S.I. 1998. Effects of p21(Cip1/Waf1) at both the G1/S and the G2/M cell cycle transitions: pRb is a critical determinant in blocking DNA replication and in preventing endoreduplication. Mol Cell Biol 18(1):629-643.

Ohta Y., Takatani K., Kawakishi S. 1995. Decomposition rate of allyl isothiocyanate in aqueous solution Biosci Biotech Biochem 59(1):102-103.

Oren M. 2003. Decision making by p53: life, death and cancer. Cell Death Differ 10(4):431-442.

Patai S., Ed. 1977. The Chemistry of Cyanates and their Thio Derivatives. Wiley, NY

Perrault S.D., Hornsby P.J., Betts D.H. 2005. Global gene expression response to telomerase in bovine adrenocortical cells. Biochem Biophys Res Commun 335(3):925-936.

Puisieux A., Galvin K., Troalen F., Bressac B., Marcais C., Galun E., Ponchel F., Yakicier C., Ji J., Ozturk M. 1993. Retinoblastoma and p53 tumor suppressor genes in human hepatoma cell lines. Faseb J 7(14):1407-1413.

Ramirez R., Carracedo J., Jimenez R., Canela A., Herrera E., Aljama P., Blasco M.A. 2003. Massive telomere loss is an early event of DNA damage-induced apoptosis. J Biol Chem 278(2):836-842.

Rojas E., Lopez M.C., Valverde M. 1999. Single cell gel electrophoresis assay: methodology and applications. J Chromatogr B Biomed Sci Appl 722(1-2):225-254.

Rose P., Armstrong J.S., Chua Y.L., Ong C.N., Whiteman M. 2005. Beta-phenylethyl isothiocyanate mediated apoptosis; contribution of Bax and the mitochondrial death pathway. Int J Biochem Cell Biol 37(1):100-119.

Rose P., Whiteman M., Huang S.H., Halliwell B., Ong C.N. 2003. beta-Phenylethyl isothiocyanate-mediated apoptosis in hepatoma HepG2 cells. Cell Mol Life Sci 60(7):1489-1503.

Royall J.A., Ischiropoulos H. 1993. Evaluation of 2',7'-dichlorofluorescin and dihydrorhodamine 123 as fluorescent probes for intracellular H2O2 in cultured endothelial cells. Arch Biochem Biophys 302(2):348-355.

Rufer N., Dragowska W., Thornbury G., Roosnek E., Lansdorp P.M. 1998. Telomere length dynamics in human lymphocyte subpopulations measured by flow cytometry. Nat Biotechnol 16(8):743-747.

Safiulina D., Veksler V., Zharkovsky A., Kaasik A. 2006. Loss of mitochondrial membrane potential is associated with increase in mitochondrial volume: physiological role in neurones. J Cell Physiol 206(2):347-353.

Saito M., Nakagawa K., Hamada K., Hirose S., Harada H., Kohno S., Nagato S., Ohnishi T. 2004. Introduction of p16INK4a inhibits telomerase activity through transcriptional suppression of human telomerase reverse transcriptase expression in human gliomas. Int J Oncol 24(5):1213-1220.

Scharf G., Prustomersky S., Knasmuller S., Schulte-Hermann R., Huber W.W. 2003. Enhancement of glutathione and g-glutamylcysteine synthetase, the rate limiting enzyme of glutathione synthesis, by chemoprotective plant-derived food and beverage components in the human hepatoma cell line HepG2. Nutr Cancer 45(1):74-83.

Shats I., Milyavsky M., Tang X., Stambolsky P., Erez N., Brosh R., Kogan I., Braunstein I., Tzukerman M., Ginsberg D., Rotter V. 2004. p53-dependent down-regulation of telomerase is mediated by p21waf1. J Biol Chem 279(49):50976-50985.

Shay J.W., Bacchetti S. 1997. A survey of telomerase activity in human cancer. Eur J Cancer 33(5):787-791.

Shen Y., White E. 2001. p53-dependent apoptosis pathways. Adv Cancer Res 82:55-84.

Shimada A., Kato S., Enjo K., Osada M., Ikawa Y., Kohno K., Obinata M., Kanamaru R., Ikawa S., Ishioka C. 1999. The transcriptional activities of p53 and its homologue p51/p63: similarities and differences. Cancer Res 59(12):2781-2786.

Silvers K.J., Eddy E.P., McCoy E.C., Rosenkranz H.S., Howard P.C. 1994. Pathways for the mutagenesis of 1-nitropyrene and dinitropyrenes in the human hepatoma cell line HepG2. Environ Health Perspect 102 Suppl 6:195-200.

Singh N.P., Danner D.B., Tice R.R., Brant L., Schneider E.L. 1990. DNA damage and repair with age in individual human lymphocytes. Mutat Res 237(3-4):123-130.

Smogorzewska A., de Lange T. 2004. Regulation of telomerase by telomeric proteins. Annu Rev Biochem 73:177-208.

Sommerlade R., Ekici P., Parlar H. 2006. Gas phase reaction of selected isothiocyanates with OH

radicals using a smog chamber-mass analyzer system. Atmospheric Environment 40:3306–3315.

Stampfer M.R., Garbe J., Nijjar T., Wigington D., Swisshelm K., Yaswen P. 2003. Loss of p53 function accelerates acquisition of telomerase activity in indefinite lifespan human mammary epithelial cell lines. Oncogene 22(34):5238-5251.

Tang L., Zhang Y. 2004. Dietary isothiocyanates inhibit the growth of human bladder carcinoma cells. J Nutr 134(8):2004-2010.

Thornalley P.J. 2002. Isothiocyanates: mechanism of cancer chemopreventive action. Anticancer Drugs 13(4):331-338.

Tice R.R., Andrews P.W., Singh N.P. 1990. The single cell gel assay: a sensitive technique for evaluating intercellular differences in DNA damage and repair. Basic Life Sci 53:291-301.

Tice R.R., Strauss G.H. 1995. The single cell gel electrophoresis/comet assay: a potential tool for detecting radiation-induced DNA damage in humans. Stem Cells 13 Suppl 1:207-214.

Tirmenstein M.A., Nicholls-Grzemski F.A., Zhang J.G., Fariss M.W. 2000. Glutathione depletion and the production of reactive oxygen species in isolated hepatocyte suspensions. Chem Biol Interact 127(3):201-217.

Triginelli S.A., Silva-Filho A.L., Traiman P., Silva F.M., Chaves-Dias M.C., Oliveira G.C., Cunha-Melo J.R. 2006. Telomerase activity in the vaginal margins of radical hysterectomy in patients with carcinoma of the cervix: correlation with histology and human papillomavirus. Int J Gynecol Cancer 16(3):1283-1288.

van Poppel G., Verhoeven D.T., Verhagen H., Goldbohm R.A. 1999. Brassica vegetables and cancer prevention. Epidemiology and mechanisms. Adv Exp Med Biol 472:159-168.

Wilkening S., Bader A. 2003. Influence of culture time on the expression of drug-metabolizing enzymes in primary human hepatocytes and hepatoma cell line HepG2. J Biochem Mol Toxicol 17(4):207-213.

Wilkening S., Stahl F., Bader A. 2003. Comparison of primary human hepatocytes and hepatoma cell line Hepg2 with regard to their biotransformation properties. Drug Metab Dispos 31(8):1035-1042.

Wright W.E., Shay J.W., Piatyszek M.A. 1995. Modifications of a telomeric repeat amplification protocol (TRAP) result in increased reliability, linearity and sensitivity. Nucleic Acids Res 23(18):3794-3795.

Wu X., Kassie F., Mersch-Sundermann V. 2005. Induction of apoptosis in tumor cells by naturally occurring sulfur-containing compounds. Mutat Res 589(2):81-102.

Wyllie A.H. 1980. Glucocorticoid-induced thymocyte apoptosis is associated with endogenous endonuclease activation. Nature 284(5756):555-556.

Xiao D., Lew K.L., Zeng Y., Xiao H., Marynowski S.W., Dhir R., Singh S.V. 2006. Phenethyl isothiocyanate-induced apoptosis in PC-3 human prostate cancer cells is mediated by reactive oxygen species-dependent disruption of the mitochondrial membrane potential. Carcinogenesis 27(11):2223-2234.

Xiao D., Srivastava S.K., Lew K.L., Zeng Y., Hershberger P., Johnson C.S., Trump D.L., Singh S.V. 2003. Allyl isothiocyanate, a constituent of cruciferous vegetables, inhibits proliferation of human prostate cancer cells by causing G2/M arrest and inducing apoptosis. Carcinogenesis 24(5):891-897.

Xu D., Wang Q., Gruber A., Bjorkholm M., Chen Z., Zaid A., Selivanova G., Peterson C., Wiman K.G., Pisa P. 2000. Downregulation of telomerase reverse transcriptase mRNA expression by wild type p53 in human tumor cells. Oncogene 19(45):5123-5133.

Xu K., Thornalley P.J. 2001. Involvement of glutathione metabolism in the cytotoxicity of the phenethyl isothiocyanate and its cysteine conjugate to human leukaemia cells in vitro. Biochem Pharmacol 61(2):165-177.

Ye L., Zhang Y. 2001. Total intracellular accumulation levels of dietary isothiocyanates determine their activity in elevation of cellular glutathione and induction of Phase 2 detoxification enzymes. Carcinogenesis 22(12):1987-1992.

Yi X., Tesmer V.M., Savre-Train I., Shay J.W., Wright W.E. 1999. Both transcriptional and posttranscriptional mechanisms regulate human telomerase template RNA levels. Mol Cell Biol 19(6):3989-3997.

Zeuner C.-R. 2005. Isothiocyanate aus Brassicaceae: quantitative und qualitative Aspekte. Diplomarbeit, Institut für Innenraum-und Umwelttoxikologie, JLU Giessen.

Zhang D.K., Ngan H.Y., Cheng R.Y., Cheung A.N., Liu S.S., Tsao S.W. 1999. Clinical significance of telomerase activation and telomeric restriction fragment (TRF) in cervical cancer. Eur J Cancer 35(1):154-160.

Zhang Y. 2000. Role of glutathione in the accumulation of anticarcinogenic isothiocyanates and their glutathione conjugates by murine hepatoma cells. Carcinogenesis 21(6):1175-1182.

Zhang Y. 2001. Molecular mechanism of rapid cellular accumulation of anticarcinogenic isothiocyanates. Carcinogenesis 22(3):425-431.

Zhang Y., Talalay P. 1994. Anticarcinogenic activities of organic isothiocyanates: chemistry and mechanisms. Cancer Res 54(7 Suppl):1976s-1981s.

Zhang Y., Tang L., Gonzalez V. 2003. Selected isothiocyanates rapidly induce growth inhibition of cancer cells. Mol Cancer Ther 2(10):1045-1052.

Zhang Y., Yao S., Li J. 2006. Vegetable-derived isothiocyanates: anti-proliferative activity and mechanism of action. Proc Nutr Soc 65(1):68-75.

Zhao J., Schmid-Kotsas A., Gross H.J., Gruenert A., Bachem M.G. 2003. Sensitivity and specificity of different staining methods to monitor apoptosis induced by oxidative stress in adherent cells. Chin Med J (Engl) 116(12):1923-1929.

Zhu X., Kumar R., Mandal M., Sharma N., Sharma H.W., Dhingra U., Sokoloski J.A., Hsiao R., Narayanan R. 1996. Cell cycle-dependent modulation of telomerase activity in tumor cells. Proc Natl Acad Sci U S A 93(12):6091-6095.

Zor T., Selinger Z. 1996. Linearization of the Bradford protein assay increases its sensitivity: theoretical and experimental studies. Anal Biochem 236(2):302-308.

VIII. LIST of PUBLICATIONS and PRESENTATIONS

Lamy E, Mersch-Sundermann V: MTBITC mediates cell cycle arrest and apoptosis induction in human HepG2 cells despite its rapid degradation kinetics in the in vitro model **(submitted)**

Lamy E, Mersch-Sundermann V: Telomerase is suppressed during the p53-dependent induction of apoptosis by 4-methylthiobutyl isothiocyanate (erucin) in human HepG2 cells **(submitted)**

Lamy E, Schröder J, Paulus S, Brenk, P, Stahl T, Mersch-Sundermann V: Studies on the genotoxic and antigenotoxic properties of *Eruca sativa* (rocket plant), erucin and erysolin towards benzo(a)pyrene in human hepatoma (HepG2) cells and mechanisms of action **Food and Chemical Toxicology 2008, April 1st,** epub ahead of print

Lamy E, Mersch-Sundermann V. Apoptosis induction and cell cycle arrest of human HepG2 cells by 4-methylthiobutyl isothiocyanate: telomerase suppression as a new component in the signaling pathway? **Naunyn-Schmiedeberg´s Archives of Pharmacology 2008** Mar; Vol. 377, Suppl. 1, p.77

Lamy E, Völkel Y, Roos PH, Kassie F, Mersch-Sundermann V. Ethanol enhanced the genotoxicity of acrylamide in human, metabolically competent HepG2 cells by CYP2E1 induction and glutathione depletion. **Int J Hyg Environ Health**. **2008** Mar;211(1-2):74-81.

Stahl T, Zeuner C-R, Krawinkel M, **Lamy E**, Mersch-Sundermann V. Identifizierung und Quantifizierung chemopräventiver Isothiocyanate in Brassicaceae. **Lebensmittelchemie 2008** 62, 9-10.

Mersch-Sundermann V, Bahorun T, Stahl T, Neergheen VS, Soobrattee MA, Wohlfarth R, Sobel R, Brunn HE, Schmeiser T, **Lamy E**, Aruoma OI. Assessment of the DNA damaging potency and chemopreventive effects towards BaP-induced genotoxicity in

human derived cells by Monimiastrum globosum, an endemic Mauritian plant. **Toxicol In Vitro. 2006** Dec;20(8):1427-34.

Aruoma OI, Colognato R, Fontana I, Gartlon J, Migliore L, Koike K, Coecke S, **Lamy E**, Mersch-Sundermann V, Laurenza I, Benzi L, Yoshino F, Kobayashi K, Lee MC. Molecular effects of fermented papaya preparation on oxidative damage, MAP Kinase activation and modulation of the benzo[a]pyrene mediated genotoxicity. **Biofactors**. **2006**; 26(2):147-59.

Lamy E, Kassie F, Gminski R, Schmeiser HH, Mersch-Sundermann V. 3-Nitrobenzanthrone (3-NBA) induced micronucleus formation and DNA damage in human hepatoma (HepG2) cells. **Toxicol Lett. 2004** Jan 15;146(2):103-9.

Lamy E, Mersch-Sundermann V: 4-Methylthiobutyl isothiocyanat induzierte Apoptose und Zellzyklusarrest in humanen HepG2-Zellen – ist Telomeraseinhibition ein neuer Baustein in dieser Signalkaskade? presented at the 49th. Congress of the DGPT, **Mainz, Germany (2008)**

Lamy E, Mersch-Sundermann V: The isothiocyanate erucin induces apoptosis by modulation of the mitochondrial membrane potential and alteration of the p53-status of human hepatoma (HepG2) cells, presented at the 48th. Congress of the DGPT, **Mainz, Germany (2007)**

Mersch-Sundermann V, **Lamy E**, Oey D, Eißmann F: Induction of apoptosis by two naturally occurring isothiocyanates in primary human ovarian carcinoma cells, presented at the 48th. Congress of the DGPT, **Mainz, Germany (2007)**

Lamy E and Mersch-Sundermann V: Growth inhibition of human HepG2 hepatoma cells by 4-Methylthiobutyl- isothiocyanate (MTBITC)-mediated induction of apoptosis; präsentiert auf der COST Konferenz "molecular and physiological effects of bioactive food compounds", **(2006) Vienna, Austria**

Lamy E, Schröder J, Völkel Y, Mersch-Sundermann V: Studies on the chemopreventive effects of Eruca Sativa (Rucola) and its Isothiocyanates in Human Cell Systems, presented at the 45th Congress of the Society of Toxicology (SOT), **San Diego, USA (2006)** and at

the 22. Congress of the Gesellschaft für Umwelt-Mutationsforschung (GUM), **Darmstadt, Germany (2006).**

Lamy E, Schröder J, Völkel Y, Roos P, Mersch-Sundermann V: Enhancement of acrylamide-mediated DNA-migration by ethanol in a human hepatoma (HepG2) cell line, presented at the 22. Congress of the Gesellschaft für Umwelt-Mutationsfroschung (GUM), **Darmstadt, Germany (2006).**

Lamy E, Schröder J, Völkel Y, Mersch-Sundermann V, Untersuchungen des chemopräventiven (antigentoxischen) Effektes von Eruca Sativa (Rucola) und seinen Isothiocyanaten in humanen Zellsystemen, presented at the 47th. Congress of the DGPT, **Mainz, Germany (2006)**

Lamy E, Mersch-Sundermann V, Hepfner E, Kassie F: 3-Nitrobenzanthrone, emitted by Diesel vehicles, caused DNA damage in human HepG2 and A549 cells using single cell gel electrophoresis and micronucleus assay; presented at the 5th Congress of Toxicology in Developing Countries (5CTDC) **Guilin, China (2003)** and at the 13. Congress of the Gesellschaft für Hygiene und Umweltmedizin (GHU), 9. Congress of the International Society of Environmental Medicine (ISEM), LGL Congress of the Öffentliche Gesundheitsdienst (ÖGD), **Erlangen, Germany (2005)**

Lamy E, Völkel Y, Schröder J, Roos, P, Mersch-Sundermann V: Beer and potato chips: Ethanol enhances the genotoxicity of acrylamide in human, metabolically competent HepG2 cells by CYP2E1 induction, presented at the 13. Congress of the Gesellschaft für Hygiene und Umweltmedizin (GHU), 9. Congress of the International Society of Environmental Medicine (ISEM), LGL Congress of the Öffentliche Gesundheitsdienst (ÖGD), **Erlangen, Germany (2005)**

Der Lebenslauf wurde aus der elektronischen Version der Arbeit entfernt.

The curriculum vitae was removed from the electronic version of the paper.

X. STATEMENT

„Ich erkläre: Ich habe die vorgelegte Dissertation selbstständig, ohne unerlaubte fremde Hilfe und nur mit den Hilfen angefertigt, die ich in der Dissertation angegeben habe. Alle Textstellen, die ich wörtlich oder sinngemäß aus veröffentlichten oder nicht veröffentlichten Schriften entnommen sind, und alle Angaben, die auf mündlichen Auskünften beruhen, sind als solche kenntlich gemacht. Bei den von mir durchgeführten und in der Dissertation erwähnten Untersuchungen habe ich die Grundsätze guter wissenschaftlicher Praxis wie sie in der „Satzung der Justus-Liebig-Universität Gießen zur Sicherung guter wissenschaftlicher Praxis“ niedergelegt sind, eingehalten.“

Schwalbach, den 20.11.07

Evelyn Lamy

XI. APPENDIX

Table 13: Proliferation of HepG2 cells assessed with the WST1 assay after 24 h

	C	SC	1 µM	3 µM	10 µM	20 µM	30 µM
Test 1	0,69	0,67	0,67	0,57	0,52	0,36	0,34
Test 2	0,6	0,53	0,46	0,51	0,48	0,48	0,34
Test 3	0,64	0,59	0,64	0,66	0,66	0,42	0,39
mean	0,64	0,60	0,59	0,58	0,55	0,42	0,36
std. dev.	0,05	0,07	0,11	0,08	0,09	0,06	0,03

Table 14: Proliferation of HepG2 cells assessed with the WST1 assay after 48 h

	C	SC	1 µM	3 µM	10 µM	20 µM	30 µM
Test 1	1,61	1,45	1,59	1,61	1,16	0,65	0,39
Test 2	0,97	0,85	0,91	1,08	0,99	0,53	0,36
Test 3	1,1	0,92	1,25	1,13	1,23	0,72	0,38
mean	1,23	1,07	1,25	1,27	1,13	0,63	0,38
std. dev.	0,34	0,33	0,34	0,29	0,12	0,10	0,02

Table 15: Proliferation of HepG2 cells assessed with the WST1 assay after 72 h

	C	SC	1 µM	3 µM	10 µM	20 µM	30 µM
Test 1	1,89	2,25	2,23	2,58	2,56	1,37	0,29
Test 2	1,84	1,61	1,75	1,94	1,75	0,78	0,27
Test 3	1,6	2,05	2,28	2,38	2,44	1,07	0,28
mean	1,78	1,97	2,09	2,30	2,25	1,07	0,28
std. dev.	0,16	0,33	0,29	0,33	0,44	0,30	0,01

Table 16: Protein concentration (µg/µl) of HepG2 cells exposed to 20 µM MTBITC for the indicated time points

	SC	24 h	48 h	72 h
Test 1	3,4	2,78	1,34	0,25
Test 2	4,71	3,26	1,57	0,26
Test 3	4,38	3,4	1,46	0,42
Test 4	4,32	3,5	1,23	0,19
mean	4,20	3,24	1,40	0,28
std. dev.	0,56	0,32	0,15	0,10

Table 17: Induction of apoptosis assessed by the "subG1" DNA content of HepG2 cells after MTBITC-treatment for 24 h

	SC	5 µM	10 µM	20 µM	30 µM	50 µM	+ control
Test 1	2,29	2,71	5,64	15,28	11,03	3,95	13,92
Test 2	2,46	2,61	7,14	15,02	8,22	3,53	17,67
Test 3	2,68	3,43	4,93	17,78	14,69	3,7	17,31
mean	2,48	2,92	5,90	16,03	11,31	3,73	16,30
std. dev.	0,20	0,45	1,13	1,52	3,24	0,21	2,07

Table 18: Apoptosis induction, assessed by the detection of ssDNA

	SC	1 h	3 h	6 h	24 h	+ control	IC
Test 1	0,29	0,14	0,12	0,48	0,6	1,27	1,59
Test 2	0,35	0,25	0,33	0,48	0,74	1,52	1,67
Test 3	0,28	0,36	0,3	0,36	0,6	1,52	1,64
mean	0,31	0,25	0,25	0,44	0,65	1,44	1,63
std. dev.	0,04	0,11	0,11	0,07	0,08	0,14	0,04

Table 19: Cell cycle distribution of HepG2 cells after 1 h-treatment with MTBITC

		Cell cycle phase		
		G1	S	G2/M
Test 1	SC	72,2	19,64	8,15
Test 2	SC	71,23	19,29	9,48
Test 3	SC	70	20,97	9,03
	mean	71,14	19,97	8,89
	std. dev.	1,10	0,89	0,68
Test 1	20 µM	75,56	15,68	8,76
Test 2	20 µM	74,69	15,5	9,81
Test 3	20 µM	74,28	15,44	10,28
	mean	74,84	15,54	9,62
	std. dev.	0,65	0,12	0,78

Table 20: Cell cycle distribution of HepG2 cells after 3 h-treatment with MTBITC

		Cell cycle phase		
		G1	S	G2/M
Test 1	SC	74,99	15,67	9,35
Test 2	SC	61,02	27,49	11,49
Test 3	SC	59,53	30	10,47
	mean	65,18	24,39	10,44
	std. dev.	8,53	7,65	1,07
Test 1	20 µM	73,85	14,4	11,75
Test 2	20 µM	71,09	14,88	14,03
Test 3	20 µM	75,81	11,02	13,17
	mean	73,58	13,43	12,98
	std. dev.	2,37	2,10	1,15

Table 21: Cell cycle distribution of HepG2 cells after 6 h-treatment with MTBITC

		Cell cycle phase		
		G1	S	G2/M
Test 1	SC	74,73	18,52	6,75
Test 2	SC	74,48	20,02	5,5
Test 3	SC	74,61	19,3	6,08
	mean	74,61	19,28	6,11
	std. dev.	0,13	0,75	0,63
Test 1	20 µM	65,65	15,99	18,35
Test 2	20 µM	67,15	9,13	23,73
Test 3	20 µM	66,15	9,08	24,77
	mean	66,32	11,40	22,28
	std. dev.	0,76	3,98	3,45

Table 22: Cell cycle distribution of HepG2 cells after 24 h-treatment with MTBITC

		Cell cycle phase		
		G1	S	G2/M
Test 1	SC	70,63	19,5	9,87
Test 2	SC	67,75	21,9	10,54
Test 3	SC	67,56	21,73	10,52
	mean	68,65	21,04	10,31
	std. dev.	1,72	1,34	0,38
Test 1	20 µM	24,87	13,35	61,78
Test 2	20 µM	25,73	15,79	58,48
Test 3	20 µM	28,55	13,44	58,01
	mean	26,38	14,19	59,42
	std. dev.	1,93	1,38	2,05

Table 23: Expression of p21^{WAF1} in HepG2 cells after Exposure to 20 µM MTBITC for the indicated time points (% of control)

Time (h)	Test 1	Test 2	mean	std. dev.
1	7,43	0,00	3,71	5,25
3	6,53	11,72	9,13	3,67
6	32,05	31,09	31,57	0,68
24	29,15	69,28	49,21	28,37
48	34,93	58,64	46,79	16,77

Table 24: GSH level of HepG2 cells after treatment with MTBITC for 6 h

	Test 1	GSH (µM)	% of control	Test 2	GSH (µM)	% of control	mean	std. dev.
DMSO	0,79	14,07	100,00	0,77	13,64	100,00	100,00	0,00
1 µM	0,97	17,43	123,89	1,02	18,22	133,64	128,77	6,90
3 µM	1,13	20,19	143,46	1,11	19,96	146,36	144,91	2,05
10 µM	1,08	19,40	137,85	0,97	17,44	127,87	132,86	7,06
20 µM	0,36	6,14	43,66	0,32	5,46	40,07	41,86	2,54
30 µM	0,37	6,42	45,59	0,30	5,10	37,38	41,48	5,81
50 µM	0,14	2,14	15,19	0,12	1,80	13,22	14,20	1,39

Table 25: GSH level of HepG2 cells after treatment with MTBITC for 24 h

	Test 1	GSH (µM)	% of control	Test 2	GSH (µM)	% of control	mean	std. dev.
DMSO	0,31	5,41	100,00	0,33	5,75	100,00	100,00	0,00
1 µM	0,50	8,72	161,22	0,56	9,95	173,00	167,11	8,34
3 µM	0,67	11,82	218,68	0,74	13,24	230,30	224,49	8,21
10 µM	0,60	10,60	196,15	0,75	13,26	230,66	213,41	24,40
20 µM	0,04	0,47	8,64	0,09	1,23	21,36	15,00	8,99
30 µM	0,02	-0,06	0,00	0,04	0,32	5,51	2,75	3,89
50 µM	-0,04	-1,01	0,00	0,02	0,05	0,87	0,44	0,62

Table 26: MMP of HepG2 cells after valinomycin-treatment for 24 h (% of control)

	0,1 µM	1 µM	10 µM	100 µM
Test 1	42,98	20,34	17,30	9,05
Test 2	59,43	32,31	22,86	9,51
Test 3	39,83	17,26	8,11	8,41
mean	47,42	23,30	16,09	8,99
std. dev.	10,53	7,95	7,45	0,55

Table 27: MMP of HepG2 cells after MTBITC-treatment for 3 h (% of control)

	3 µM	10 µM	20 µM	30 µM	+ control
Test 1	113,36	94,80	103,15	93,92	26,78
Test 2	107,31	92,64	82,92	101,71	64,72
Test 3	88,47	89,87	87,91	83,36	36,52
mean	103,05	92,44	91,33	93,00	42,67
std. dev.	12,98	2,47	10,54	9,21	19,70

Table 28: MMP of HepG2 cells after MTBITC-treatment for 6 h (% of control)

	3 µM	10 µM	20 µM	30 µM	+ control
Test 1	82,67	121,00	74,70	60,78	17,01
Test 2	111,66	104,63	84,37	33,86	6,65
Test 3	70,37	94,01	83,79	71,87	24,54
mean	88,23	106,55	80,95	55,50	16,07
std. dev.	21,20	13,60	5,42	19,55	8,98

Table 29: MMP of HepG2 cells after MTBITC-treatment for 24 h (% of control)

	3 µM	10 µM	20 µM	30 µM	+ control
Test 1	72,90	29,63	5,43	8,47	8,81
Test 2	58,40	39,48	5,48	8,75	10,69
Test 3	90,57	57,24	14,44	6,22	12,45
mean	73,96	43,44	8,45	7,81	10,65
std. dev.	16,11	19,52	5,19	1,39	1,82

Table 30: Expression of Bclxl in HepG2 cells after Exposure to 20 µM MTBITC for the indicated time points (% of control)

Time (h)	Test 1	Test 2	Test 3	mean	std. dev.
1 h	125,49	105,59	85,08	114,39	34,56
3 h	152,26	59,82	57,80	89,96	53,96
6 h	56,72	45,70	15,41	39,27	21,39
24 h	44,87	56,27	22,65	41,26	17,09
48 h	40,00	56,27	37,21	44,49	10,29

Table 31: Conversion of 5 µM DHR123 to RH123 in HepG2 cells by H_2O_2 (% of control)

	Test 1	Test 2	mean	std. dev.
10 µM	79,98	65,67	72,83	10,12
30 µM	223,90	191,70	207,80	22,77
100 µM	620,12	531,94	576,03	62,35
300 µM	1612,35	1376,19	1494,27	166,99

Table 32: Conversion of 10 µM DHR123 to RH123 in HepG2 cells by H_2O_2 (% of control)

	Test 1	Test 2	mean	std. dev.
10 µM	89,65	68,05	78,85	15,27
30 µM	247,92	186,24	217,08	43,61
100 µM	639,10	508,90	574,00	92,07
300 µM	1636,51	1297,34	1466,92	239,83

Table 33: Conversion of 50 µM DHR123 to RH123 in HepG2 cells by H_2O_2 (% of control)

	Test 1	Test 2	mean	std. dev.
10 µM	76,79	61,20	68,99	11,02
30 µM	207,70	152,74	180,22	38,87
100 µM	527,95	405,43	466,69	86,64
300 µM	1065,19	818,58	941,88	174,38

Table 34: Production of ROS in HepG2 cells exposed to MTBITC for 1 h (% of control)

	Test 1	Test 2	Test 3	Test 4	mean	std. dev.
1 µM	12,52	12,00	16,30	11,99	13,20	2,08
3 µM	11,48	11,40	12,62	9,82	11,33	1,15
10 µM	10,03	10,85	12,47	10,77	11,03	1,03
20 µM	11,51	8,89	9,76	9,03	9,80	1,20
30 µM	13,04	10,83	12,95	12,23	12,26	1,02

Table 35: Production of ROS in HepG2 cells exposed to MTBITC for 3 h (% of control)

	Test 1	Test 2	Test 3	Test 4	mean	std. dev.
1 µM	9,01	11,68	14,40	11,71	11,70	2,20
3 µM	9,97	10,12	13,42	11,41	11,23	1,60
10 µM	9,40	10,79	13,63	12,71	11,63	1,90
20 µM	13,75	10,80	13,31	14,92	13,20	1,74
30 µM	17,61	16,94	20,25	19,60	18,60	1,58

Table 36: Production of ROS in HepG2 cells exposed to MTBITC for 6 h (% of control)

	Test 1	Test 2	Test 3	Test 4	mean	std. dev.
1 µM	3,95	5,12	5,58	4,89	4,89	0,69
3 µM	4,58	5,19	6,03	5,12	5,23	0,60
10 µM	7,55	8,23	8,35	9,06	8,30	0,62
20 µM	9,17	8,25	10,10	9,44	9,24	0,77
30 µM	10,68	11,38	11,81	11,61	11,37	0,49

Table 37: DNA damage in HepG2 cells after 1 h-treatment with 20 µM MTBITC

	SC	20 µM	+ control
Test 1	0,91	1,91	2,55
Test 2	0,89	2,12	2,52
Test 3	0,77	2,34	2,80
mean	0,86	2,12	2,62
std. dev.	0,07	0,22	0,16

Table 38: Expression of p53 in HepG2 cells after Exposure to MTBITC for 1 h (% of control)

	3 µM	10 µM	20 µM	30 µM
Test 1	109,66	143,21	279,45	147,86
Test 2	142,93	229,27	310,44	229,57
Test 3	144,86	229,81	375,06	160,73
mean	132,48	200,76	321,65	179,39
std. dev.	19,79	49,84	48,78	43,93

Table 39: Expression of p53 in HepG2 cells after Exposure to MTBITC for 3 h (% of control)

	3 µM	10 µM	20 µM	30 µM
Test 1	106,74	98,38	57,62	53,09
Test 2	103,37	74,4	31,11	24,09
Test 3	102,95	78,73	43,2	46,72
mean	104,35	83,84	43,98	41,30
std. dev.	2,08	12,78	13,27	15,24

Table 40: Expression of p53 in HepG2 cells after Exposure to MTBITC for 6 h (% of control)

	3 µM	10 µM	20 µM	30 µM
Test 1	95,52	106,9	215,54	96,44
Test 2	115,91	114,71	146,47	87,24
Test 3	119,44	138,61	209,17	73,68
mean	110,29	120,07	190,39	85,79
std. dev.	12,91	16,52	38,17	11,45

Table 41: Expression of p53 in HepG2 cells after Exposure to MTBITC for 24 h (% of control)

	3 µM	10 µM	20 µM	30 µM
Test 1	95,08	86,47	44,64	59,73
Test 2	96,71	81,57	80,59	61,18
Test 3	90,89	105,47	74,96	40,76
mean	94,23	91,17	66,73	53,89
std. dev.	3,00	12,62	19,34	11,39

Table 42: Expression of p63 in HepG2 cells after Exposure to MTBITC for the indicated time points (% of control)

	1 h	3 h	6 h	24 h	48 h
Test 1	127,09	142,79	170,60	444,85	543,78
Test 2	106,05	59,81	237,99	494,66	502,85
Test 3	173,08	92,10	228,40	417,42	513,08
mean	135,40	98,23	212,33	452,31	519,90
std. dev.	34,28	41,83	36,45	39,16	21,30

Table 43: Expression of MDM2 in HepG2 cells after Exposure to 20 µM MTBITC for the indicated time points (% of control)

	Test 1	Test 2	Test 3	mean	std. dev.
1 h	1	0	0	0	0,23
3 h	7	6	6	6	0,58
6 h	174	128	197	167	35,29
24 h	941	860	886	895	41,08
48 h	679	582	729	663	74,96

Table 44: Expression of hTERT in HepG2 cells after Exposure to 20 µM MTBITC for the indicated time points (% of control)

	Test 1	Test 2	Test 3	mean	std. dev.
1 h	89,2	99,46	103,34	97,34	7,30
3 h	75,6	69,92	88,57	78,04	9,55
6 h	70,9	53,17	66,91	63,67	9,31
24 h	51,8	61,98	44,58	52,79	8,74
48 h	61,16	70,19	50,89	60,75	9,66

Table 46: Telomerase activity of HepG2 cells after 20 µM MTBITC-treatment for the indicated time points (% of control)

	6 h	24 h	48 h	72 h	+ control
Test 1	97,84	92,10	83,61	50,87	11,56
Test 2	99,20	89,37	76,82	45,36	12,44
Test 3	102,63	91,96	75,24	58,75	5,80
mean	99,89	91,14	78,56	51,66	9,93
std. dev.	2,47	1,53	4,45	6,73	3,61

Table 47: Telomerase activity of HepG2 cells after exposure to TMPyP4 for 24 h (% of control)

	100 µM	200 µM	300 µM
Test 1	76,16	41,87	11,56
Test 2	92,19	24,91	12,44
Test 3	92,23	33,03	5,80
mean	86,86	33,27	9,93
std. dev.	9,27	8,48	3,61

Table 48: Expression of HSP90 in HepG2 cells after Exposure to 20 µM MTBITC for the indicated time points (% of control)

	Test 1	Test 2	mean	std. dev.
1 h	147,74	164,55	156,15	11,88
3 h	202,16	239,35	220,76	26,30
6 h	282,20	277,79	279,99	3,11
24 h	322,73	292,90	307,82	21,09
48 h	472,37	416,89	444,63	39,23

Table 49: Expression of HSP70 in HepG2 cells after Exposure to 20 µM MTBITC for the indicated time points (% of control)

	Test 1	Test 2	Test 3	mean	std. dev.
1 h	48,42	62,82	87,39	66,21	19,70
3 h	71,42	83,73	68,95	74,70	7,92
6 h	192,62	92,33	115,52	133,49	52,51
24 h	222,06	280,99	298,42	267,16	40,02
48 h	421,12	219,65	330,65	323,81	100,91

Table 50: Determination of the telomere length of HepG2 cells after exposure to 20 µM MTBITC for the indicated time points

	SC	1 h	6 h	24 h	48 h
Test 1	22,79	22,45	24,31	21,47	22,54
Test 2	23,02	22,25	23,58	25,98	23,5
Test 3	21,81	21,56	22,28	20,45	28,17
mean	22,54	22,09	23,39	22,63	24,74
std. dev.	0,64	0,47	1,03	2,94	3,01

Table 51: Degradation kinetic of MTBITC in culture medium containing 1 x 10^6 HepG2 cells (% of control)

Time (min.)	Test 1	Test 2	Test 3	mean	std. dev.
30	65,1	65,42	66,11	65,54	0,52
60	44,82	53,88	53,46	50,72	5,11
180	36,36	34,23	33,48	34,69	1,49
360	28,68	29,57	16,92	25,06	7,06
1440	0,00	0,00	0,00	0,00	0,00

Table 52: Degradation kinetic of MTBITC in culture medium w/o cells (% of control)

Time (min.)	Test 1	Test 2	mean	std. dev.
30	90,25	70,17	80,21	14,20
60	73,21	55,24	64,23	12,71
180	45,83	46,6	46,22	0,54
360	34,88	27,75	31,32	5,04
1440	0,00	0,00	0,00	0,00

Table 53: Degradation kinetic of MTBITC in destilled water with gas exchange (% of control)

Time (min.)	Test 1	Test 2	mean	std. dev.
30	83,3	68,5	75,90	10,47
60	69,86	56,55	63,21	9,41
180	41,87	51,02	46,45	6,47
360	36,1	32,05	34,08	2,86
1440	28,35	23,24	25,80	3,61

Table 54: Degradation kinetic of MTBITC in destilled water w/o gas exchange (% of control)

Time (min.)	Test 1	Test 2	Test 3	mean	std. dev.
30	66,07	67,42	77,45	70,31	6,22
60	57,72	60,06	65,23	61,00	3,84
180	49,77	54,3	53,05	52,37	2,34
360	45,87	47,38	52,85	48,70	3,67
1440	29,98	35,27	40,79	35,35	5,41

Table 55: Determination of the "point of no return" in HepG2 cells after exposure to 20 µM MTBITC (% of control)

	1 h	6 h	24 h
Test 1	98,73	5,97	4,28
Test 2	76,39	3,99	2,28
Test 3	89,57	6,07	4,01
mean	88,23	5,34	3,52
std. dev.	11,23	1,17	1,09